AD-A107 263 AIR FORCE INST OF TECH WRIGHT-PATTERSON AFB OH F/G 8/12
DETERMINATION OF ICE CRYSTAL GROWTH PARAMETERS IN A SUPERCOOLED--ETC(U)
JUN 81 M W KOWA
UNCLASSIFIED AFIT-CI-81-36T NL

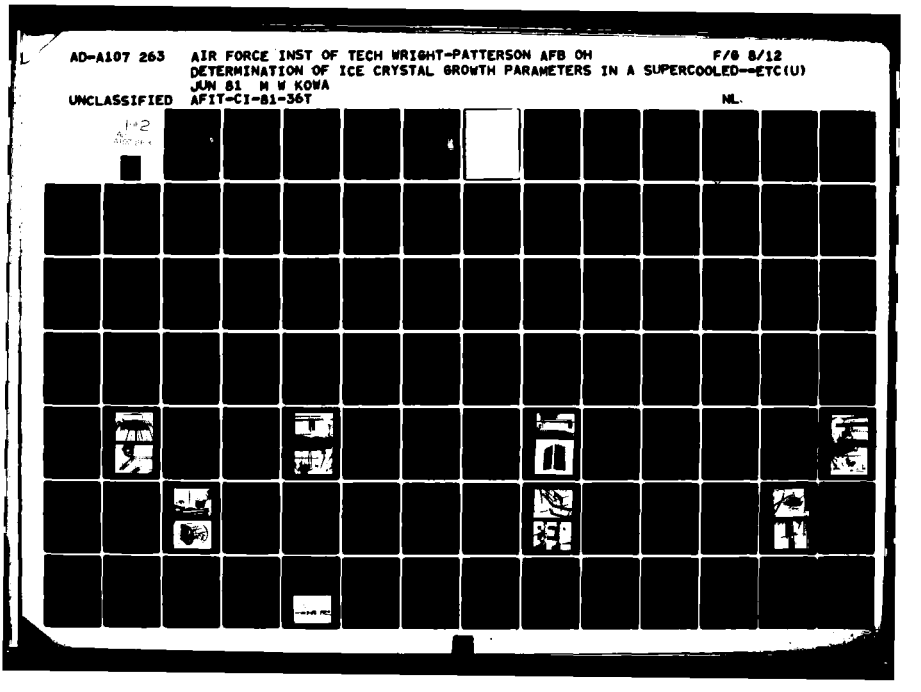

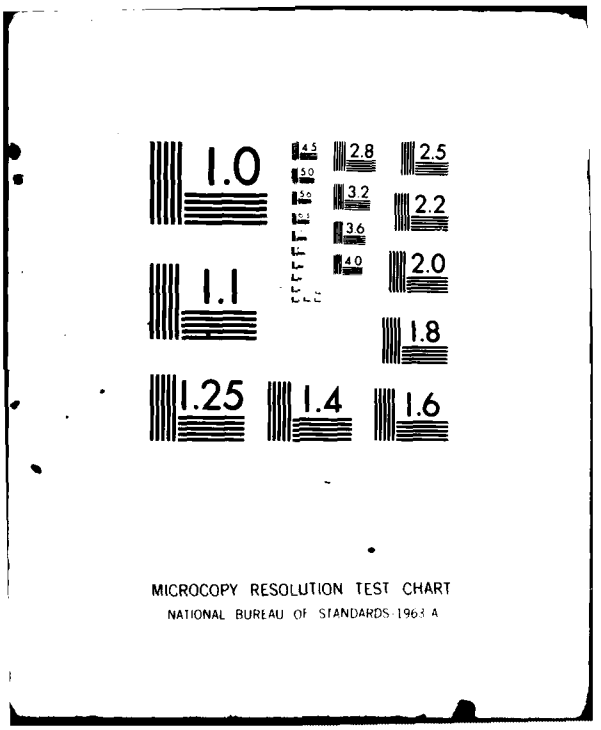
1.0
1.1
1.25
1.4
1.6
1.8
2.0
2.2
2.5
2.8
3.2
3.6
4.0
4.5
5.0
MICROCOPY RESOLUTION TEST CHART
NATIONAL BUREAU OF STANDARDS 1963 A

UNCLASS

SECURITY CLASSIFICATION OF THIS PAGE (When Data Entered)

REPORT DOCUMENTATION PAGE	READ INSTRUCTIONS BEFORE COMPLETING FORM
1. REPORT NUMBER: AFIT-CI-81-36T (6)	2. GOVT ACCESSION NO.: AD-A107263
3. RECIPIENT'S CATALOG NUMBER	
4. TITLE (and Subtitle): Determination of Ice Crystal Growth Parameters in a Supercooled Cloud Tunnel,	5. TYPE OF REPORT & PERIOD COVERED: THESIS/DISSERTATION
	6. PERFORMING ORG. REPORT NUMBER
7. AUTHOR(s): (10) Capt Mike Wayne Kowa	8. CONTRACT OR GRANT NUMBER(s): Master's Thesis
9. PERFORMING ORGANIZATION NAME AND ADDRESS: AFIT STUDENT AT: University of Utah	10. PROGRAM ELEMENT, PROJECT, TASK AREA & WORK UNIT NUMBERS
11. CONTROLLING OFFICE NAME AND ADDRESS: AFIT/NR, WPAFB OH 45433	12. REPORT DATE: (11) June 1981
	13. NUMBER OF PAGES: 128 (12) 146
14. MONITORING AGENCY NAME & ADDRESS (if different from Controlling Office)	15. SECURITY CLASS. (of this report): UNCLASS
	15a. DECLASSIFICATION/DOWNGRADING SCHEDULE

16. DISTRIBUTION STATEMENT (of this Report)

APPROVED FOR PUBLIC RELEASE; DISTRIBUTION UNLIMITED

17. DISTRIBUTION STATEMENT (of the abstract entered in Block 20, if different from Report)

16 OCT 1981

Air Force Institute of Technology (ATC)
Wright-Patterson AFB, OH 45433

18. SUPPLEMENTARY NOTES

APPROVED FOR PUBLIC RELEASE: IAW AFR 190-17

Fredric C. Lynch
FREDRIC C. LYNCH, Major, USAF
Director of Public Affairs

19. KEY WORDS (Continue on reverse side if necessary and identify by block number)

20. ABSTRACT (Continue on reverse side if necessary and identify by block number)

ATTACHED

81 10 27 250

DD FORM 1 JAN 73 1473 EDITION OF 1 NOV 65 IS OBSOLETE

UNCLASS

SECURITY CLASSIFICATION OF THIS PAGE (When Data Entered)

012200

AD A107263

DTIC FILE COPY

DTIC ELECTE NOV 6 1981 S D H

ABSTRACT

In order to completely understand the behavior of a dynamically changing ice crystal as it falls through a supercooled cloud, the simultaneous determination of the crystal size, mass, apparent density, and fall velocity is desirable. Based on the experience obtained in our two previous ice crystal growth studies, a new supercooled cloud tunnel has been developed. It has successfully demonstrated the capability of accurately simulating the crystal growth under free-fall conditions in a natural supercooled cloud. The new vertically converging design for the working/observation section of the tunnel permits ice crystals to be stably suspended in a supercooled cloud airstream for indefinite lengths of time. A new fog chamber is used to make the supercooled fog homogeneous with respect to droplet number and concentration, and temperature, before entering the working/observation section. A method has been developed by which the moisture content in the supercooled fog can be controlled and held constant. The flow rate through the working/observation section is controlled by a specially designed valve which also maintains the total flow into the chamber at a constant level. This configuration keeps the supercooled fog condition constant throughout an experimental run. A special method is devised to preserve the collected ice crystals so they can be photographed from both the top and side. This method also allows for accurate crystal mass determination by melting. The flow velocity, and therefore crystal fall velocity, is continually measured by an electronic manometer while a

thermocouple continually records the supercooled fog temperature.

Using this new apparatus, growing ice crystals were freely suspended in the supercooled fog for periods from three to ten minutes and temperatures between -3.0 to -23.0°C. Single and double plates were observed about -4.5°C, columns between -4.5 and -7.0°C, isometric crystals (2a/c = 1) near 9.0°C, dendrites between -13.0 and -16.0°C, vaned crystals between -16.0 and -18.0°C, and complex crystals between -18.0 and -23.0°C. The complex crystals appear to result from a combination of riming growth and vapor diffusion growth. The maximum crystal fall velocity was observed near -9.0° where the isometric crystals were observed. This was the temperature where the ice crystal mass minimum and the ice crystal apparent density maximum were detected. This indicates the importance of the crystal spatial form in controlling the fall velocity. By closely observing the crystals while freely suspended, it was found that columns were oriented with the prism faces down while at the same time rotating horizontally about an axis perpendicular to the prism plane. Dendrites and plates were oriented with the basal faces down while at the same time rotating about their vertical axis. The speeds of rotation became larger as the fall velocity increased. Dendrites and large double plates were aerodynamically the most stable while vaned crystals were the least. The vanes on the vaned crystals did not begin to affect the aerodynamic characteristics until after five to six minutes of growth.

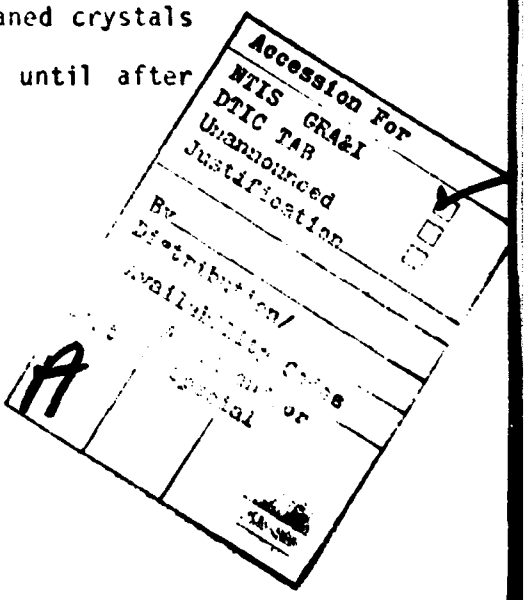

81-36T

AFIT RESEARCH ASSESSMENT

The purpose of this questionnaire is to ascertain the value and/or contribution of research accomplished by students or faculty of the Air Force Institute of Technology (ATC). It would be greatly appreciated if you would complete the following questionnaire and return it to:

AFIT/NR
Wright-Patterson AFB OH 45433

RESEARCH TITLE: Determination of Ice Crystal Growth Parameters in a Supercooled Cloud Tunnel

AUTHOR: Capt Mike Wayne Kowa

RESEARCH ASSESSMENT QUESTIONS:

1. Did this research contribute to a current Air Force project?

( ) a. YES ( ) b. NO

2. Do you believe this research topic is significant enough that it would have been researched (or contracted) by your organization or another agency if AFIT had not?

( ) a. YES ( ) b. NO

3. The benefits of AFIT research can often be expressed by the equivalent value that your agency achieved/received by virtue of AFIT performing the research. Can you estimate what this research would have cost if it had been accomplished under contract or if it had been done in-house in terms of manpower and/or dollars?

( ) a. MAN-YEARS _____ ( ) b. $_____

4. Often it is not possible to attach equivalent dollar values to research, although the results of the research may, in fact, be important. Whether or not you were able to establish an equivalent value for this research (3. above), what is your estimate of its significance?

( ) a. HIGHLY SIGNIFICANT ( ) b. SIGNIFICANT ( ) c. SLIGHTLY SIGNIFICANT ( ) d. OF NO SIGNIFICANCE

5. AFIT welcomes any further comments you may have on the above questions, or any additional details concerning the current application, future potential, or other value of this research. Please use the bottom part of this questionnaire for your statement(s).

NAME GRADE POSITION

ORGANIZATION LOCATION

STATEMENT(s):

FOLD DOWN ON OUTSIDE - SEAL WITH TAPE

AFIT/NR
WRIGHT-PATTERSON AFB OH 45433

OFFICIAL BUSINESS
PENALTY FOR PRIVATE USE. $300

NO POSTAGE
NECESSARY
IF MAILED
IN THE
UNITED STATES

BUSINESS REPLY MAIL
FIRST CLASS PERMIT NO. 73236 WASHINGTON D.C.

POSTAGE WILL BE PAID BY ADDRESSEE

AFIT/ DAA
Wright-Patterson AFB OH 45433

FOLD IN

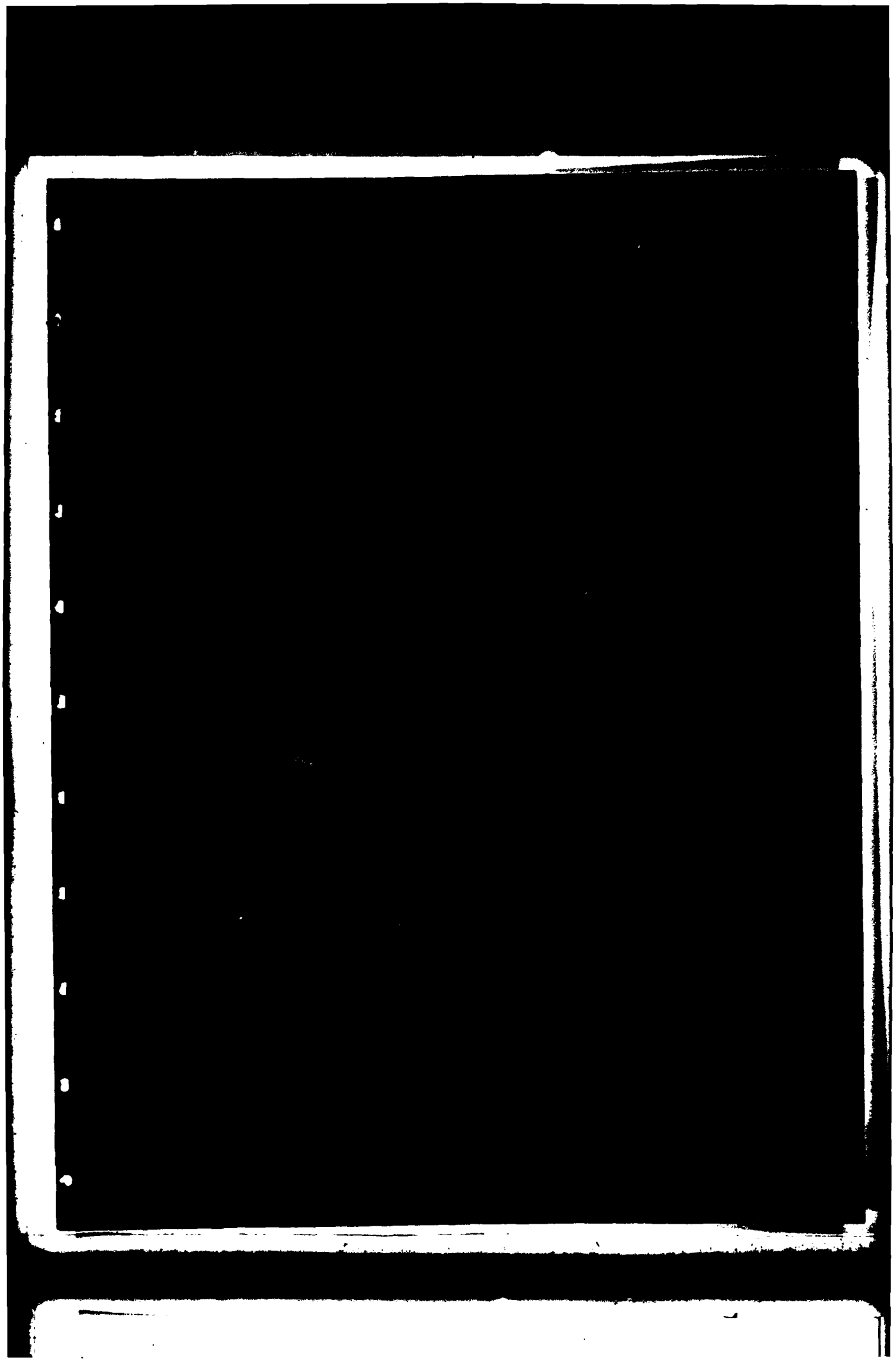

DETERMINATION OF ICE CRYSTAL GROWTH PARAMETERS IN A SUPERCOOLED CLOUD TUNNEL

by

Mike Wayne Kowa

A thesis submitted to the faculty of
The University of Utah
in partial fulfillment of the requirements for the degree of

Master of Science

Department of Meteorology

The University of Utah

June 1981

THE UNIVERSITY OF UTAH GRADUATE SCHOOL

SUPERVISORY COMMITTEE APPROVAL

of a thesis submitted by

Mike Wayne Kowa

I have read this thesis and have found it to be of satisfactory, quality for a master's degree.

June 8, 1981 — Norihiko Fukuta.
Date — Norihiko Fukuta
Chairman, Supervisory Committee

I have read this thesis and have found it to be of satisfactory quality for a master's degree.

8 June 1981 — Kenneth Sassen
Date — Kenneth Sassen
Member, Supervisory Committee

I have read this thesis and have found it to be of satisfactory quality for a master's degree.

June 8, 1981 — Elford G. Astling
Date — Elford G. Astling
Member, Supervisory Committee

3-79

THE UNIVERSITY OF UTAH GRADUATE SCHOOL

FINAL READING APPROVAL

To the Graduate Council of The University of Utah:

I have read the thesis of Mike Wayne Kowa in its final form and have found that (1) its format, citations, and bibliographic style are consistent and acceptable; (2) its illustrative materials including figures, tables, and charts are in place; and (3) the final manuscript is satisfactory to the Supervisory Committee and is ready for submission to the Graduate School.

June 8, 1981
Date

Norihiko Fukuta
Norihiko Fukuta
Member, Supervisory Committee

Approved for the Major Department

L. H. Lattman
Chairman/ Dean

Approved for the Graduate Council

James L. Clayton
Dean of The Graduate School

ABSTRACT

In order to completely understand the behavior of a dynamically changing ice crystal as it falls through a supercooled cloud, the simultaneous determination of the crystal size, mass, apparent density, and fall velocity is desirable. Based on the experience obtained in our two previous ice crystal growth studies, a new supercooled cloud tunnel has been developed. It has successfully demonstrated the capability of accurately simulating the crystal growth under free-fall conditions in a natural supercooled cloud. The new vertically converging design for the working/observation section of the tunnel permits ice crystals to be stably suspended in a supercooled cloud airstream for indefinite lengths of time. A new fog chamber is used to make the supercooled fog homogeneous with respect to droplet number and concentration, and temperature, before entering the working/observation section. A method has been developed by which the moisture content in the supercooled fog can be controlled and held constant. The flow rate through the working/observation section is controlled by a specially designed valve which also maintains the total flow into the chamber at a constant level. This configuration keeps the supercooled fog condition constant throughout an experimental run. A special method is devised to preserve the collected ice crystals so they can be photographed from both the top and side. This method also allows for accurate crystal mass determination by melting. The flow velocity, and therefore crystal fall velocity, is continually measured by an electronic manometer while a

thermocouple continually records the supercooled fog temperature.

Using this new apparatus, growing ice crystals were freely suspended in the supercooled fog for periods from three to ten minutes and temperatures between -3.0 to -23.0°C. Single and double plates were observed about -4.5°C, columns between -4.5 and -7.0°C, isometric crystals (2a/c = 1) near -9.0°C, dendrites between -13.0 and -16.0°C, vaned crystals between -16.0 and -18.0°C, and complex crystals between -18.0 and -23.0°C. The complex crystals appear to result from a combination of riming growth and vapor diffusion growth. The maximum crystal fall velocity was observed near -9.0° where the isometric crystals were observed. This was the temperature where the ice crystal mass minimum and the ice crystal apparent density maximum were detected. This indicates the importance of the crystal spatial form in controlling the fall velocity. By closely observing the crystals while freely suspended, it was found that columns were oriented with the prism faces down while at the same time rotating horizontally about an axis perpendicular to the prism plane. Dendrites and plates were oriented with the basal faces down while at the same time rotating about their vertical axis. The speeds of rotation became larger as the fall velocity increased. Dendrites and large double plates were aerodynamically the most stable while vaned crystals were the least. The vanes on the vaned crystals did not begin to affect the aerodynamic characteristics until after five to six minutes of growth.

TABLE OF CONTENTS

LIST OF FIGURES

ACKNOWLEDGEMENTS

I wish to express my sincere gratitude to Dr. Norihiko Fukuta, chairman of my supervisory committe, for his invaluable assistance, guidance, encouragement, and most of all, patience. I would also like to thank Dr. Sassen and Dr. Astling for serving on my supervisory committee.

I am very grateful to my fellow students who offered their encouragement and assistance throughout my stay at the University of Utah. A special thanks goes to Doug Swoboda for his many helpful suggestions, assistance, and patience while working together for the past 18 months.

I wish to express my deepest gratitude to my wife, Mildred, for her love, understanding, support, and assistance during the many difficult times which arose during the past two years.

This material is based upon work supported by National Science Foundation, Division of Atmospheric Science Foundation, under Grant ATM-8004108.

Chapter 1

INTRODUCTION

Ice phase processes play dominant roles in producing most forms of precipitation that occur in all but tropical regions of the earth (Mason, 1971). In liquid phase clouds, condensation by itself is not usually adequate for producing precipitation. By condensation alone, without coalescence process, droplets seldom reach a size large enough to fall from the cloud and reach the ground before entirely evaporating. It wasn't until 1935, when Bergeron published his hypothesis, that the important role that the ice phase processes play in the formation of precipitation became widely understood and accepted. Bergeron explained that only through the process of ice crystals growing in a supercooled cloud could precipitation elements grow to a size large enough to fall from a cloud and reach the ground. If the temperature above the ground is entirely or predominantly below freezing, some type of frozen precipitation results. If warm layers of adequate depth exist, the ice crystals will melt before reaching the ground and rain results.

Without precipitation, obviously life on earth could not exist. History abounds with examples of the rise, fall, and forced migration of civilizations as a result of the lack of or abundance of precipitation. Since the ice phase processes are necessary for the formation of precipitation over much of the earth's surface, it is necessary that we study and fully understand these processes.

Until recently man was at the mercy of nature to provide the necessary precipitation for his survival. Over the past few decades, however, use of weather modification techniques have shown promise in inducing and augmenting precipitation. This is of particular significance in the arid western regions of the United States where ice phase precipitation provides most of the water supply, primarily in the form of mountain snowpack. In other areas, weather modification has been used in an attempt to suppress crop destroying hailstorms. A full understanding of ice phase cloud processes is a must in order to guide these weather modification methods to a success.

Ice phase processes also significantly influence atmospheric dynamics through releasing or absorbing latent heats and hydrometeor loading (Mason, 1971; Pruppacher and Klett, 1978). Additional development of a supercooled cloud happens when it glaciates (Fukuta, 1973). Hydrometeor loading, along with cooling due to evaporation of precipitation, often results in the development of strong downdrafts. These downdrafts present a severe hazard to aircraft during landing and take off. Again, an accurate knowledge of the ice phase processes occuring in the atmosphere is required to fully investigate and understand these phenomena.

To understand these ice phase processes an accurate study of ice crystal growth parameters is paramount. A review of the previous methods of ice crystal growth study is presented in Chapter 2. Chapter 3 includes the design and construction of a new supercooled cloud tunnel used in this study. Chapter 4 describes the experimental procedures employed in conducting the experiments. Results and discussions are included in Chapter 5 while Chapter 6 contains conclusions.

Chapter 2

PAST ICE CRYSTAL GROWTH STUDIES

One of the objectives of studying the processes of ice crystal growth is to describe the growth processes that occur in actual clouds in nature. Many different approaches have been used to investigate these ice crystal growth processes but they can be grouped into two general categories. One studies ice crystals collected in their natural cloud environment and the other the crystals grown in the laboratory where the natural cloud conditions are simulated as accurately as possible.

Field Studies

Several field investigations of ice crystal growth have been conducted (Mason, 1971). Some of the earliest field studies were carried out by Nakaya and Terada in the 1930's. They measured the fall velocity of individual ice crystals observed on Mt. Tokati, Japan at temperatures between -8 and -15°C. The crystals were collected on a glass plate, photographed, and their linear dimensions were determined. The crystals were then melted and the drop diameters were measured, allowing the mass to be calculated. From this data, the relationship between the fall velocity and the dimensions of the crystals were determined. The interesting feature of these relationships is that the fall velocities of the plane dendritic, spatial dendritic, and powder

snow crystals were nearly independent of their dimenisions. It should be noted, however, that only medium to very large crystals were collected in this study. Therefore, the results do not necessarily apply to the early stages of crystal growth. Nakaya and Terada also determined relationships between the mass and maximum linear dimensions of the crystals.

Several early field experiments gave indications that the temperature and crystal habit were related (Mason, 1971). In the early 1900's Heim conducted observations in the Antarctic and Westmann on Spitzbergen. Both studies were among the first to relate temperature and crystal habit. During the period from 1930 and 1960, the field observations of Nakaya and his colleagues in Japan further revealed the temperature and habit relationships.

Field investigations have also shown the effects of supersaturation on crystal habit. In 1962 at Yellowstone Park, crystals growing at air temperatures of -30°C on grass stems near hot springs with a water temperature of +10°C were studied to determine the habit variations under high supersaturations (Hallett, 1965).

More recently, Auer and Veal (1970) have reported on their study of ice crystal dimensions in natural clouds. Crystals were collected from orographic and cumulus clouds at a mountain top observation station and their replicas were studied under a microscope.

All of the investigations mentioned thus far have one fact in common in that the ice crystals were collected near the ground. Therefore, only the growth characteristics of crystals just prior to ground impact were observed. We now know that the temperature at which the ice crystals grow is the controlling factor in habit development.

Obviously, except for the Yellowstone Park experiments, the temperature near the ground where the crystals were collected would only rarely be the temperature at which they grew. It wasn't until ice crystals were collected from their actual growth environment that definitive relationships between crystal habit and temperature were observed.

Several attempts have been made to study ice crystals in their natural growth environment (Mason, 1971). In the 1940's Weickmann conducted some of the first observations of ice crystals in natural clouds. Observations were made by aircraft, in the troposphere as high as the cirrus levels. Crystal habit variations in different cloud types, from nimbostratus in the lower troposphere to cirrostratus in the upper troposphere, were observed and compiled. Nearly ten years later, similar aircraft observations were made in Russia by Borovikov. His observations were very similar to those of Weickmann.

More recently, growth characteristics of crystals in natural clouds have been investigated by means of aircraft by Ono (1969 and 1970). Replicas of ice crystals sampled from clouds over southeast Australia at temperatures between -2 and -32°C were studied. Results for crystal habit variations with temperature were similar, but much more detailed, to those compiled earlier by Weickmann. Investigation was also made on the riming growth and crystal free fall characteristics.

Even though these studies of ice crystals collected from their growing environment were an improvement over the earlier ground based measurements, many disadvantages still existed. A major problem with measurements made from aircraft was the damage done to the crystals during the collection process. Even with the use of decelerator tubes to slow down the crystals before they were received on the collection

surface, it was impossible to entirely eliminate crystal damage. It was also impossible to determine what effects the airframe may have had upon the crystals before they were collected.

An attempt to eliminate these problems associated with aircraft measurements was made by Magono and Tazawa (1966). An instrument called a snow crystal sonde was designed. As it ascended through the clouds, ice crystals were collected undamaged. At the same time, a conventional radio-sonde was used to measure the temperature and humidity of the environment in which the crystals were collected.

A problem with these and all field investigations is the inability to control the conditions of the environment. Without this ability it is difficult to determine exactly the effect of the various environmental conditions upon the different growth parameters. It is also impossible to observe the entire life history of ice crystals. To bypass these pitfalls it is necessary to rely upon ice crystal growth studies in the laboratory where the natural cloud conditions are simulated as accurately as possible.

Laboratory Studies

Laboratory studies are usually of two general types. One type of study uses static methods to grow the crystals. With this approach, ice crystals are held stationary and grown on a flat surface or a fiber of various materials. The other type of study uses dynamic methods to grow the crystals. With this approach the crystals are either freely suspended in updrafts of supercooled fog or allowed to fall freely through it.

Static Chambers

One of the first chambers for investigating ice crystal growth in the laboratory was developed by Nakaya (1954). A fine rabbit hair, upon which crystals were grown, was stretched across an air-stream whose temperature and supersaturation could be varied. Despite the chamber's inability to maintain the temperature and supersaturation at constant values throughout the crystal growth period, relationships of air temperature and crystal habit similar to those observed earlier in the natural clouds were produced. Nakaya also observed dendritic growth at temperatures between -14 and -17°C, but only under relatively high supersaturations. Thus the first indication of a possible link between supersaturation and crystal habit was obtained.

In order to grow crystals under accurately controlled temperatures and supersaturations, Hallett and Mason (1958) developed a chamber. A nylon or glass fiber, upon which ice crystals were grown, was suspended vertically through the center of a vapor diffusion chamber. Capabilities of this chamber allowed crystals to be grown at temperatures from 0 to 50°C and supersaturations from a few per cent to approximately 300 per cent. Since the fiber had a temperature gradient along its length, it was possible to simultaneously grow several ice crystals at various temperatures and supersaturations. As a result, is was observed for the first time that the variations of crystal habit with temperature are characterized by sharp, well-defined boundaries. Hallett and Mason also observed closely the effects of supersaturation on crystal habit. They found that high supersaturation does not affect the basic crystal habit. However, it was observed that the supersaturation controls crystal shape development such as the transition from

prisms to needles and plates to dendrites. The unique design of their chamber also made it possible to study the effect of changing the temperature and supersaturation during the crystal growth process. They observed that when the environment of the growing crystal was changed it continued to grow but at the habit associated with the new temperature and supersaturation. Hallett and Mason also found that, in addition to the habit characteristics of crystals, there are zones of temperature where growth rates are higher than elsewhere. They observed that growth rate maxima occur between 0 to -2°C, -4 to -6°C, and -14 to -16°C.

Hallett (1965), using data collected by the static method, determined that the mass growth rate of a crystal at water saturation varies with temperature. A minimum occurs near -8°C while maxima are observed near -5 and -15°C.

Laboratory studies by Kobayashi (1961) used a similar apparatus to grow ice crystals on a fiber. He conducted measurements over a wide range of supersaturations in order to further refine the earlier observations made by Hallett and Mason (1958) concerning the effects of supersaturation on crystal habit.

Recently, laboratory experiments using the static methods were carried out to investigate, in addition to the habit variations with temperature and supersaturation, the actual mechanism responsible for this habit change. One such experiment was reported by Lamb and Hobbs (1971).

The static type chamber, used in all of the above discussed laboratory studies, is ideal for the investigation of the microscopic ice crystal growth mechanisms. However, since the crystals are held

static on a foreign material, the natural cloud conditions are not accurately simulated. Most important, however, is the inability, when using the static chambers, to measure the fall velocity of the crystals, and the associated effect on other growth parameters. To measure more accurately the crystal growth parameters under simulated natural conditions, the dynamic type chambers are necessary.

Dynamic Chambers

The first ice crystal growth studies conducted in the laboratory, though quite simple, were carried out in dynamic type chambers. These first studies, reported by aufm Kampe, et al. (1951) and Mason (1953), simply made use of artificially produced supercooled clouds in which ice crystals were nucleated, allowed to grow, and as they settled, collected on slides coated with Formvar solution. The clouds were produced by injecting steam into room-size cold chambers or smaller cold boxes in which the temperature could be controlled. The plastic replicas of ice crystals, produced by a process developed by Schaefer (1946), were examined under a microscope and photographed. Relationships between the growth temperature and crystal habit were determined. The habit sequence of plate, column, plate, column with decreasing temperatures was observed, which closely resembled the relationships observed in the natural environment. These early laboratory studies not only proved that natural ice crystal growth could be simulated in the laboratory, but also that more detailed and accurate results could be attained since growing conditions could be controlled.

When ice crystals grow in natural supercooled clouds, microphysical changes such as habit and dendritic developments occur as the

crystals fall relative to the cloudy air. There is evidence that crystals which fall with respect to the supercooled cloud show slightly different habit transitions than those grown under static conditions (Hallett, 1965). As the crystal falls, the local concentration of water vapor near the crystal surface is enhanced. Thus, the habit transitions dependent upon supersaturation, plates to dendrites and prisms to needles, occur at lower supersaturations.

As the ice crystals grow in the supercooled cloud, they develop fall velocities depending on their shape, size, mass, etc. Knowledge of the crystal fall velocity is essential in understanding the development of precipitation and the movement through the cloud. This knowledge is of particular importance in understanding the change in the growth mode of the crystal; i.e., from vapor diffusional growth to riming growth. Fukuta (1978) has shown that during vapor diffusional growth the crystal mass increase is proportional to $t^{1.5}$, where t is time, while during riming growth the crystal mass increase is proportional to t^{6}. This is shown graphically in Figure 1. Since fast fall velocities favor riming growth (Rogers, 1979), it is obvious why a clear understanding of this parameter is necessary.

Early laboratory studies attempting to determine the fall velocity of ice crystals were carried out by Jayaweera and Mason (1966) and Jayaweera and Cottis (1969). They investigated the fall behavior of steel, aluminum, and plastic cylinder and disc models, of various diameters in a viscous liquid. The results were used to estimate the terminal velocities of plate-like and columnar ice crystals. However, due to the complex habit and dendritic developments of actual ice crystals as they fall through the supercooled cloud environment,

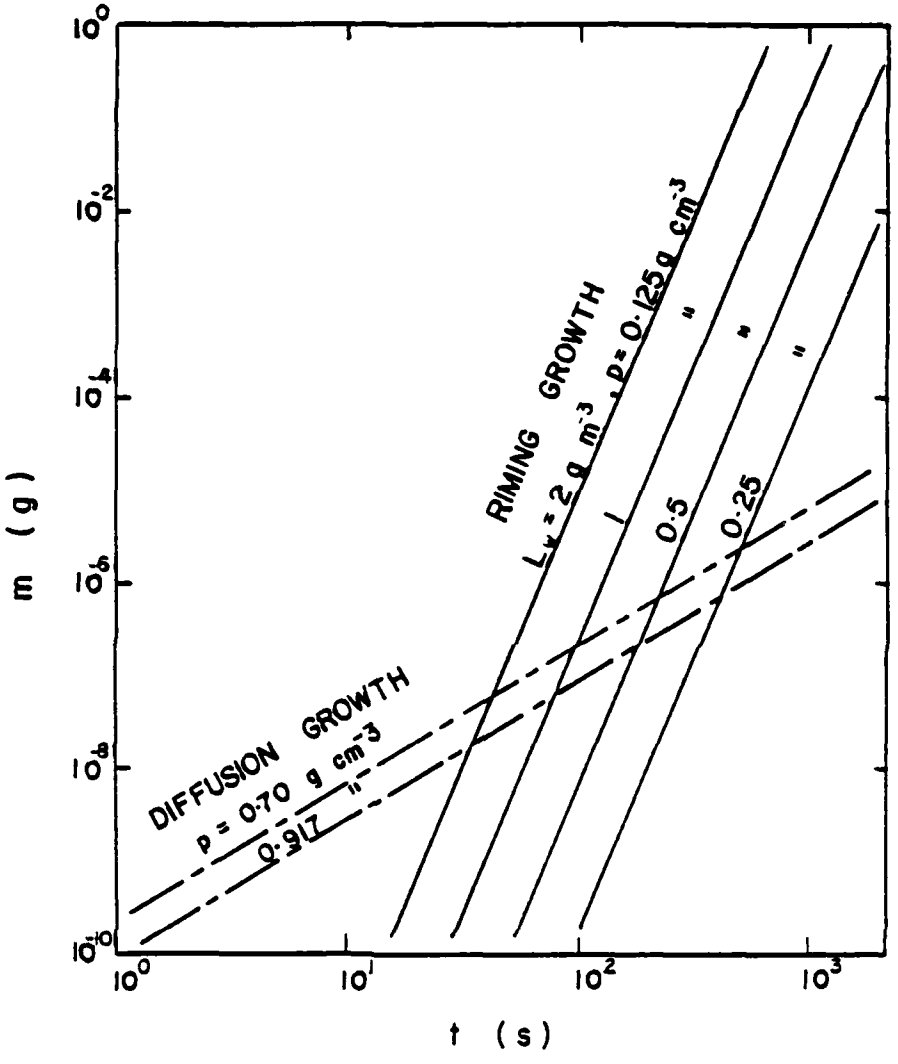

Figure 1. Relationship between the ice crystal mass m and the time t for vapor diffusion and riming growth (Fukuta et al., 1979).

calculations based on the behavior of simplified physical models are not necessarily applicable to natural crystals. As an ice crystal falls through a supercooled cloud, its shape, size, and mass change. These changes, in turn, continually affect the fall velcoity of the crystal. To completely understand the behavior of a dynamically changing ice crystal, it is preferable to simulataneously determine the size (in a- and c-directions), apparent density, mass and fall velocity of the crystal under conditions that accurately simulate the natural cloud conditions. The first attempt was made by Fukuta (1969).

The experimental apparatus used by Fukuta, shown in Figure 2, was the first generation of apparatus used to simultaneously determine the above parameters. The apparatus consisted of a Plexiglass double-walled chamber with inside dimensions of 9.6 cm × 9.6 cm × 61.5 cm and outside dimensions of 15.5 cm × 15.5 cm × 61.5 cm. The chamber was chilled by coolant circulated between inner and outer wall at a predetermined temperature. Placed on top of the main chamber was a cooled copper chamber with inside dimensions of 10.5 × 10.5 cm × 50.5 cm and outside dimensions of 14 cm × 14 cm × 50.5 cm. Moisture was supplied by warmed water in a semipermeable membrane at the top of the copper chamber. The fog temperature was continuously measured by two thermocouples and recorded on a strip chart recorder. The supercooled fog was seeded with ice crystals by insertion of a brass rod, chilled indirectly with dry ice, through a hole near the base of the copper chamber. As the crystals grew and fell through the main chamber, their fall velocity was measured by the chopped light method. A beam of light, chopped at a known time interval by a chopper, illuminated the bottom portion of the chamber through a slit in the wall. As the

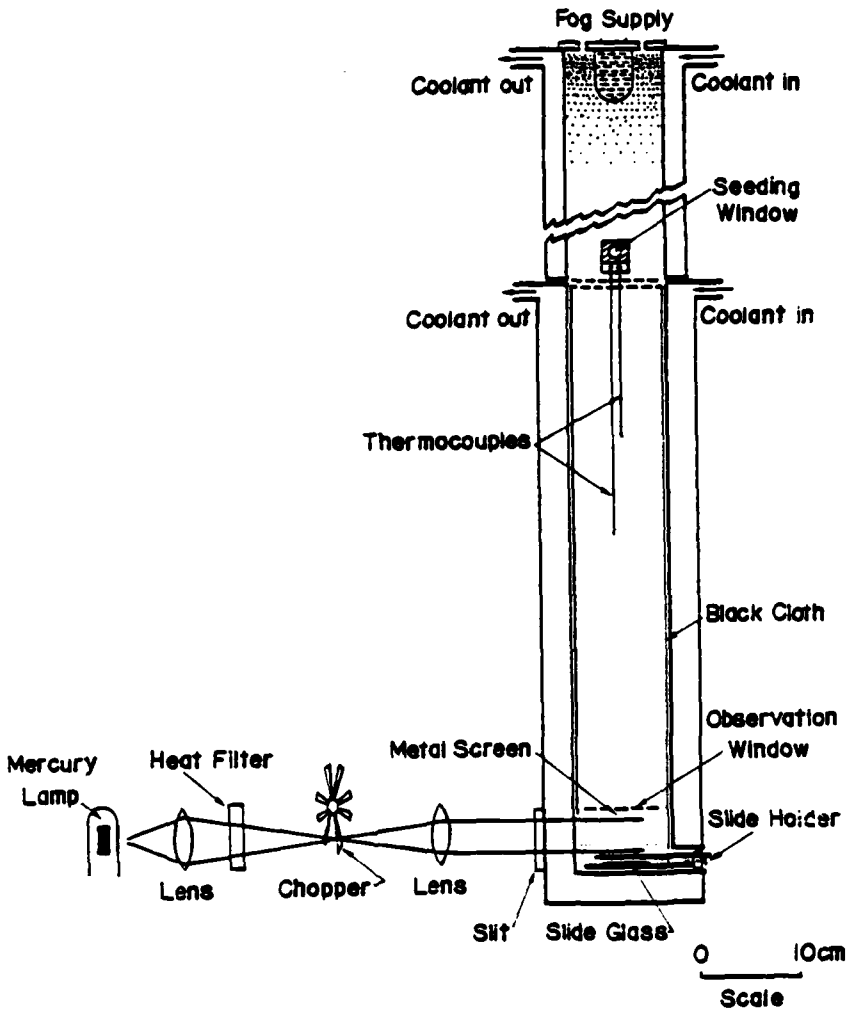

Figure 2. Experimental apparatus used by Fukuta (Fukuta, N., 1969: Experimental studies on the growth of small ice crystals. J. Atmos. Sci., 26, 522-531.

crystals fell through the light, they were photographed. The resulting photographed light streaks, when measured, indicated the crystals' fall velocity. As the falling crystals reached the bottom of the chamber, they were collected on a glass slide coated with chilled silicone oil. A cover slide coated also with silicone oil was placed over the crystals and a photomicrograph was taken. Since the silicone oil used was denser than the ice, the crystals would slowly rise to the cover slide. Therefore, it was necessary to photograph the crystals as quickly as possible after collection. However, this method proved superior to the previously used Formvar replicas, the crystals being photographed in greater detail and mass determination being more accurate. From the photomicrograph, the crystal dimensions were determined. The crystals were then melted by heating the cover slide. By measuring the diameter of the resulting droplets, the crystal mass was determined. From the photomicrographs the crystal habit relationship with the growth temperature was investigated. The habit sequence of plate, column, plate, column agreed closely with that observed by aufm Kampe et al. (1951) and Mason (1953). The a-axis and c-axis dimensions were measured from the photomicrographs (see Figure 3). The crossovers in the figure clearly show the temperatures at which the habit change occurred.

From the values of crystal mass, determined by measuring the diameter of the melted crystal, Fukuta analyzed the relationship between crystal mass and temperature for constant growth times (Figure 4). The general relationships found were similar to those reported by Hallett (1965), from his static chamber measurements. Fukuta divided the crystal mass by the apparent volume of the ice crystal which

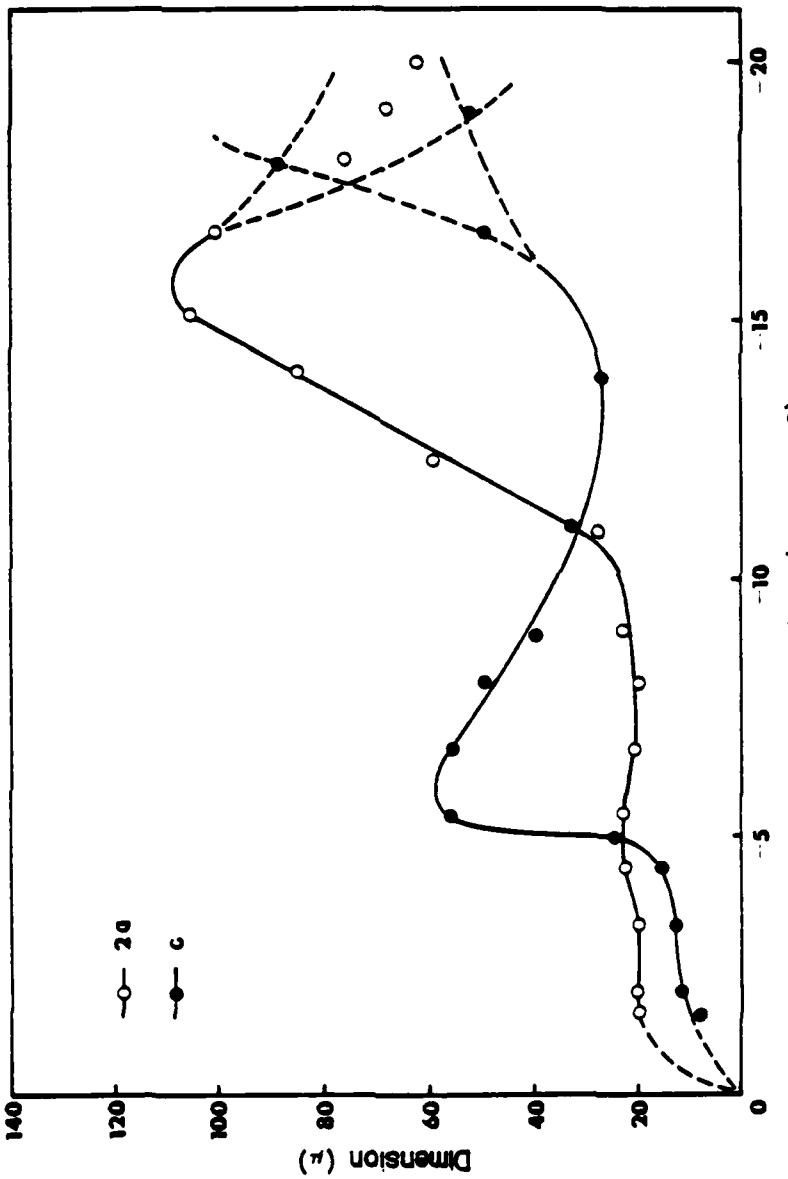

Figure 3. Ice crystal dimensions plotted as a function of temperature T (Fukuta, 1969; see page 13).

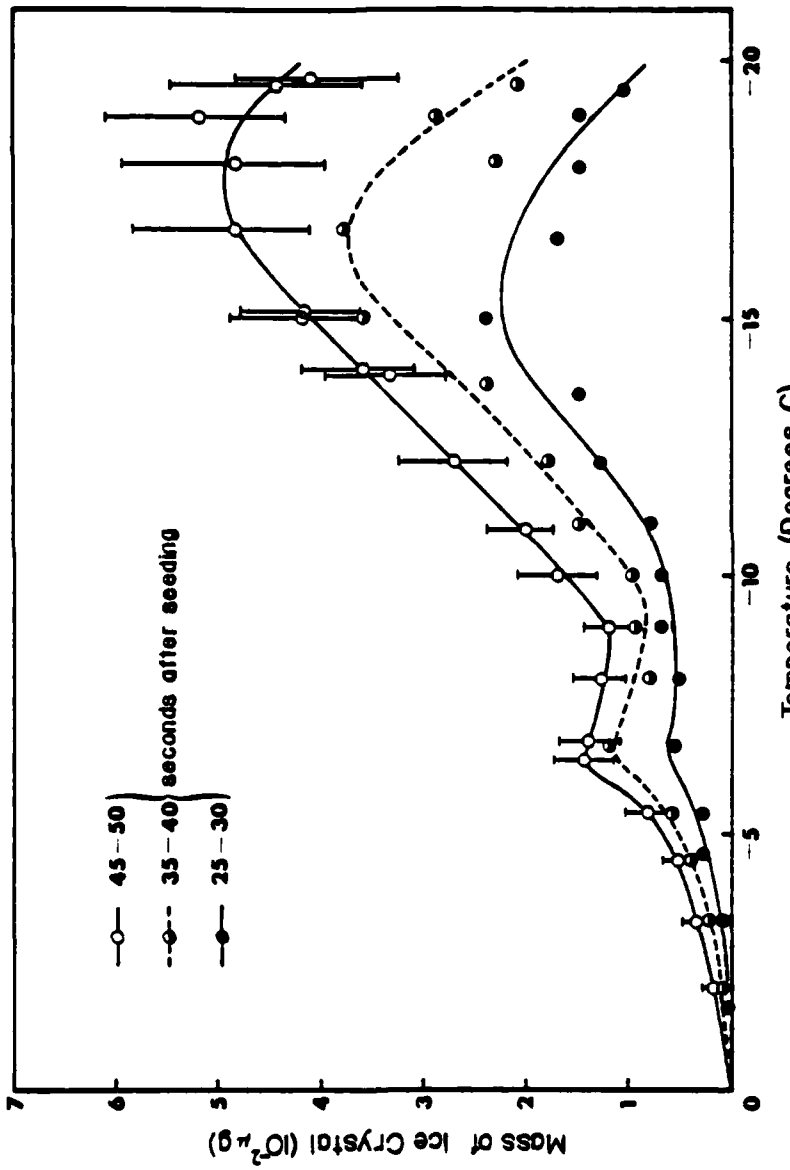

Figure 4. Ice crystal mass plotted as a function of temperature for various growth periods from 25 to 50 seconds (Fukuta, 1969; see page 13).

yielded an estimate of the crystal apparent density (Figure 5). Of particular interest is the coincidence of the crystal mass maxima and the apparent density minima. This clearly suggests the advantage of the spatial form of ice in the vapor diffusional growth.

From his crystal fall velocity measurements, Fukuta obtained the following two relationships. Figure 6 shows the relationships of crystal fall velocity with respect to the temperature of the growth environment after a set period of growth time. Two fall velocity plateaus, one from -5 to -8°C and the second from -10 to -18°C, were observed. An interesting observation was the fact that a fall velocity maximum did not necessarily coincide with an observed mass maximum as might be expected. Figure 7 shows the relationship he obtained between crystal fall velocity and the time after seeding at different temperatures. It was found that for periods up to approximately 20 seconds after seeding, all crystals had nearly the same fall velocity, regardless of the temperature of their environment. This indicated that the factor, or factors, controlling the fall velocity profile of a crystal did not begin to vary with temperature significantly until after approximately 20 seconds. During the first few seconds of growth the ice crystal habit apparently did not become well developed and the a-axis and c-axis dimensions were nearly equal. It appeared from the study that the crystal shape variation and the resultant change in aerodynamic fall characteristics were controlling factors in the variation of the crystal fall velocity.

This experimental technique worked quite well in simultaneously determining the crystal fall velocity, mass, apparent density, and habit and provided much valuable data. However, since the technique

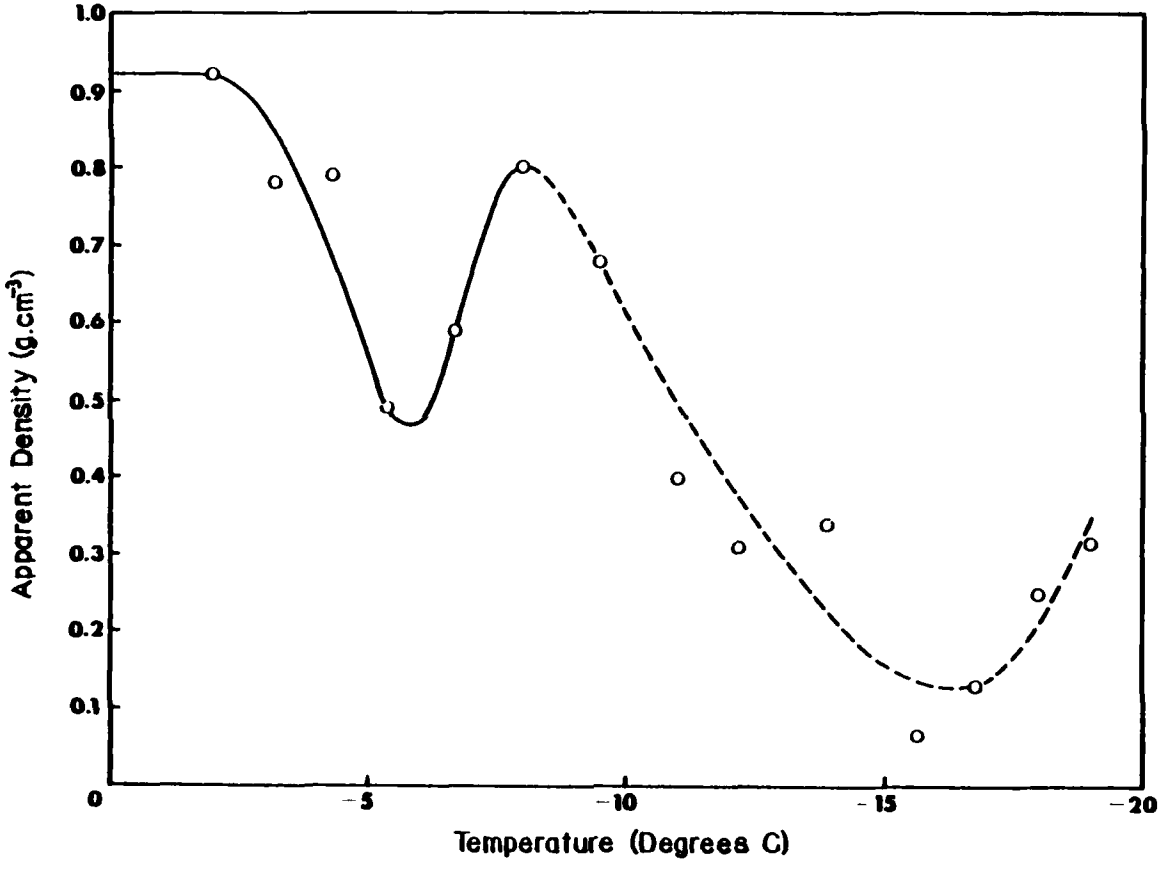

Figure 5. Ice crystal apparent density plotted as a function of temperature for growth period of 45 - 50 seconds (Fukuta, 1969; see page 13).

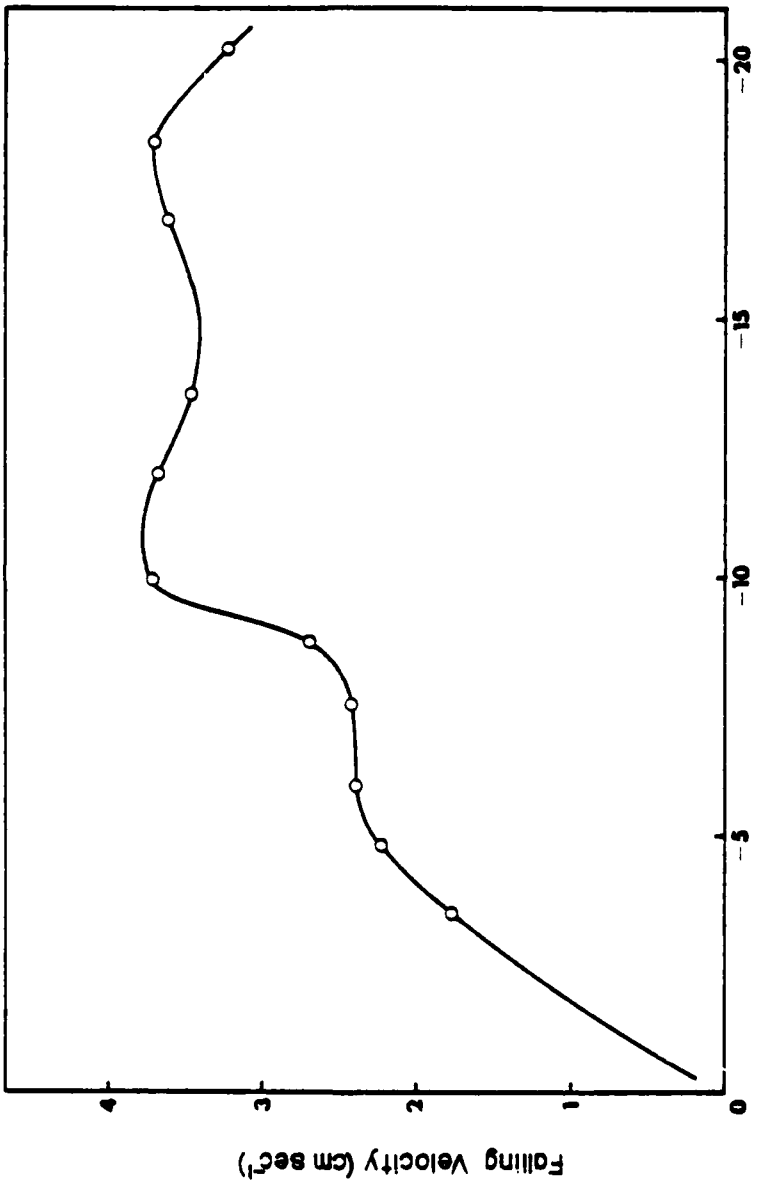

Figure 6. Ice crystal fall velocity plotted as a function of temperature for growth period of 40 - 45 seconds (Fukuta, 1969; see page 13).

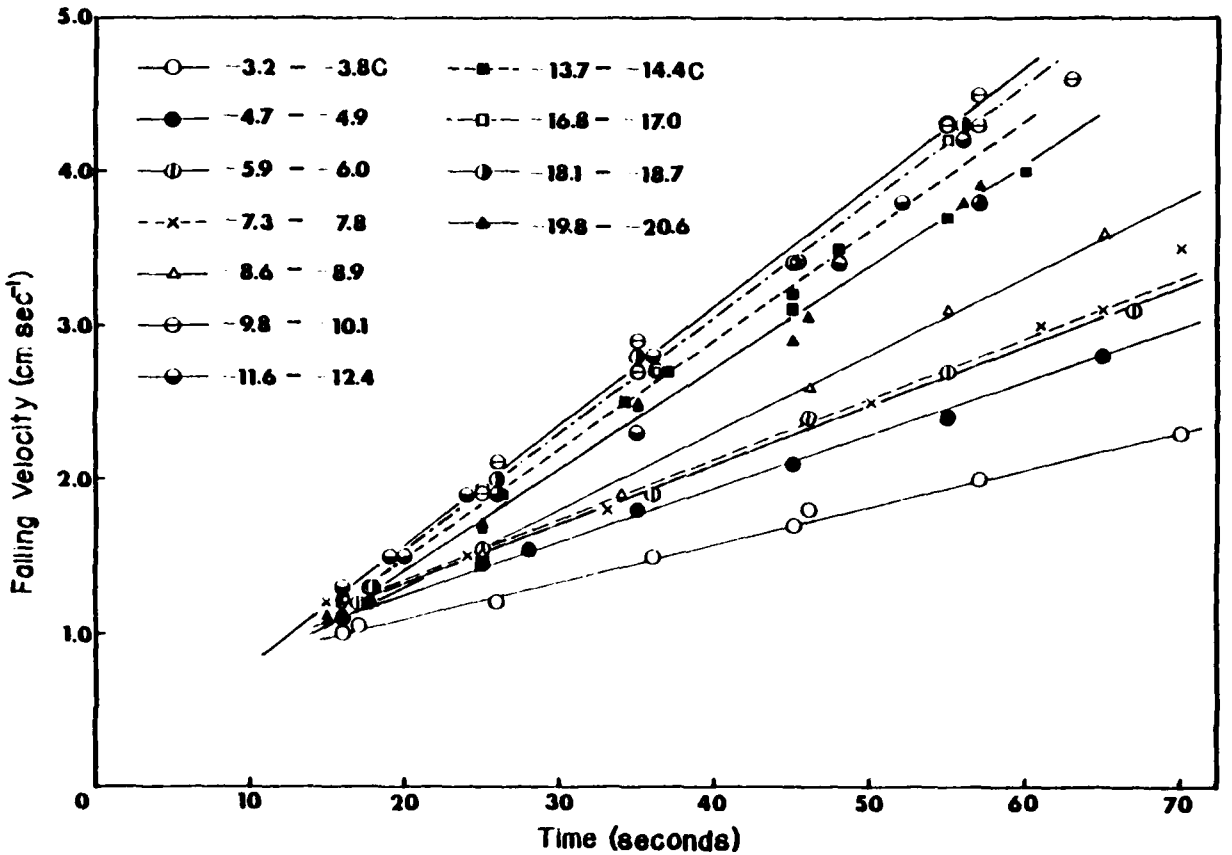

Figure 7. Ice crystal fall velocity plotted as a function of time at different temperatures from -3.2 to -20.6°C (Fukuta, 1969; see page 13).

could only permit ice crystal growth for up to 1 minute after seeding, further studies were badly needed that could grow the crystals in freely suspended conditions for longer periods of time.

Using a larger chamber, the growth rates and densities of freely falling ice crystals at temperatures between -5 and -9°C as a function of time, for periods up to 3 minutes, were measured by Ryan et al. (1974) and for temperatures between -3 and -21°C by Ryan et al. (1976). Michaeli and Gallily (1976) measured the mass growth rates of freely falling ice crystals between -1 and -20°C as a function of time for growth times of 60 and 100 seconds. Unfortunately, in all three of these studies, crystal fall velocity measurements were not carried out, making the data incomplete. It wasn't until Fukuta et al. (1979) freely suspended ice crystals in a simple wind tunnel that Fukuta's 1969 data was extended to longer periods of time.

Various types of vertical wind tunnels have been used in the study of cloud physics since the middle to late 1940's. Vertical tunnels were used for hail growth studies by Macklin (1961). In these tunnels, however, the hailstones were not freely suspended in the air flow. Instead, the stones were held in a stationary position within the air flow by mechanical means. Other tunnels were used to study the behavior and growth of water drops freely suspended in the air flow (Telford, 1955; Kinzer and Gunn, 1951; Kinzer and Cobb, 1956 and 1958). All of these tunnels, however, were incapable of maintaining the conditions of natural clouds for other than relatively short periods of time. This goal was accomplished in a cloud tunnel designed and constructed at the University of California at Los Angeles (U.C.L.A.) (Pruppacher and Neiburger, 1968). Several studies using this U.C.L.A. tunnel

(Beard and Pruppacher, 1969 and 1970) have been carried out to investigate such topics as fall velocity characteristics, behavior during free fall, and collection efficiencies of small water droplets. The U.C.L.A. tunnel, upon modification for use at temperatures below 0°C, was also used for several studies (Pitter and Pruppacher, 1973; Pflaum et al., 1978; Pflaum and Pruppacher, 1979) investigating the freezing threshold and behavior of freely falling water drops and the growth and fall velocity behavior of freely falling graupel. In a similar vertical wind tunnel at the University of Nevada (Hoffer and Mallen, 1968 and 1970), water droplets were freely suspended in the air stream in order to study their freezing properties under conditions simulating the natural atmosphere and their evaporation rates. Another vertical wind tunnel, designed and constructed at the University of Toronto (Iribarne and Klemes, 1970), was used to suspend water droplets and study the electrical effects associated with the breakup of the droplets in free fall.

It should be noted that the above wind tunnels were used only to suspend relatively heavy precipitation elements. The flow speeds produced in these tunnels in order to suspend these heavier precipitation elements make the tunnels unsuitable for suspending much lighter ice crystals. The simple tunnel used by Fukuta et al. (1979) was one of the first used to freely suspend small ice crystals.

The L-shaped tunenl used by Fukuta et al is illustrated in Figure 8. The tunnel, constructed of Masonite, was operated in a walk-in cold room. The vertical section of the tunnel was approximately 2 m high, while the horizontal section was 2.5 m long. The tunnel cross-section (dimensions: 0.5 m × 0.5 m) was the same in both the horizontal

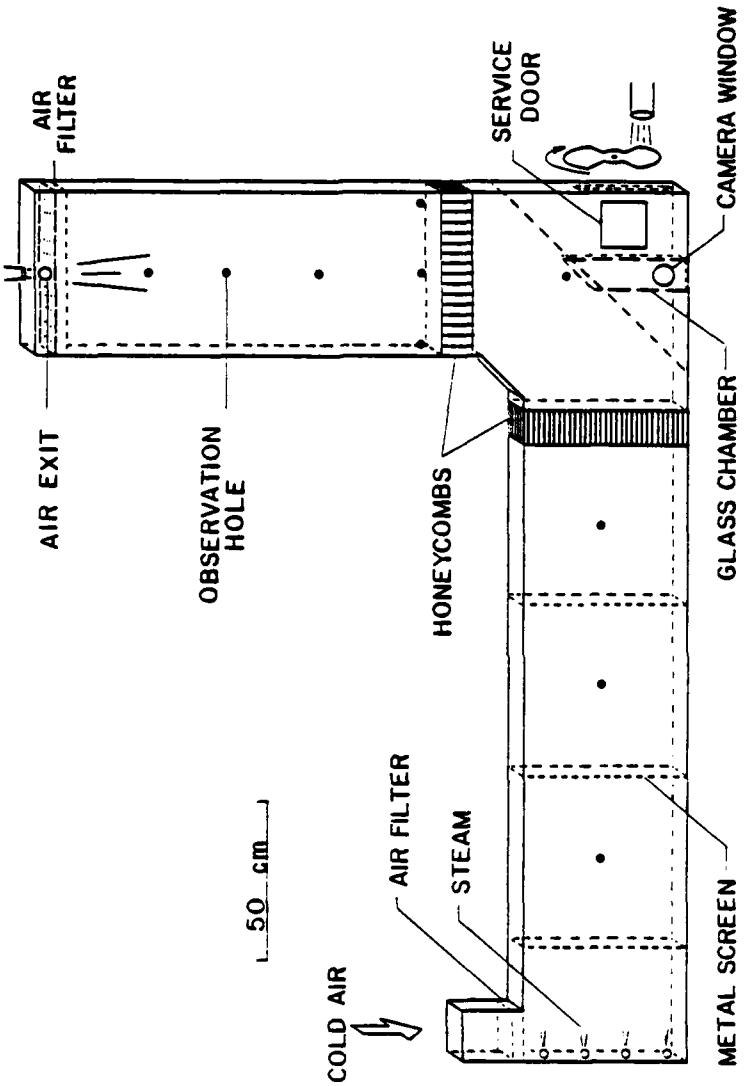

Figure 8. The L-shaped supercooled cloud tunnel used by Fukuta et al. (1979).

and vertical sections. In order to reduce turbulence within the tunnel, metal screens and honeycombs were used. Air from the cold room was introduced into the tunnel through an air filter at the left end of the horizontal section. At that point, steam, produced in a pressure cooker heated on a hot plate, was injected into the cold air to produce a supercooled fog. The supercooled fog was pulled through the tunnel by a small vacuum cleaner attached at the top of the vertical section of the tunnel. The temperature of the supercooled fog was measured by a thermometer inserted into the tunnel through holes along the length of the horizontal and vertical sections. Illumination of the tunnel interior was accomplished by a microscope lamp directed down through the center of the vertical section through an opening in the top of the vertical section. Ice crystals, generated in a pre-seeding chamber, were injected in known quantity into the tunnel near the bottom of the vertical section. The vertical velocity of the supercooled fog, adjusted by means of a variac on the vacuum cleaner motor and a leak valve in the suction line, was set at a speed just adequate to freely suspend the ice crystals in the vertical section of the tunnel. As the crystals grew and their fall velcotiy increased, the suction was increased in order to keep the crystals suspended. At the end of the desired period of time (up to 3 minutes), the suction was shut off and the crystals allowed to fall through a glass chamber in the bottom of the vertical section. The fall velocity of the crystals was measured by photographing them under a chopped light beam as they fell through the glass chamber. A new method for crystal collection and study under a microscope was used. The crystals were collected on a slide glass with a depression which is filled with silicone oil. A cover glass

coated with motor oil was then placed over the slide glass with the crystal. The crystal remained at the interface of the two oils for indefinite periods of time since it was denser than the motor oil and less dense than the silicone oil. Upon melting, the formed droplet remained at the interface. With this improved method of preserving the ice crystals, photomicrographs were more easily taken than in earlier studies.

From the photomicrographs, the variation of crystal habit with growth temperature was examined. At temperatures between -13 and -19°C double plates and vaned plates were observed. Various crystal nucleating agents were used and in each case the double and vaned plates were observed. This observation of double and vaned plates agreed quite well with the findings of Fukuta (1968) during his studies of the use of "vapor activated" metaldehyde as an ice nucleation agent. At other temperatures the familiar crystal habits found in the earlier studies were also confirmed.

From the photomicrographs, the ice crystal mass was determined. Figure 9 shows the relationship between the crystal mass and growth temperature. Of particular significance is the minimum at -10°C and the maxima at -7 and -15°C. These results agreed well with those of Fukuta (1969) and reasonably well with those of Ryan et al. (1974 and 1976) and Hallett (1965). Since no indications of crystal riming were observed, it was presumed that the mechanism of growth for the crystals was vapor diffusion.

From the crystal fall velocity measurements the relationship between fall velocity and growth temperature was investigated (Figure 10). Several significant relationships between crystal shape, growth

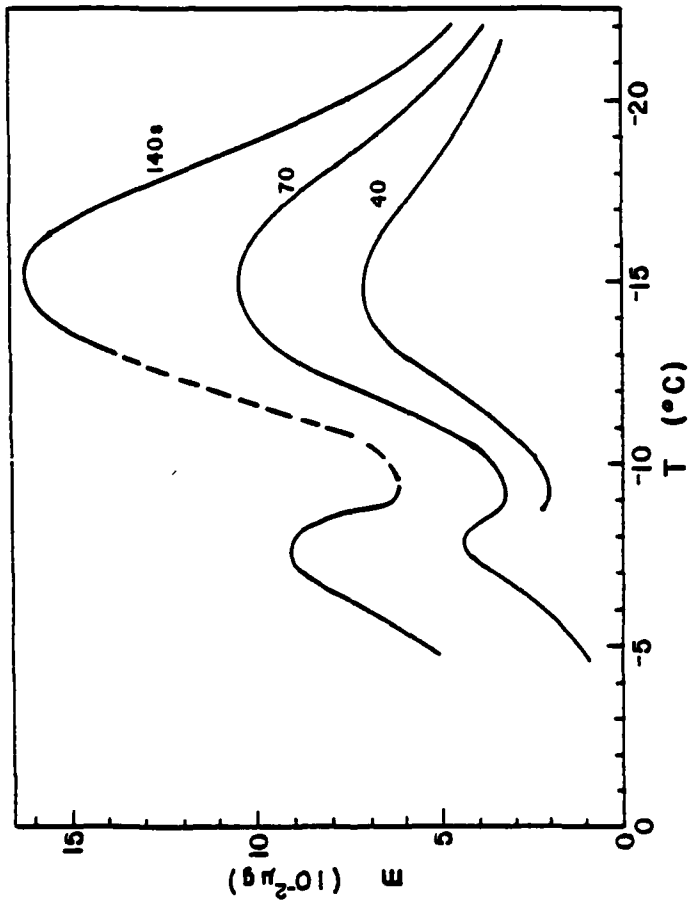

Figure 9. Ice crystal mass m plotted as a function of temperature T for growth periods of 40, 70, and 140 seconds (Fukuta et al., 1979).

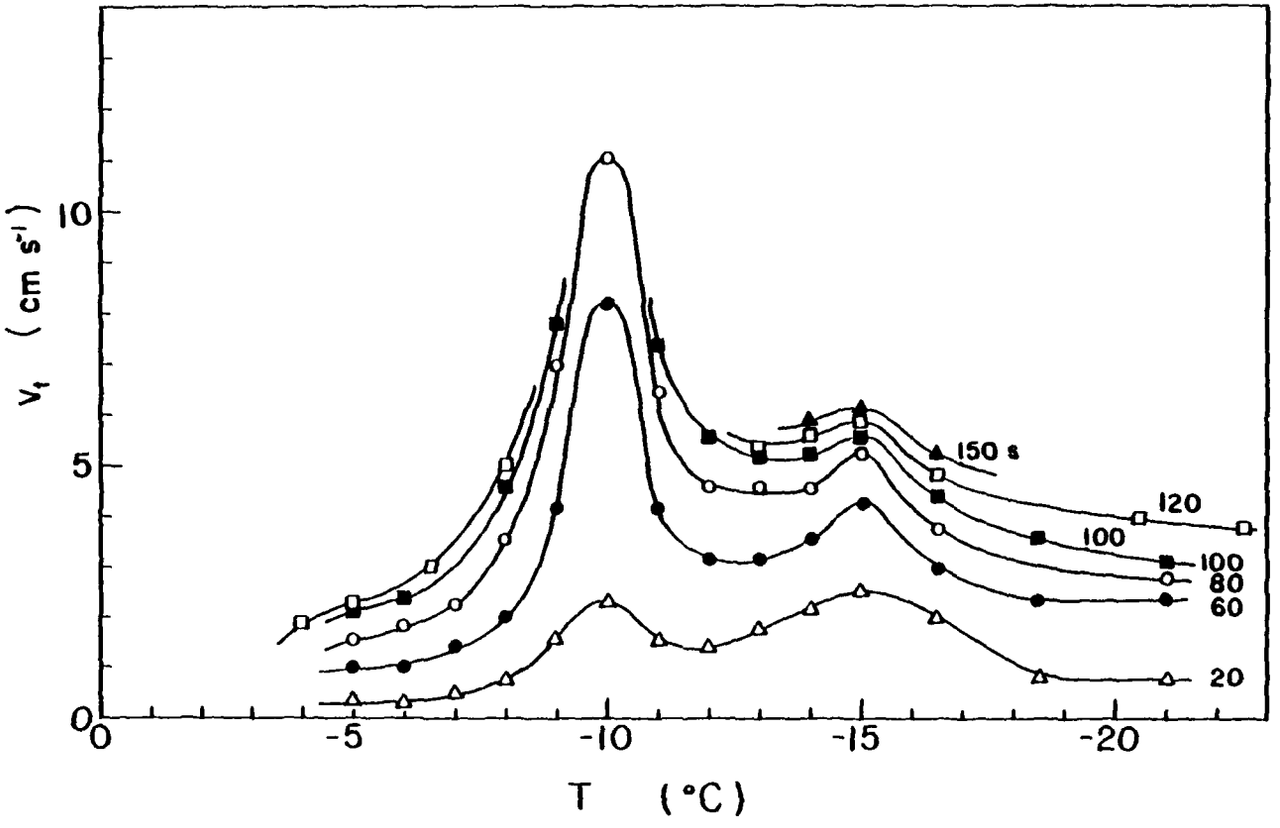

Figure 10. Ice crystal fall velocity V_t plotted as a function of temperature T for various growth times between 20 and 150 seconds (Fukuta et al., 1979).

mechanism and fall velocity are evident in this figure. Since ice crystal habit is not well developed early in the growth process, the 2a/c axial ratio is near unity and the crystal fall velocity is not significantly affected by aerodynamic drag. Since the rate of increase in size of the crystal is proportional to the total vapor flux arriving at the crystal surface and the vapor flux is greatest at around -15°C, the crystal mass increases most rapidly at -15°C during the initial period of growth. This explains why, for growth periods of up to 20 seconds, the fall velocity is greatest at -15°C. In this early stage of growth, the crystal mass appears to be a primary factor controlling the crystal fall velocity. As the crystal continues to grow by vapor diffusion, it begins to develop shape and habit. A falling crystal that develops a shape well spread in space (plate, dendrite, or needle) becomes significantly influenced by aerodynamic resistance. Crystals growing at temperatures around -10°C have a 2a/c axial ratio near unity since this is the temperature zone where the switch-over of habit occurs from column to plate as the temperature lowers. Therefore, the shapes of crystals growing in this temperature zone are near spherical, the shape which provides the minimum aerodynamic resistance. This explains why for growth periods beyond 20 seconds, the fall velocity of a crystal at -10°C becomes faster than crystals at other temperatures. After habit development begins, the aerodynamic drag of a crystal becomes an increasingly dominant factor in interfering with fall velocity development.

After determining the apparent density of the crystal, its relationship with crystal growth temperature was investigated (Figure 11). Of particular significance is the marked apparent density peak

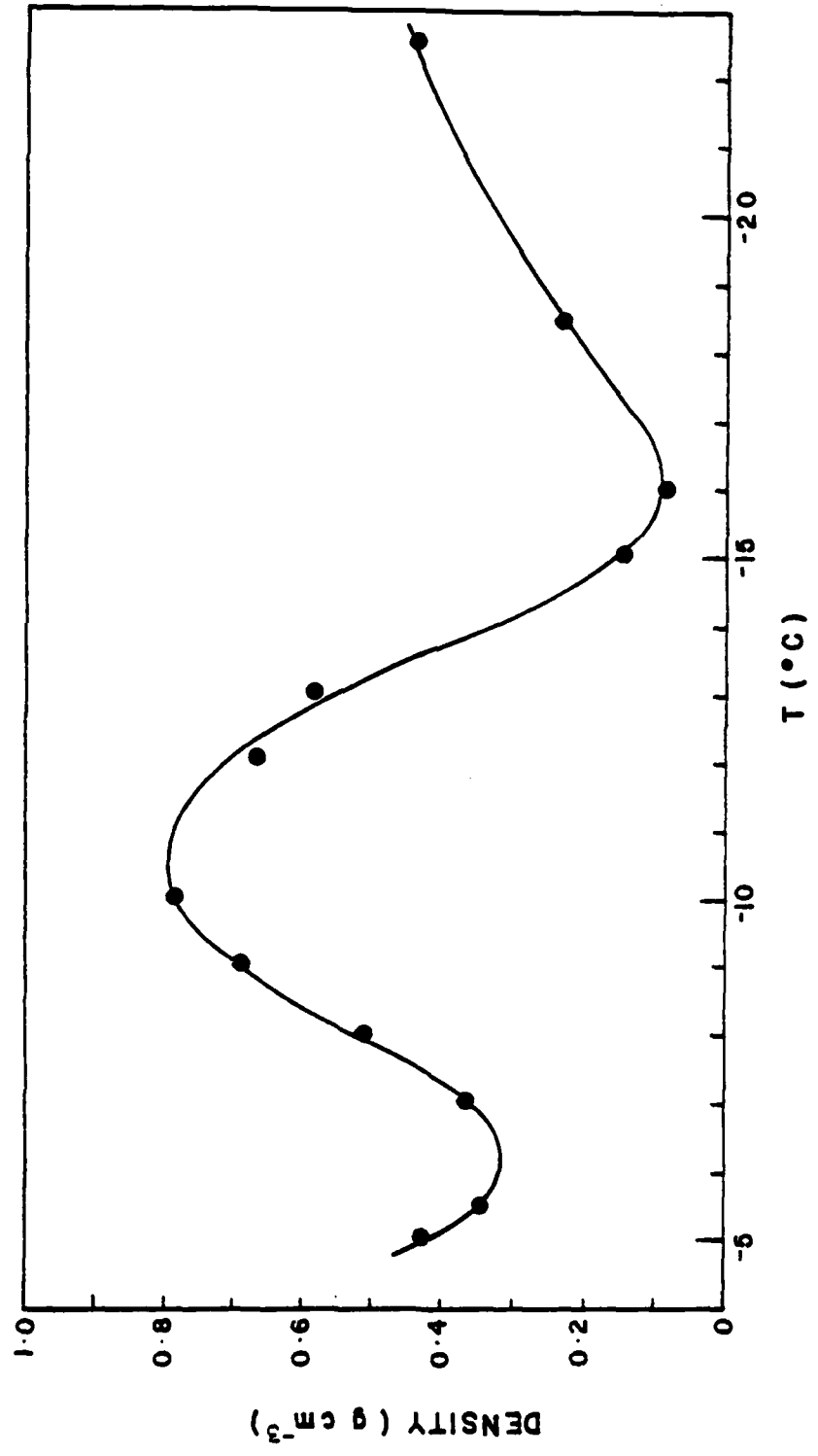

Figure 11. Ice crystal apparent density plotted as a function of temperature T (Fukuta et al., 1979).

near -10°C, the temperature of maximum fall velocity. This in turn demonstrates the importance of the spatial form of the crystal in determining its fall velocity development.

This supercooled cloud tunnel represented the second generation of apparatus capable of simultaneously determining the fall velocity, shape, size, mass, and apparent density of an ice crystal. The major advantage of this tunnel was its capability to extend the period that ice crystals could be freely suspended in a supercooled cloud for as long a period as 3 minutes. However, disadvantages still existed. It was very difficult, with the pressure cooker used in the manner described above, to maintain the amount of steam injected into the tunnel at a constant level. This induced a problem of controlling the liquid water content of the supercooled fog, an important parameter in determining the growth characteristics of a crystal. Also, due to the short distance between the point of steam injection into the tunnel and the vertical section of the tunnel, with only the horizontal section of the tunnel in between them, it was difficult to make the supercooled fog homogeneous with respect to temperature and droplet concentration at the point where the ice crystals were suspended. In addition, due to the fixed and large cross-sectional area of the tunnel and the limits of the amount of suction obtainable from the vacuum cleaner, it was impossible to suspend the ice crystals falling faster than about 12 cm/s. Also due to the constant cross-sectional area of the tunnel, it was difficult to stabilize the crystals in the horizontal and vertical directions within the vertical section of the tunnel. It wasn't until the apparatus used in the present study was constructed that these difficulties were eliminated.

Chapter 3

APPARATUS

The objective of this study was to design and construct an apparatus capable of freely suspending an ice crystal in a supercooled cloud for extended periods of time and conduct measurements. From the collected data, simultaneous determination of ice crystal size, shape, mass, apparent density, and fall velocity, as a function of time and temperature, was to be made.

Factors Considered in the Apparatus Design

As shown in the previous chapter, the most common and reliable method for freely suspending precipitation elements in the laboratory for extended periods of time is the vertical wind tunnel. Several factors were considered in the design of the vertical wind tunnel used in the current study to freely suspend ice crystals in a supercooled fog for indefinite periods of time.

In order to suspend an ice crystal in the working/observation section of the vertical wind tunnel, a capability is needed to hold the crystal in essentially a fixed position for extended periods of time. To make this possible, it is necessary to provide a position of vertical as well as horizontal stability within the tunnel. A laminar flow is necessary to achieve this stability. Therefore, a method must be developed to suppress the turbulence within the tunnel working section.

Since visual tracking of the ice crystal is necessary to position and hold it in the zone of stability, the observation section of the tunnel must be, at least partially, constructed of a transparent material. In addition, for tracking of the ice crystal in this manner, proper illumination must be provided to make all sizes of crystals clearly visible.

In order to position and maintain the crystal at its point of stability within the working/observation section, it is necessary to adjust the flow speed through the chamber. While the crystal is being suspended in the supercooled fog environment, it grows and becomes heavier. Therefore, as the crystal grows and becomes heavier, the flow through the tunnel must be gradually increased to keep the crystal from "falling out." Accordingly, a method must be used that will allow for convenient and continuous adjustment of the flow speed through the tunnel. When the crystal is held at a fixed position within the tunnel, the flow speed at that point equals the fall velocity of the crystal. Therefore, in order to determine the crystal fall velocity, a method must be employed to measure the flow speed within the tunnel. A continuous record of the velocity during the entire crystal growth period is desirable for the post experimental data analysis.

To produce the supercooled cloud within the tunnel, a continuous source of moisture is needed. In order to keep the liquid water content of the supercooled cloud constant during each experiment, two design considerations are necessary. First, a method must be developed by which the amount of moisture from the source can be controlled and held constant. Second, the amount of moisture per unit volume of air passing through the tunnel working/observation section must remain

constant, at least with respect to time. As the amount of flow through the observation section changes, the amount of moisture passed through the section must be proportionally adjusted. In addition, as the supercooled fog passes through the working/observation section, it must be homogeneous with respect to temperature and droplet concentration. A method must be developed to assure this condition is sustained.

One of the aims of the present study is to grow ice crystals at varying temperatures between -3 to -25°C. Therefore, a method is necessary that will cool and maintain the tunnel at any desired temperature in this range. Since the crystal habit is dependent upon the ambient air temperature surrounding the crystal at that moment, the air temperature within the tunnel must be maintained as stable as possible during the entire period of each crystal growth experiment. Due to the importance of the ambient air temperature stability in the crystal growth environment, an accurate method of measuring the temperature must be used. In addition, since the temperature has to remain nearly constant throughout each experiment, a method of continuous temperature recording that also allows constant monitoring is advantageous. The continuous record of the temperature during the entire crystal growth period will aid in the post experimental data analysis.

It has been shown that when two ice crystals growing in a supercooled cloud are in very close proximity to each other, they compete for the available moisture. Due to this competition for moisture, neither crystal will show its true growth characteristics at water saturation. Since direct seeding of the supercooled fog within the tunnel could result in large numbers of ice crystals, the method is likely to induce competition for moisture among the crystals. Therefore, a

method of ice crystal seeding by which the number of crystals can be accurately controlled has to be devised. The method of ice crystal nucleation is also an important consideration. When using heterogeneous nucleation techniques, a possibility exists that contamination from the seeding material may occur in addition to formation of complex crystals. In this study, only the growth behavior of pure ice crystals is intended. Therefore, some form of homogeneous nucleation is desirable in order to eliminate possible effects of the various nucleants used in heterogeneous nucleation.

After growing an ice crystal for the desired length of time, it is necessary to remove the crystal from the tunnel so that photomicrographs can be made. The method used must assure that the ice crystal is collected undamaged and that no melting, evaporation, or growth has taken place after the end of the experiment and before collection on the microscope slide.

The method of preserving the ice crystals for examination and photographing under the microscope is of critical importance. Several methods have been used in past studies (Schaefer, 1941, 1949 and 1962; Smith-Johansen, 1965; Bigg, 1953; Fukuta, 1969). Each of these methods, however, had certain disadvantages. The methods used by Schaefer and Smith-Johansen produced replicas of the ice crystals instead of preserving the original crystals. Therefore, mass determination was not accurate, some crystal details were lost, and the crystals could not be viewed from the side. The method used by Bigg was originally intended for ice nucleation studies at the interface between two water-immiscible and mutually immiscible liquids, one lighter and the other heavier than water. But when applied for the present purpose, the side

side view position of an ice crystal cannot be stably maintained. The limitations of Fukuta's 1969 method were discussed earlier. Several improvements of these methods are necessary for the current study. The method used in this study is a modified version of that used by Fukuta et al. (1979). The ice crystal must be received between the microscope slide and cover glass and kept there for extended periods of time without coming in contact with either. The crystal must maintain its original shape, size, and detailed structure while being kept between the cover glass and slide. In order to facilitate the determination of crystal mass, the water droplet resulting from melting the ice crystal must remain between the slide and cover glass without coming in contact with either. If they come in contact with each other, the droplet loses its exact spherical identity. Also, in order to accurately measure both the a- and c-axis of the ice crystal, it is desirable to rotate the crystal. This allows the crystal to be viewed and photographed from both the top and side.

The apparatus designed for and used in this study satisfies all of the above requirements. The vertical wind tunnel is designed with four primary sections, i.e., the fog chamber, the honeycomb section, the working/observation section, and the suction section. Support equipment for the tunnel includes the ice crystal generation chamber, the steam generator, the suction system, the crystal sampling device, the microscope, and the data recorder.

Final Design and Construction

The wind tunnel was constructed entirely in our laboratory and was made of 3.18 mm thick clear acrylic sheets. The acrylic was

selected because of its transparency, reasonable strength, light weight, and ease of fabrication. The acrylic was easily cut to the desired pattern by a sabre saw and the pieces easily bonded together by using an acrylic solvent, ethylene or methylene dichloride. At locations where the connected acrylic pieces were subjected to a great deal of force, a solution of acrylic resin in ethylene dichloride was applied instead. In constructing the fog chamber section, large sheets of acrylic were required. Aluminum corner brackets were used to connect these larger sheets and provided the necessary support to keep the chamber upright. The four tunnel sections, constructed separately, were connected together by using 6.35 mm thick acrylic sheet flanges plus nuts and bolts (Figure 12(a)). By constructing the tunnel entirely of the acrylic and by using acrylic flanges to connect the sections and acrylic solvent and solution to bond the various pieces, the entire tunnel assembly contracts and expands at the same rate with varying temperature, avoiding undesirable structural failure.

The tunnel is placed in an environmental walk-in cold room in our laboratory. This walk-in cold room has dimensions of 3.3 m × 2.7 m × 2.3 m and is capable of reaching temperatures as low as -25°C.

Figures 12(b) and 13 show the basic tunnel. The various sections and support equipment will be discussed in detail in the following sections.

Fog Chamber

The fog chamber is 1.22 m long, 1.55 m high, and 0.47 m wide. Three shelves are used to divide the chamber into four sections. A photograph of the fog chamber is shown in Figure. 14(a).

Figure 12(a). Photograph of connection flange.

(b). Photograph of entire supercooled cloud tunnel.

(a)

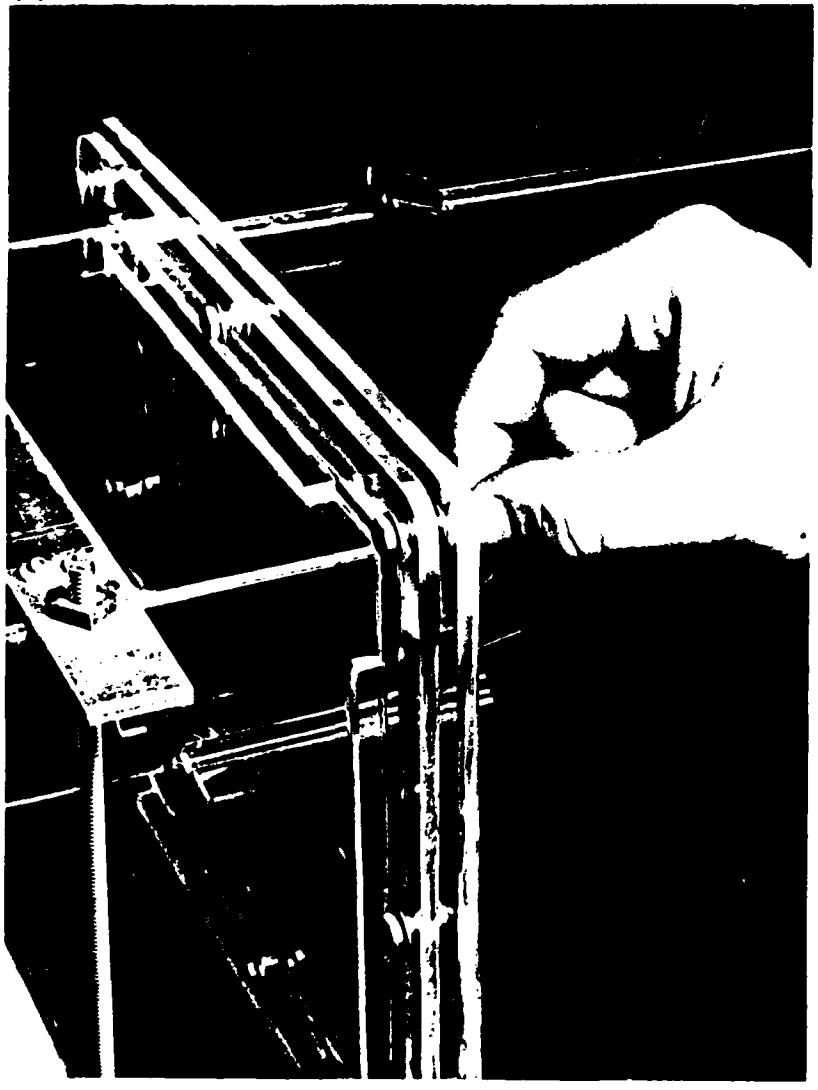

(b)

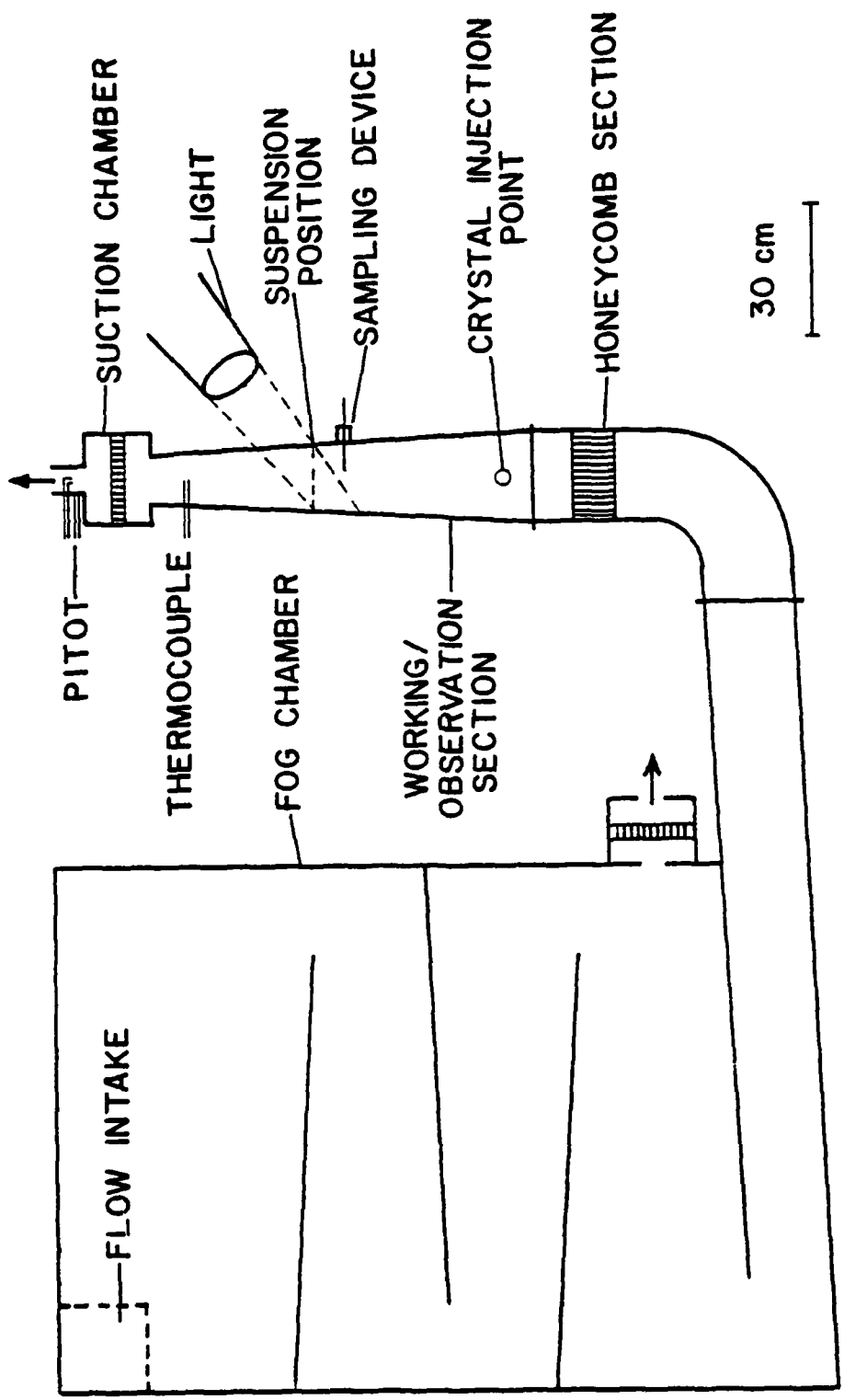

Figure 13. Diagram of the entire supercooled cloud tunnel.

Figure 14(a). Photograph of the fog chamber.

(b). Photograph of the honeycomb section.

(a)

(b)

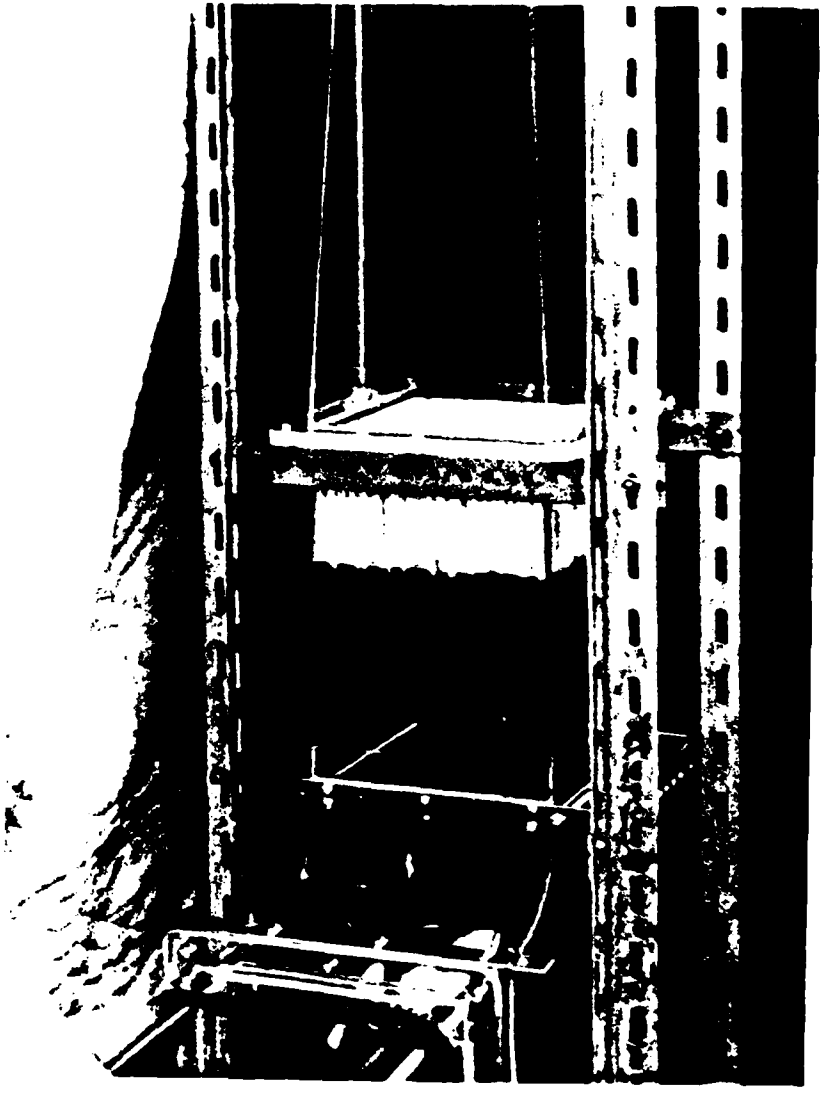

Cold room air is drawn into the chamber at the upper left rear corner. At the same point, steam is injected into the chamber producing a supercooled fog. Due to cold air and steam introduction, there is a large amount of turbulence at the top of the chamber which helps to thoroughly mix the steam and cold air. As the supercooled fog passes from the top section to the lower sections, the turbulence dies down and the fog vertically stratifies. By the time the supercooled fog reaches the bottom section, it is well mixed and homogeneous with respect to both temperature and droplet concentration.

As the supercooled fog passes through the chamber, the inside walls begin to accumulate frost. This makes observation of the fog conditions inside the chamber difficult. To eliminate this problem, an automobile rear window heater was applied to the front wall of the chamber. The heater is connected to a variac in order to control the amount of heating provided by the heater. A maximum of 5 volts A.C. is applied to the heater, which results in adequate heating to stop the formation of frost.

Illumination of the inside of the fog chamber is accomplished by shining a 12 volt high intensity light through the side wall. To further aid in the viewing of the supercooled fog, a black cloth is hung across the outside of the chamber back wall.

Honeycomb Section

As the supercooled fog passes into the vertical portion of the tunnel, it must be as turbulence-free as possible. A common method of suppressing turbulence in wind tunnels is the application of honeycombs (Pankhurst and Holder, 1952).

The honeycomb used in this tunnel was constructed entirely in our laboratory. Plastic soda straws, with a diameter of 6 mm and a length of 10 cm, were placed in a frame made of 6.35 mm thick acrylic sheets. The frame, with dimensions of 20 cm × 20 cm × 10 cm, fits snuggly within the tunnel at a position near the bottom of the vertical portion. A photograph of the honeycomb section is shown in Figure 14(b).

As the supercooled fog passes through the honeycomb, frost begins to form after a certain period of time, depending upon the liquid water content of the fog. As the frost crystals grow at the expense of the supercooled fog, the amount of moisture passing into the working/observation section of the tunnel varies. To eliminate this problem, the honeycomb was made replaceable. An opening, slightly larger than the honeycomb frame, was cut in the front wall of the tunnel. Three separate honeycomb were constructed. When the frost begins to develop on the honeycomb, it is easily removed and replaced with a new, frost free honeycomb. A photograph of the removed honeycomb is shown in Figure 15(a).

Working Observation Section

This section is perhaps the most critical of the entire tunnel. It is here that the ice crystals are freely suspended in the supercooled fog and observed as they grow. A photograph of this section is shown in Figure 15(b).

The working/observation section is 89 cm tall. The bottom of the section is 20 cm square, converging to the top where it is 11 cm square. We discovered that this convergent configuration provides an excellent stability for the crystal as it is freely suspended in the

Figure 15(a). Photograph of the removed honeycomb.

(b). Photograph of the working/observation section

(a)

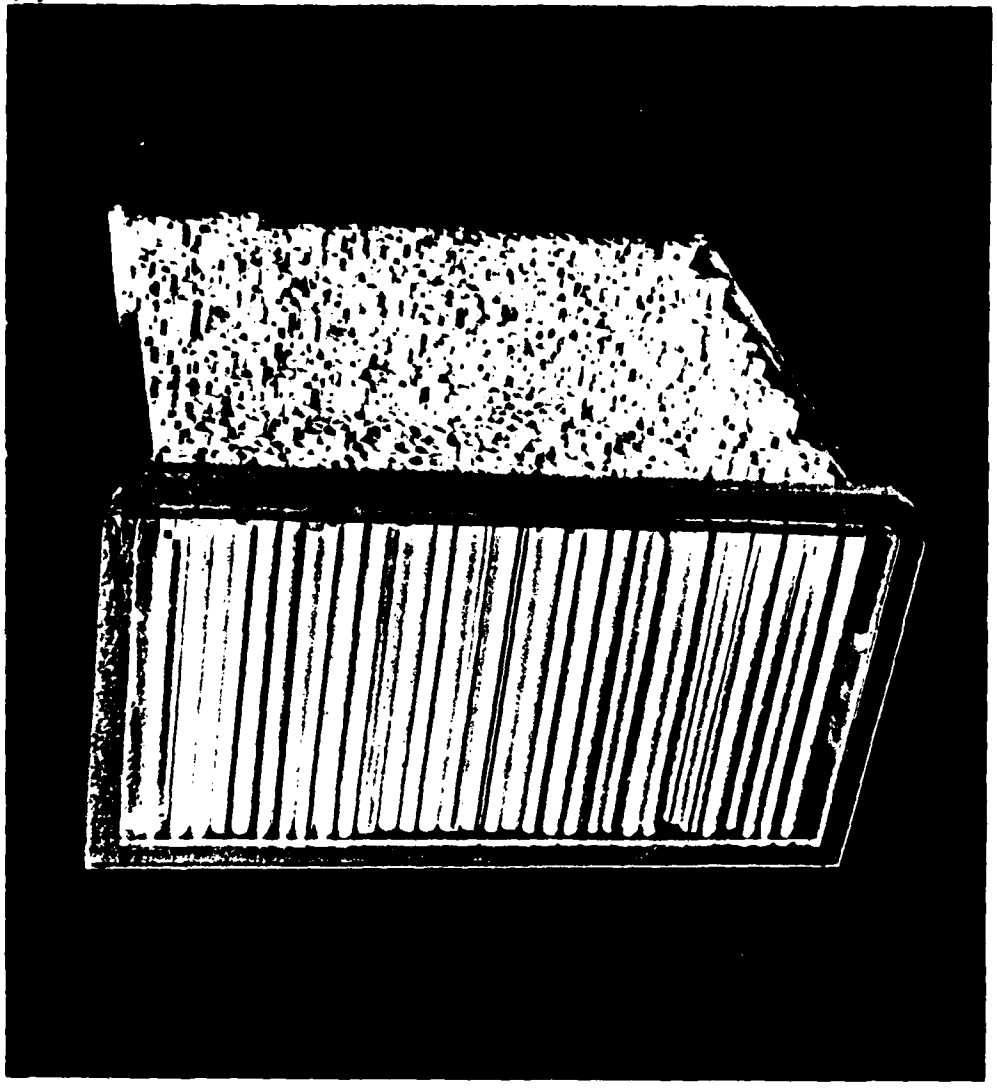

(b)

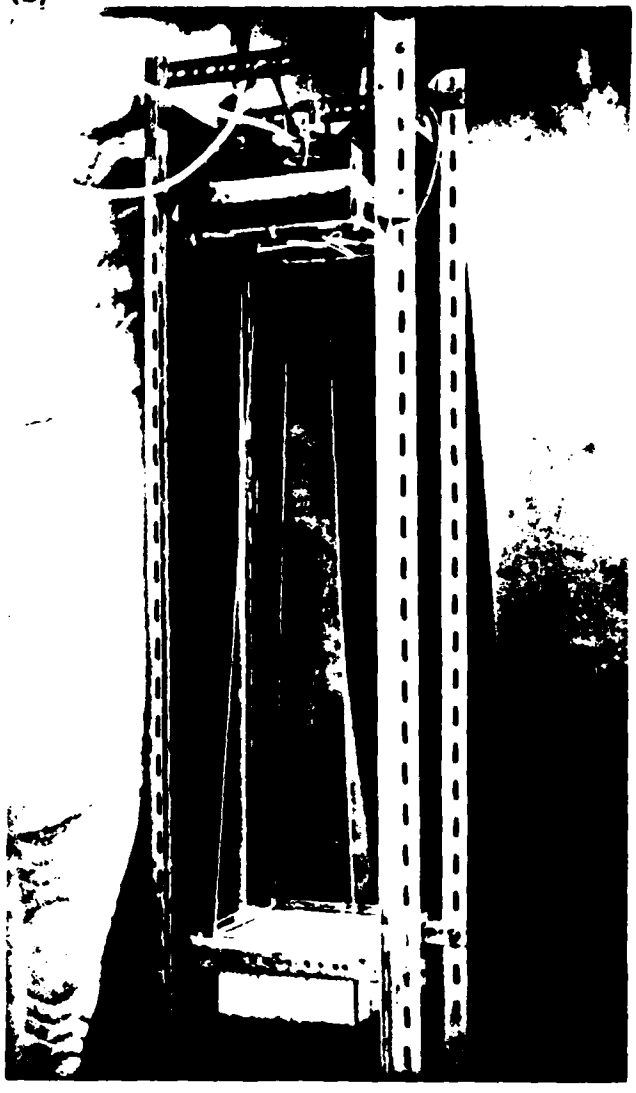

stream of supercooled fog. With constant flow rate through the tunnel, the flow speed through the working/observation section increases from the bottom to the top due to the decreasing cross-sectional area and the law of continuity. In this design, the vertical stability was anticipated to be not as good as that found in a vertically diverging design. However, due to the relatively slow fall speed of ice crystals, the instability is easily overcome by manual adjustment of the flow speed and the crystals can be suspended for indefinite periods, at any point along the vertical direction within this convergent section. The convergent design does provide a superb crystal stability in the horizontal directions within this section. As the flow passes through the convergent section, a velocity peak is developed just inside the chamber walls, apparently due to the flow enertia. This results in a velocity minimum in the center regions of the chamber. Therefore due to this smooth "velocity trap" in the center regions of the chamber, ice crystals remain away from the walls and near the center. Figure 16, (a) and (b) shows the relative velocity profiles along the horizontal plane for the slower flow speeds (less than 17.5 cm/s) and the faster flow speeds. For speeds less than 17.5 cm/s, the velocity trap is relatively large and broad and the suspended crystals remain within approximately 4 cm of the chamber centerline. At higher flow speeds, the velocity trap is much better defined and the crystals remain within approximately 1 cm of the chamber centerline.

Two sources of illumination are used in this portion of the tunnel. For general illumination, a light fixture with two 1.2 m long fluorescent tubes is used. In order to restrict the light into a narrow beam, a light shade was constructed of Masonite. The light fixture

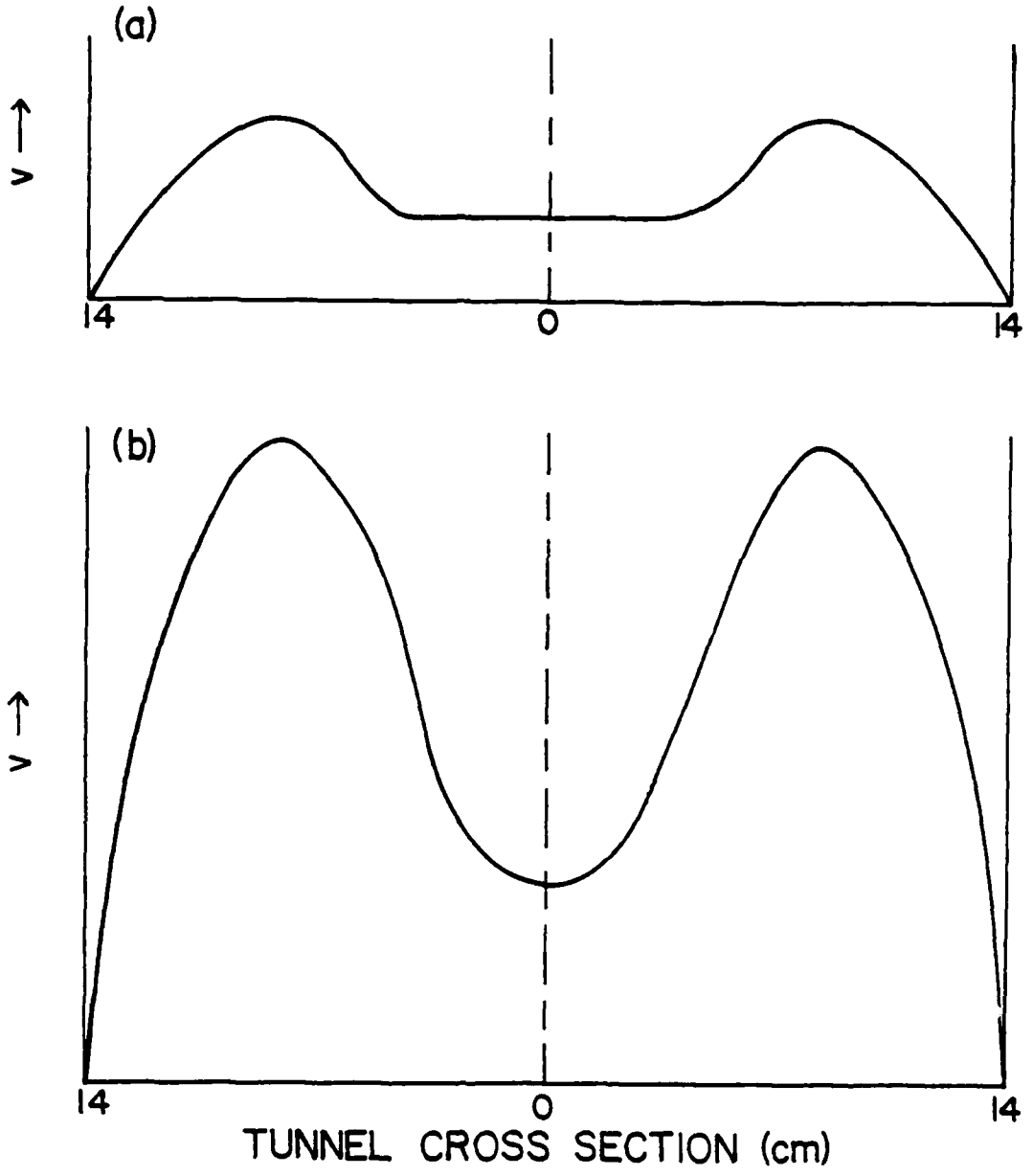

Figure 16. Relative velocity profile along the horizontal plane at the 14 cm square vertical position in the working/observation section for; (a). Flow speeds less than 17.5 cm/s. (b). Flow speeds greater than or equal to 17.5cm/s.

and shade are positioned vertically along the left side of working/observation section. This light source is adequate for illumination of the larger ice crystals and the supercooled fog. However, it does not provide adequate illumination to comfortably view the small ice crystals present in this section during their early stages of growth. For easy viewing of smaller crystals, a much brighter light source is required. Initially a slide projector with a 500 watt bulb was used. However, the cold temperatures within the cold room proved too harsh for the bulb and it lasted for only a few hours. To eliminate this problem, a quartz-halogen automobile driving light is used. Not only does this light provide the necessary brightness with rather small wattage but also is rugged enough to withstand the cold temperatures. A box was constructed of aluminum to house the light. This serves to form a light beam, directed into the tunnel through the right wall at the level where the crystals are suspended. In addition, a 10.2 cm diameter flexible duct hose, attached to the rear of the box and connected to a vent in the top of the cold room, provides a means to remove the heat generated by the light bulb. Figure 17(a) is a photograph of this light in position.

Suction Chamber

Positioned above the working/observation section is the suction chamber (Figure 17(b)). It serves the purpose of assuring that the air flow suction is applied evenly across the entire cross-section of the working/observation section. The chamber is 20 cm square and 15.2 cm tall. At the top center is located a 5.7 cm inside diameter, 7 cm long, acrylic pipe. To this pipe is attached the suction hose. Midway

Figure 17(a). Photograph of light in position beside the working/ observation section and the crystal sampling device in its pre-collection position.

(b). Photograph of the suction chamber.

(a)

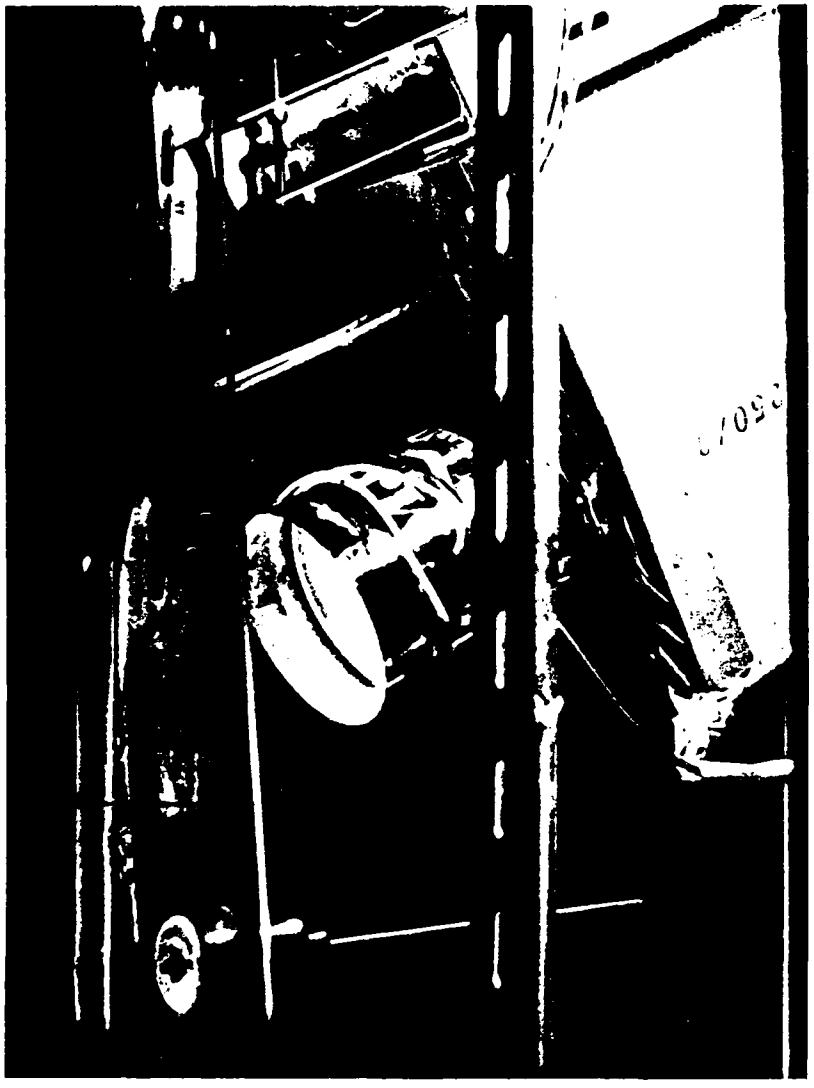

(b)

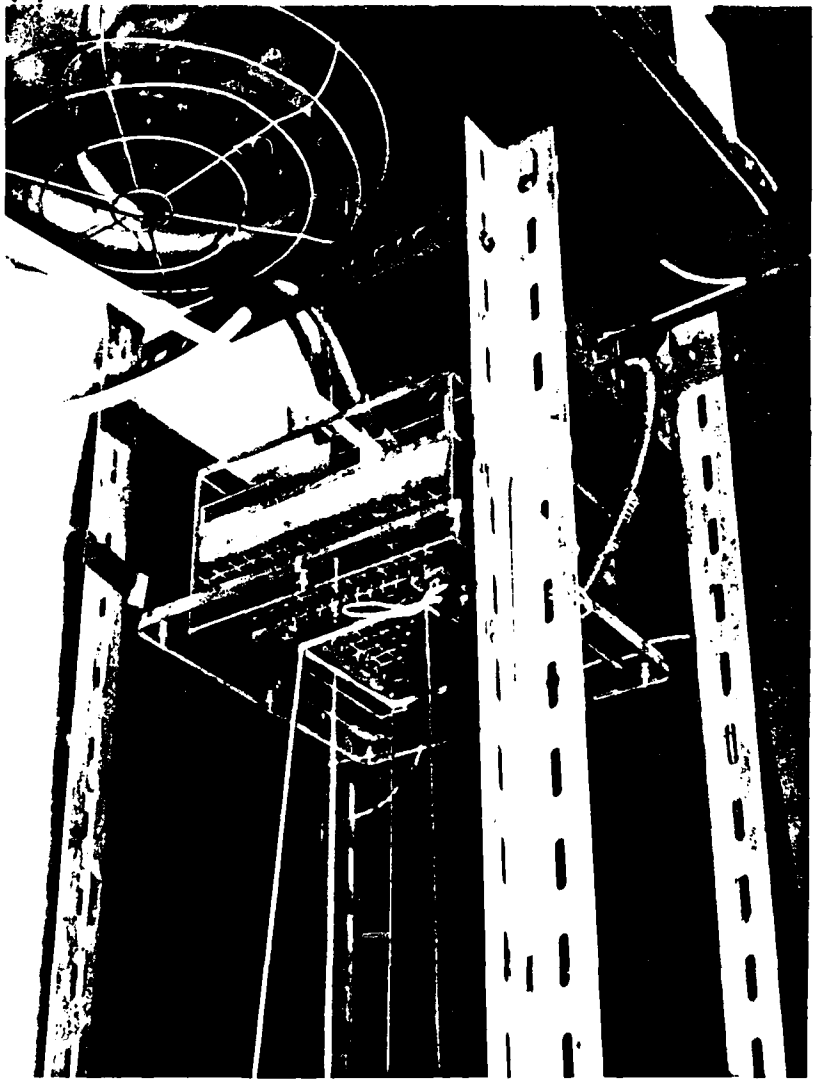

between the top and bottom of the chamber is a 6.1 mm thick sheet of acrylic with 225 evenly spaced holes of 3.56 mm diameter. (The total area of these holes equals the cross-sectional area of the suction line.) Immediately below the acrylic divider is a 2.5 cm thick piece of foam rubber. As air is pulled through the tunnel, a difference in pressure is established between both sides of the foam rubber divider. The result is even flow across the entire cross-section of the chamber.

Steam Generator

The steam generator consists of a specially modified pressure cooker (Figure 18(a)). In order to control the amount of steam produced, two considerations are given. First, it is necessary to accurately control the temperature of the water in the pressure cooker. This is accomplished by using a 1000 watt, 1.2 m long, immersion heater. The heater, of the flexible type, is shaped into a coil that exactly fits into the bottom of the cooker. This provides even heating of the water. Power to the heater is supplied through an Omega Engineering Model 49 temperature controller. The temperature controller uses a thermister to measure the water temperature and accordingly controls the electrical current supplied to the heater to maintain the water at a constant 82.2°C. Second, since the water temperature is held at a level below the boiling point, compressed air must be injected uniformly into the water to form the necessary steam and develop pressure. Copper tubing with holes is shaped into a coil and placed at the bottom of the pressure cooker. Compressed air is then passed through a flow meter into the copper tubing. Since the water temperature is held constant by the temperature controller, the only variable determining

Figure 18(a). Photograph of the steam generator.

(b). Photograph of the velocity control valve.

(a)

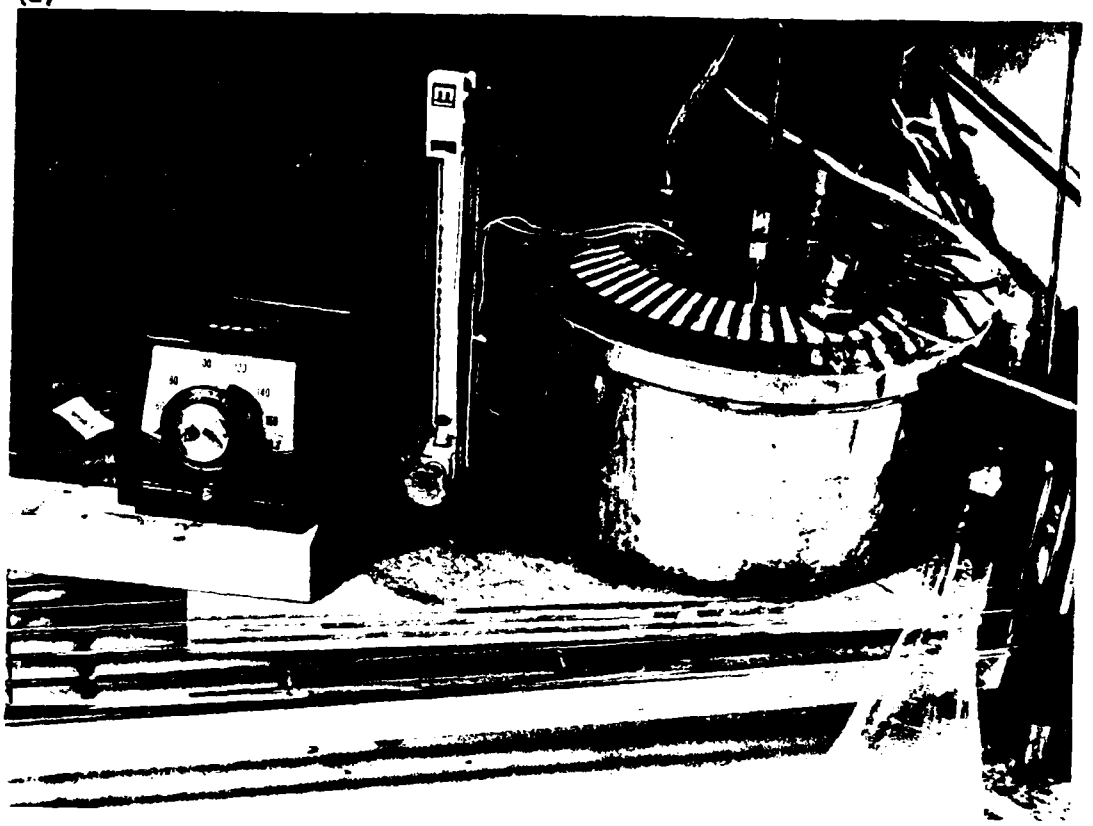

(b)

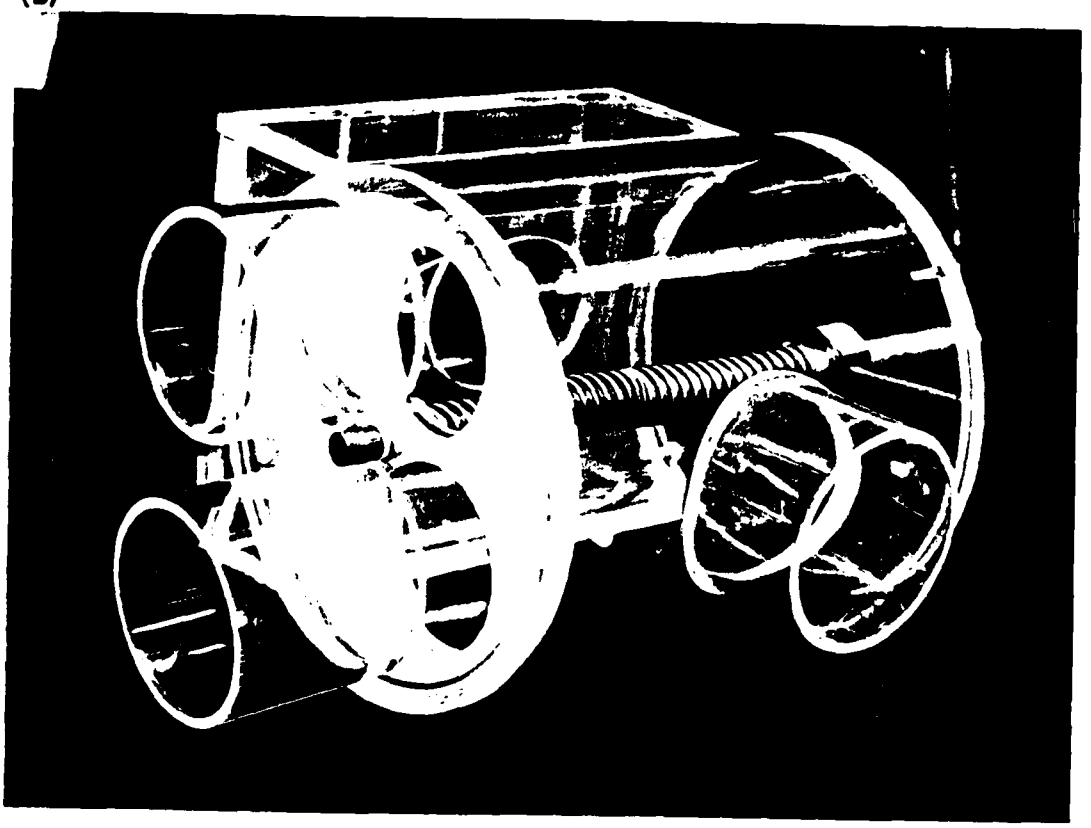

the amount of steam produced is the compressed air flow bubbling through the hot water. Therefore, the amount of water vapor used to produce supercooled fog is controlled by the setting of the flow meter in the compressed air line.

Because of the heat generated, the pressure cooker is placed outside the cold room. The steam is passed through the cold room and then into the fog chamber via a copper tube well insulated with foam rubber. The steam line is oriented in a way to assure that, when steam is not being produced, any condensed moisture in the line flows downhill out of the cold room. A water trap is placed in the line outside the cold room to collect the condensed moisture. This arrangement assures that the steam line does not become clogged with ice between periods of use. The flow meter is located in the cold room for easy access where it can be continually monitored to assure it remains at a constant setting.

Suction System

The suction to pull air through the wind tunnel is provided by a large vacuum cleaner. We found that the 16 gallon Wet-Dry Shop Vac marketed by Sears, Roebuck and Company was ideal. This vacuum provides more than adequate flow rates through tunnel and is rugged enough to withstand the low temperatures of the cold room for extended periods of operation. In order to reduce the suction provided by the vacuum cleaner, so that the flow speeds produced in the tunnel are within the range suitable for suspending ice crystals, a variac is attached to the vacuum cleaner motor. The voltage supplied to the motor is reduced to and held constant at 60 volts by means of this variac.

To vary the flow rate through the working/observation section without delay, a control valve is positioned in the suction line between the vacuum cleaner and the wind tunnel. The valve was designed and constructed entirely in our laboratory (Figure 18(b)). It is made of a 14.6 cm long clear acrylic pipe with an inside diameter of 14.6 cm and a wall thickness of 6.1 mm. Top and bottom plates are constructed of 6.1 mm thick acrylic sheets. Through the side of the pipe is inserted a smaller acrylic pipe with inside diameter of 5.7 cm and wall thickness of 3.1 mm. Into this side pipe is connected the suction line from the vacuum cleaner. Through the bottom plate are connected two smaller acrylic pipes of the same size as the pipe from the side of the valve. A flexible hose connects one of these bottom plate pipes to the suction chamber above the working/observation section. The other pipe is connected by a flexible hose to a similar suction chamber near the bottom of the fog chamber. (This suction chamber will be described later). Placed inside the valve, against the bottom plate, is a 6.1 mm thick, 14.0 cm diameter, plate made of polyethylene which provides low friction, sliding motion. Two holes, equal in diameter to those in the valve bottom plate, are cut in this inside plate. The holes in the inside plate are positioned such that when one hole is lined up with a hole in the bottom plate, the other holes in the inside and outside plates do not line up. In this position, when suction is applied, all of the flow passes through one of the bottom hoses and none through the other. If the inside plate is rotated to the point where half of one of the bottom plate holes is open, half of the other hole in the bottom plate is also open. In this position, when suction is applied, half of the total flow passes through each of the bottom hoses. The total flow

passing through both bottom hoses remains approximately constant, permitting a constant total suction while the flow rate into working/observation section is adjusted. A brass shaft, attached to the inside plate, extends through the top plate and has a handle attached. By turning the handle, the inside plate is rotated and the ratio of flow passing through the two bottom hoses is varied. A spring, placed between the inside and top plates, keeps the inside polyethylene plate forced tightly against the bottom plate, thus keeping the amount of leakage between the two plates to a minimum. A second hole, or "leak valve", is located in the side of the valve which serves the same purpose as the variac on the vacuum cleaner motor. A cover plate is used to vary the area of the hole opening. It is used to "leak off" a controlled amount of flow so that the total flow passing through the tunnel can be pre-adjusted to the desired working range.

As was mentioned above, one hose connects the control valve to the top of the vertical portion of the tunnel and the other connects the valve to the lower portion of the fog chamber. With this arrangement, the total volume of air pulled into the fog chamber remains constant and since the rate of water vapor injection into the chamber is constant, the fog condition remains unchanged even if the fog flow rate through the working/observation section changes. By the time the supercooled fog reaches the bottom of the fog chamber, it is well mixed. Therefore, if 75% of the flow is pulled from the tunnel at this point, 75% of the moisture is also removed. The 25% of the flow pulled through the working/observation section contains 25% of the total moisture.

At the point where the suction branch from bottom of the fog

chamber is located, a configuration similar to the previously discussed suction chamber is used (Figure 19(a)). The dimensions of both are identical. However, under normal use, an average of 75% of the total flow is drawn through the fog chamber suction branch and therefore 75% of the supercooled fog. This larger percentage of supercooled fog causes icing, and therefore clogging, of the foam rubber divider. To eliminate this problem, a heater was constructed and placed over the fog chamber suction opening. The heater consists of high resistance wire wound on a hardwood frame (Figure 19(a)). Total resistance of the heater is 54 ohms. Electrical current is supplied to the heater through a variac set of 90 volts. As the resistance wire heats, it also expands. To eliminate the possibility of the wires touching and causing a short circuit, the wires were electrically insulated with segments of fine glass tubes. As the supercooled fog passes through the heater, it is warmed and the amount of icing is greatly reduced.

Velocity Measurement System

As discussed earlier, the flow speed required to freely suspend an ice crystal at a stationary point in the tunnel equals the fall velocity of the ice crystal. To measure the crystal fall velocity, it is necessary to accurately determine the flow speed at any vertical position within the working/observation section.

In our tunnel, the flow speed is measured by a standard pitot tube arrangement (Anderson, 1978). The pitot tube, oriented perpendicular to the flow, senses the flow total pressure. The static pressure orifice, oriented parallel to the flow, senses the flow static pressure. The pitot tube and static pressure ports are connected by rigid walled

Figure 19(a). Photograph of the fog chamber with suction chamber.

(b). Photograph of the resistance cylinders positioned in the pressure line for velocity measurement.

(a)

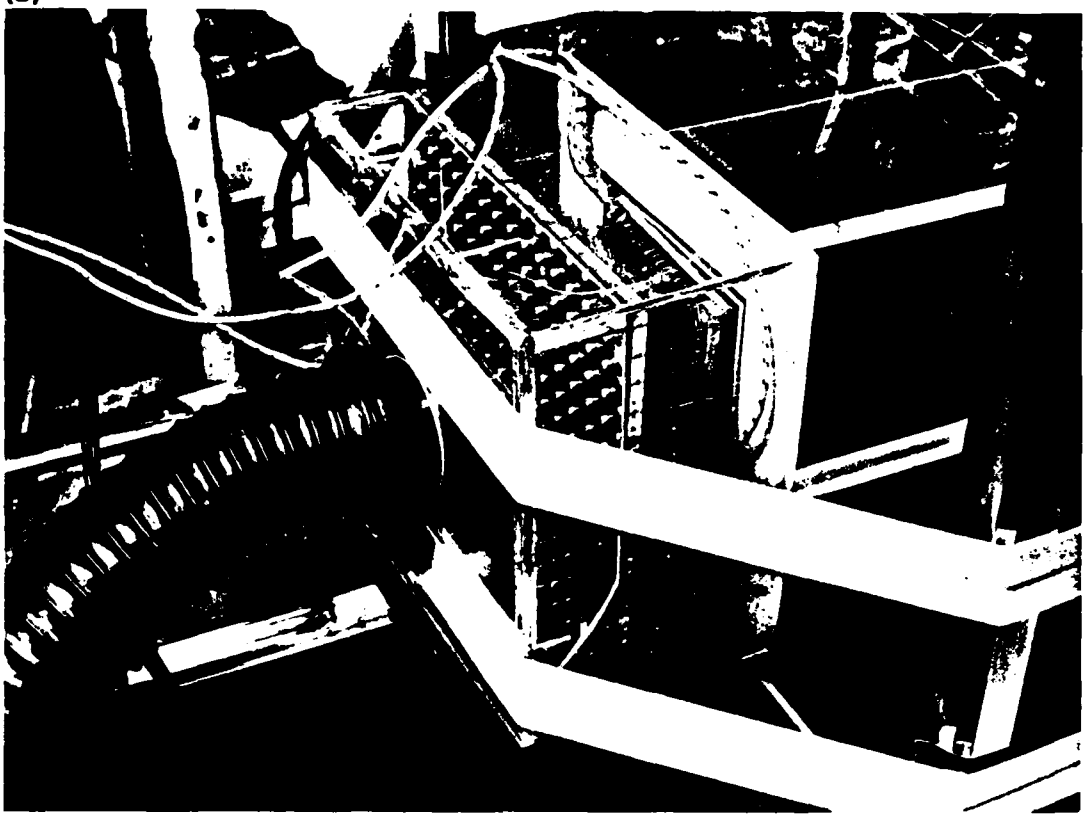

(b)

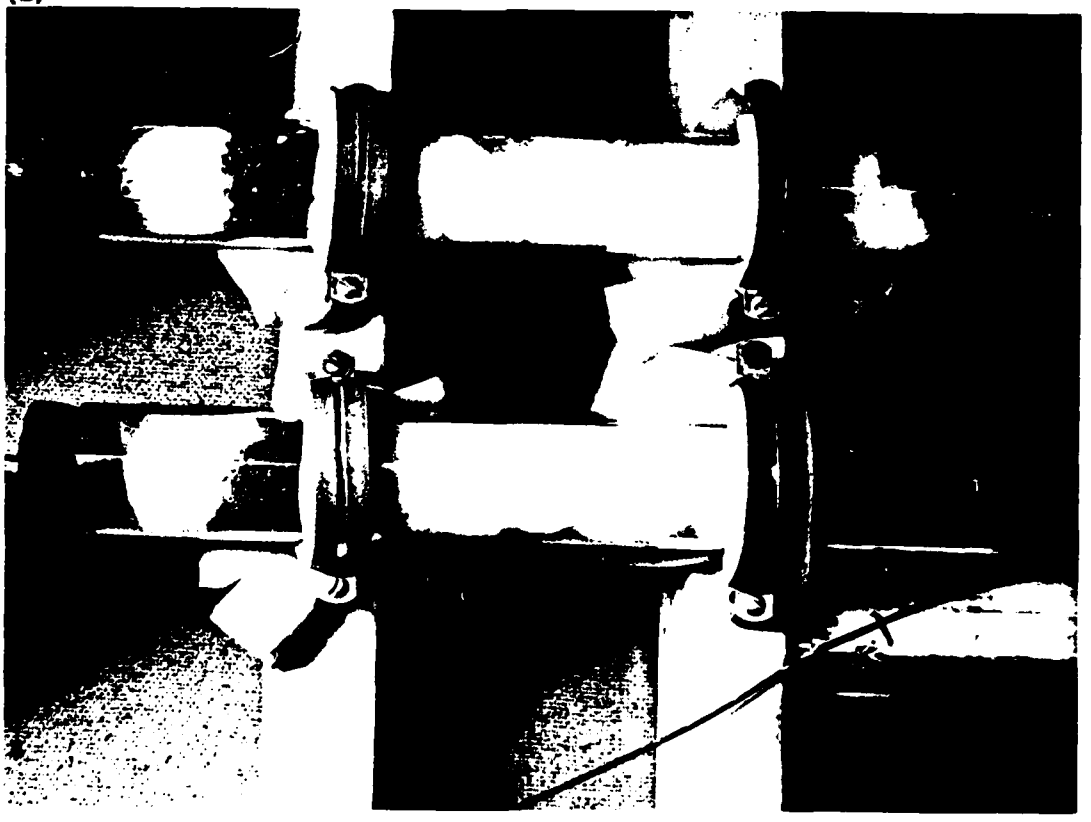

plastic tubing to an MKS Baratron Type 220B Electronic Differential Pressure Manometer. The pitot line is connected to one side of a metal diaphram while the static pressure line is attached to the other side. The displacement of the metal diaphram is an indicator of the differential pressure. Electrodes measure the displacement of the diaphram and provide an output voltage that is calibrated to indicate the differential pressure.

Small scale pressure variations, caused by the vacuum cleaner motor, were encountered in the wind tunnel. This resulted in excessive "noise" in the manometer output voltage. One method of damping such "noise" is to increase the resistance in the total and static pressure lines (Pankhurst and Holder, 1953). However, if too much resistance were adopted, the manometer response would become slow. To provide the necessary resistance to damp the noise in our apparatus, a resistance cylinder was placed in each pressure line (Figure 19(b)). Each cylinder consists of a 30.5 cm long, 3.8 cm inner diameter, acrylic pipe. Glass wool, loosely packed inside each pipe, was used to provide the necessary resistance. A thin layer of silica gel was also placed in each cylinder. This layer assured the air within each pressure line remained dry and thus eliminated the likelihood of clogging by icing.

Due to the relatively slow flow speeds required to freely suspend an ice crystal, placement of the pitot tube arrangement presented a problem. The flow speeds in the working/observation section were well below the lower threshold of speeds that could be sensed by the manometer. For this reason,the pitot tube arrangement could not be placed in that section. Because of its small cross-sectional area, the 5.7 cm diameter pipe above the suction chamber was the only location

where the flow speeds were within the range of the manometer sensor. Therefore, the pitot tube arrangement was placed in this location (Figure 20(a)).

Our original intent was to convert the measured differential pressure directly to the flow speed by using Bernoulli's equation (Pankhurst and Holder, 1952). However, we found that due to poor flow conditions in the lower portion of the pipe where the pitot tube arrangement was located, simple Bernoulli equation conversion was not accurate. By making smoke tests, we first confirmed that a one-to-one correspondence did exist between the differential pressure and the actual flow speed through the working/observation section. Next, to obtain the relationship between the manometer voltage output and the flow speed in the working/observation section, additional smoke tests were conducted. A puff of smoke was released in the center of the working/observation section near the bottom. A stopwatch was used to determine the time needed for the puff of smoke to reach the top of the section. Because of the convergent shape of this section, the flow speed varied depending on the vertical position. An expression was derived to estimate the flow speed at an arbitrary vertical position out of the experimental data (see appendix). Figure 21 shows the relationship between manometer voltage output and flow speed.

Temperature Measurement

To accurately measure the temperature of the air flow in the working/observation section, a copper-constantan thermocouple was placed at various locations throughout the section. This verified that the supercooled fog was homogeneous with respect to temperature throughout

Figure 20(a). Photograph of the pitot tube arrangement.

(b). Photograph of the crystal sampling device in its collective position.

(a)

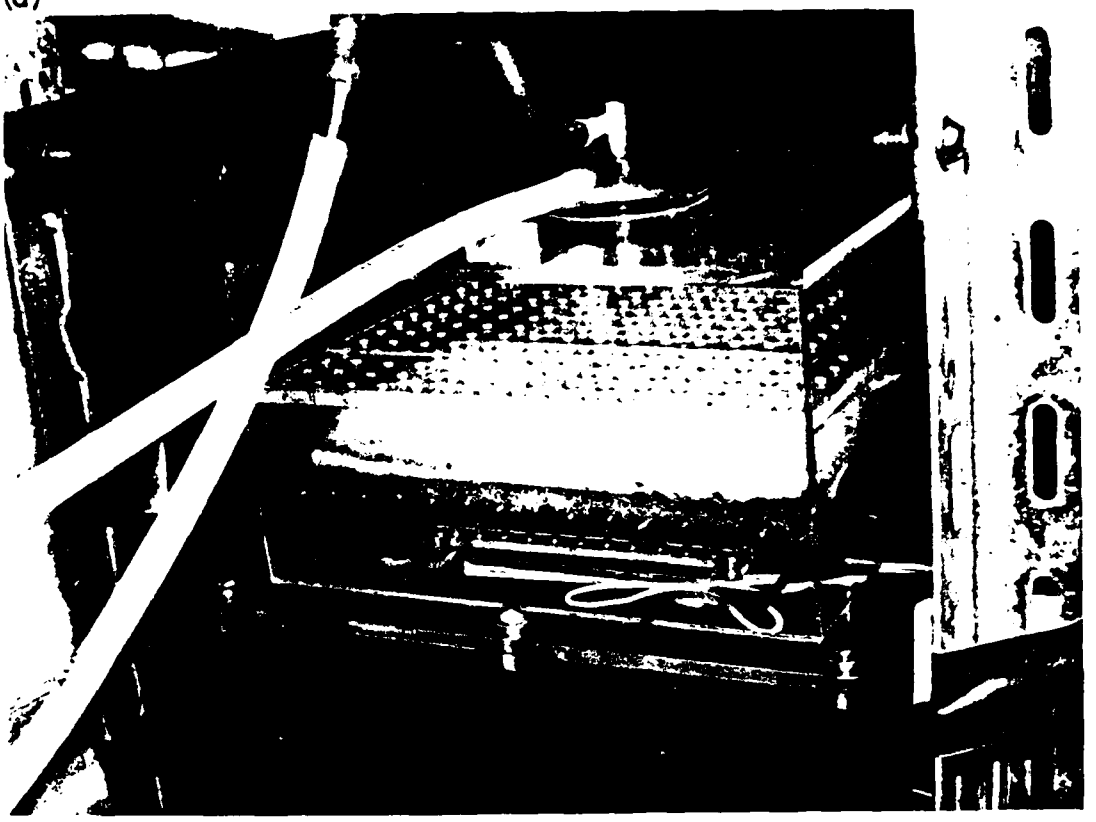

(b)

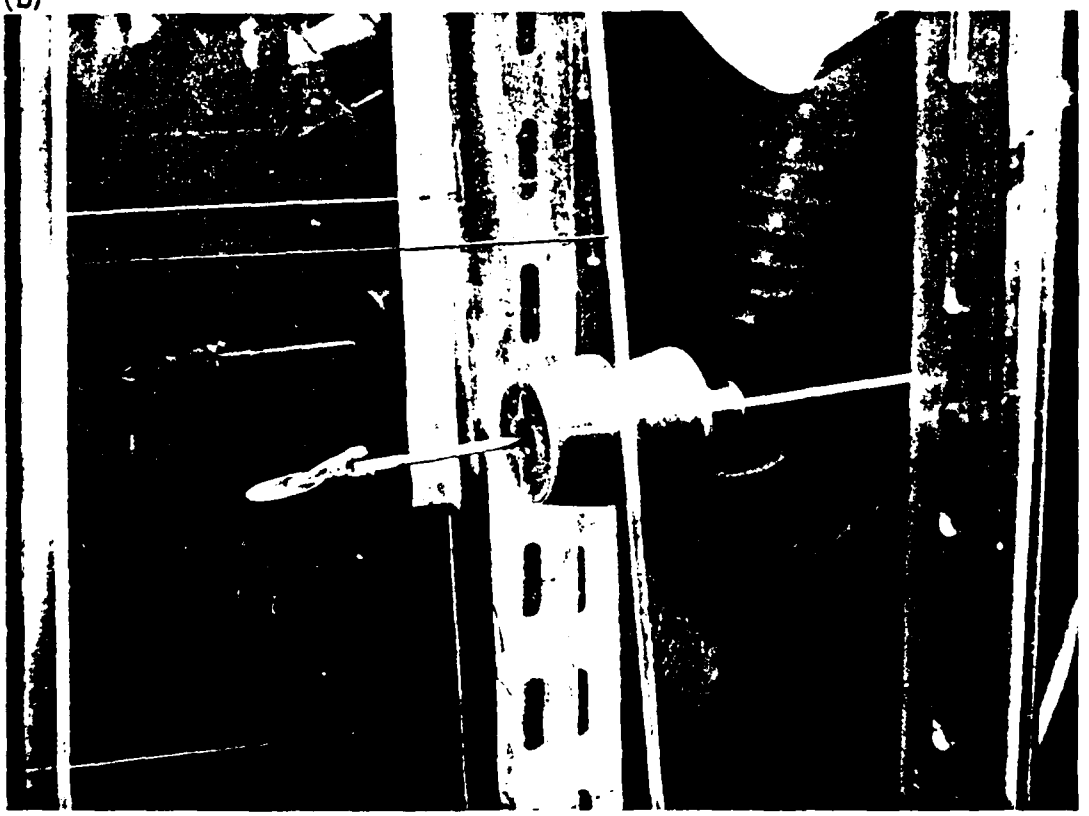

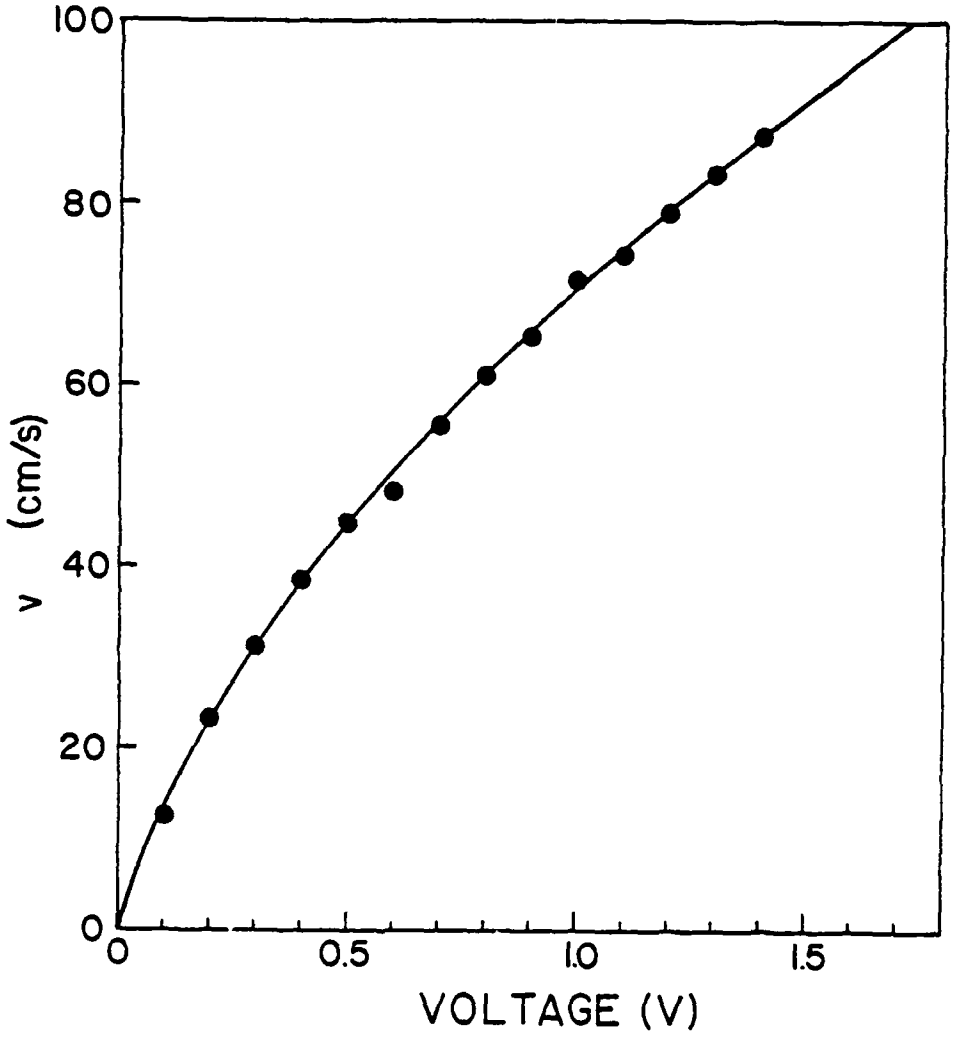

Figure 21. The flow velocity v plotted as a function of the manometer output voltage.

the working/observation section. To monitor the flow temperature during each experiment, a thermocouple was placed near the top center of the working/observation section, well above the point where the ice crystal was suspended, in order not to disturb the flow. Due to the low flow speeds encountered in the tunnel, the true airflow temperature was accurately determined directly from the thermocouple reading and no correction for the flow speed was necessary (Pope and Harper, 1966).

Ice Crystal Generation Chamber

To eliminate the possibility of competition for available moisture in the tunnel among the growing ice crystals, a separate chamber was used for ice crystal nucleation. The chamber consisted of a 20 liter plastic jug with its inside walls coated with flat black paint. The chamber was illuminated using a bright microscope lamp directed through the side of the chamber. A supercooled fog was produced inside the jug by breathing into it. A few seconds after the breathing, ice crystals were nucleated homogeneously by the "popping bubble" technique. A small plastic bubble (the type often used as packing material) was popped inside the jog which, through adiabatic expansion, caused homogeneous ice nucleation. Within a few seconds ice crystals were removed from the jug with a cooking baster and injected into the working/observation section of the tunnel through a small hole in the bottom center of the front wall.

Initially difficulties were experienced when transferring the crystals from the ice crystal generation chamber to the tunnel. In order to keep the crystals from subliming in the baster, the baster interior had to be coated with ice. This ice coating was produced by

breathing into the baster before it was used to transfer the crystals.

Crystal Sampling Device

The method used to capture and withdraw an ice crystal from the tunnel is based on a principle used by the University of California at Los Angeles (U.C.L.A.) in their wind tunnel (Pruppacher, private communication). The sampler consists of a brass rod with a small alligator slip attached to the end. A round microscope slide cover glass coated with oil is placed in the alligator clip. The brass rod fits through a three rubber stopper assembly which in turn fits into a hole in the right wall of the working/observation section. The inside rubber stopper is hollowed out so that when the sampler is not in use, the cover glass can be withdrawn from the chamber into the stopper assembly (Figure 17(a)). This assures that, during an experiment, unwanted ice crystals are not collected on the cover glass. After the crystal has been suspended and grown for a desired period of time, the sampler is extended into the working/observation section. Initially the cover glass is oriented parallel to the flow in order not to disturb the flow. In this orientation, the cover glass is positioned below the suspended crystal. The flow speed is then reduced slightly until the ice crystal is suspended immediately above the sampler cover glass. The sampler is then quickly turned so that the cover glass is perpendicular to the flow (Figure 20(b)). A dead air space results just above the cover glass and the ice crystal falls softly onto the oil coated cover glass. The entire sampling apparatus is then removed from the chamber, the cover glass removed, and the crystal prepared for study under the microscope.

Data Recorder

Voltage outputs from the electronic manometer and the thermocouple are fed into a Yokogawa Type 3066 Flatbed Pen Recorder. Three separate channels with 19 voltage ranges from 5 μV/cm to 5 V/cm are available and 8 chart speeds from 60 cm/min to 2 cm/hr are possible. We found that a chart speed of 20cm/hr was ideal for our use. The thermocouple voltage output is fed into channel 1 with a voltage setting of 1 mV/cm, providing good resolution over the temperature ranges used in our study. The manometer voltage output is fed into channel 2 with a voltage setting of 0.1 V/cm, 0.25 V/cm, or 0.5 V/cm, depending upon the fall velocity range of the particular crystal type being grown. Channel 3 is used as an event marker. A 9 volt battery is combined in series with a foot-operated momentary contact switch. By simply depressing the switch for a second, an instantaneous 9 volt change is fed into channel 3, which results in a marker line on the strip chart. This data recording arrangement is excellent for our study, since a continuous recording of both flow speed and airstream temperature is made throughout each growth experiment. The use of the event marker makes post data analysis easy and accurate. Figure 22(a) is a photograph of a typical readout.

One problem was encountered with the use of the flatbed recorder. The recorder is designed for use only at temperatures between +5 to +40°C. Therefore, an acrylic box was constructed in which to enclose the recorder. A 100 watt light bulb is placed inside the box to provide illumination as well as heat to maintain the temperature within the recorder operating range.

Figure 22(a). Photograph of a sample recorder readout.

(b). Photograph of the crystal melting device.

(a)

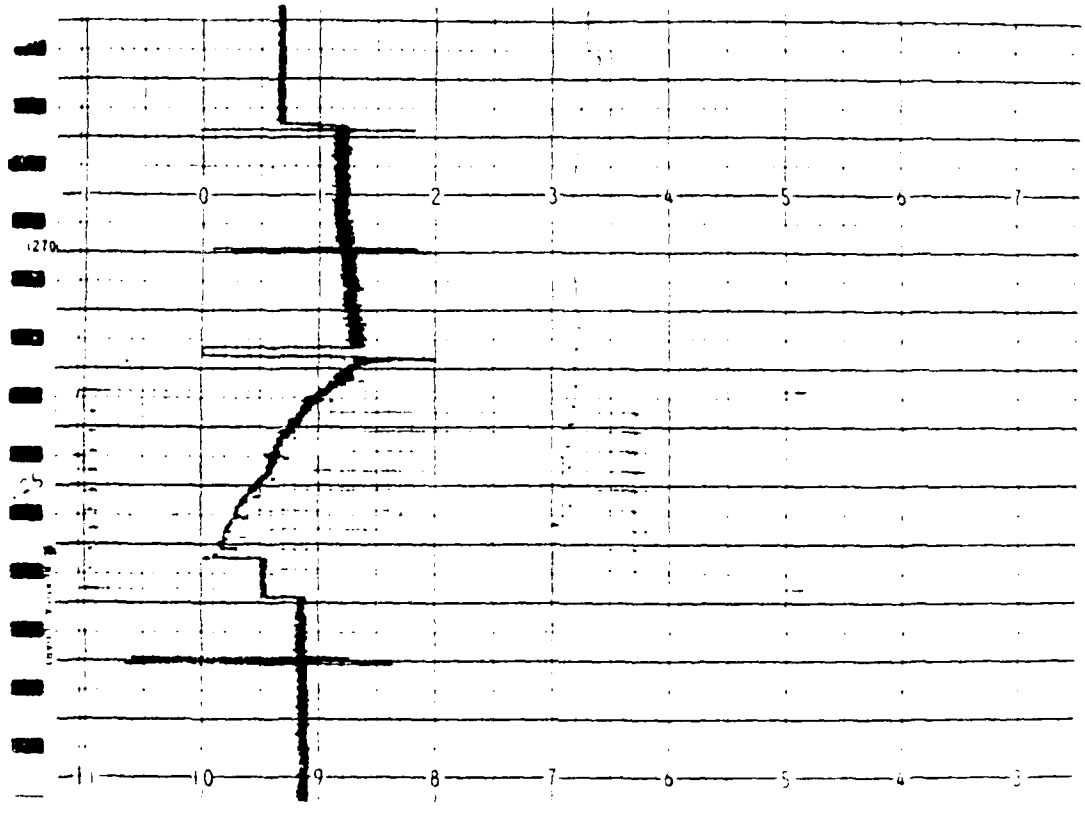

(b)

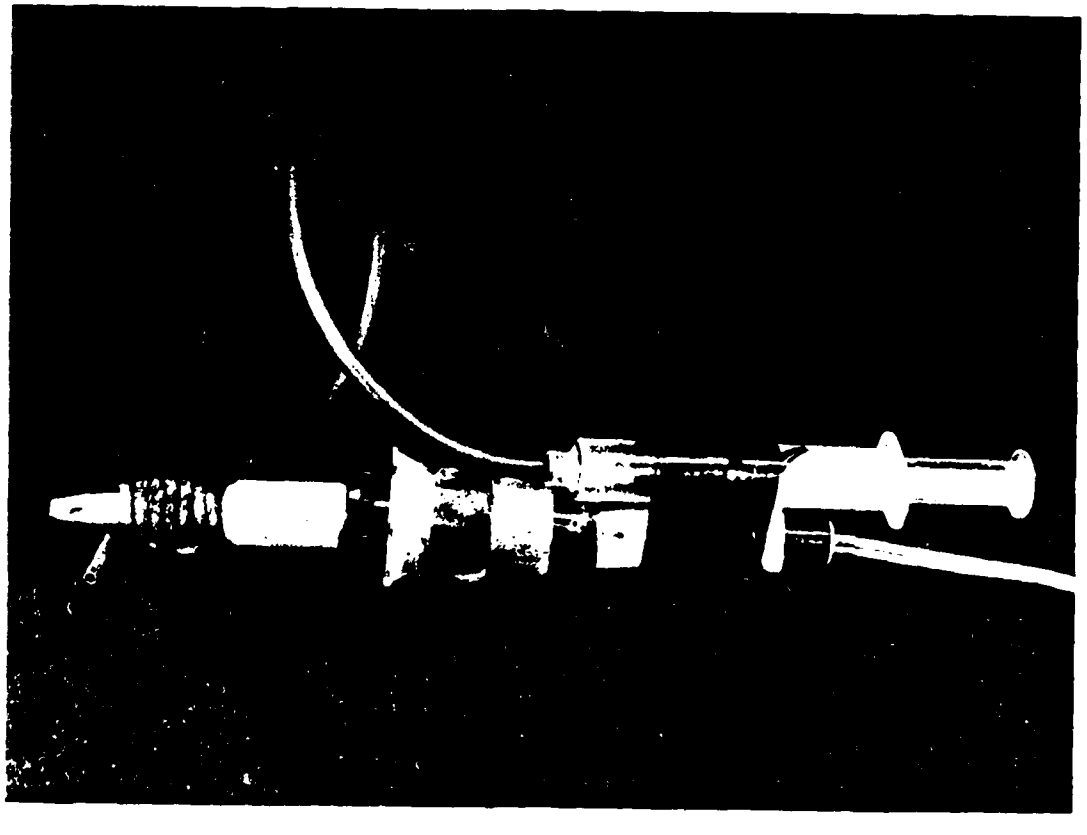

Microscope

A Nikon Optiphot Biological Microscope with Differential Interference Contrast "NT", Nomarsky Prism, and automatic exposure 35 mm photomicrograph attachments is used to study and photograph the ice crystals after they are removed from the tunnel. To eliminate any possibility of the ice crystal melting during its examination under the microscope, the entire microscope assembly is placed in the environmental cold room. This presented a problem similar to that encountered in the use of the data recorder.

We were advised by engineers from the Nikon Company that prolonged exposure of the microscope to temperatures below 0°C could severely damage the microscope lenses and prisms. A solution was found by using plumbing heat tape (normally wrapped around water pipes to prevent freezing). A 2.75 m length of heat tape was wrapped around the critical parts of the microscope. Cloth and foam rubber were then wrapped and taped over the heat tape to provide insulation. The heat tape is plugged into a 115 volt electrical outlet. A thermostat automatically turns the heat tape on when the temperature drops below 3.3°C. The heat tape and insulation work quite well in keeping the critical components of the microscope above 0°C, yet does not excessively heat the microscope stage.

Timer

In order to time the growth period, an accurate timing device is required. We used a General Electric spring operated darkroom timer. This timer is capable of accurately measuring time from 30 seconds to 120 minutes. The timer has an audio alarm that sounds at the end of

the desired time period. An audio alarm is a must, since it is nearly impossible to watch the time while at the same time concentrating on the suspended ice crystal.

Chapter 4

EXPERIMENTAL PROCEDURE

Liquid Water Content Determination

In order to clearly describe the ice crystal growth environment in our tunnel, the liquid water content of the supercooled fog in which the crystals are grown must be determined. The liquid water content of the supercooled fog in our chamber was measured by using a glass tube filled with grains of plaster of paris.

First, the grains of plaster of paris are kept for several hours just above water in a sealed container in order to assure that the plaster of paris is saturated with respect to water. Second, the plaster of paris grains are placed in a glass tube and the tube and contents are weighed to within 0.1 mg. Third, the tube of plaster of paris grains is placed in the cold room and allowed to reach equilibrium temperature. Fourth, a known volume of supercooled fog is drawn from the center of the working/observation section, through the tube of plaster of paris. Fifth, the tube of plaster of paris is allowed to warm to the room temperature and again weighed to within 0.1 mg. The difference between the two weights gives the liquid water content for the volume of air pulled through the tube of plaster of paris.

Liquid water content measurements were taken, at various cold room temperatures, with the flow rate of compressed air in the steam generator held constant at 3,825 cc/min. Figure 23 shows the results

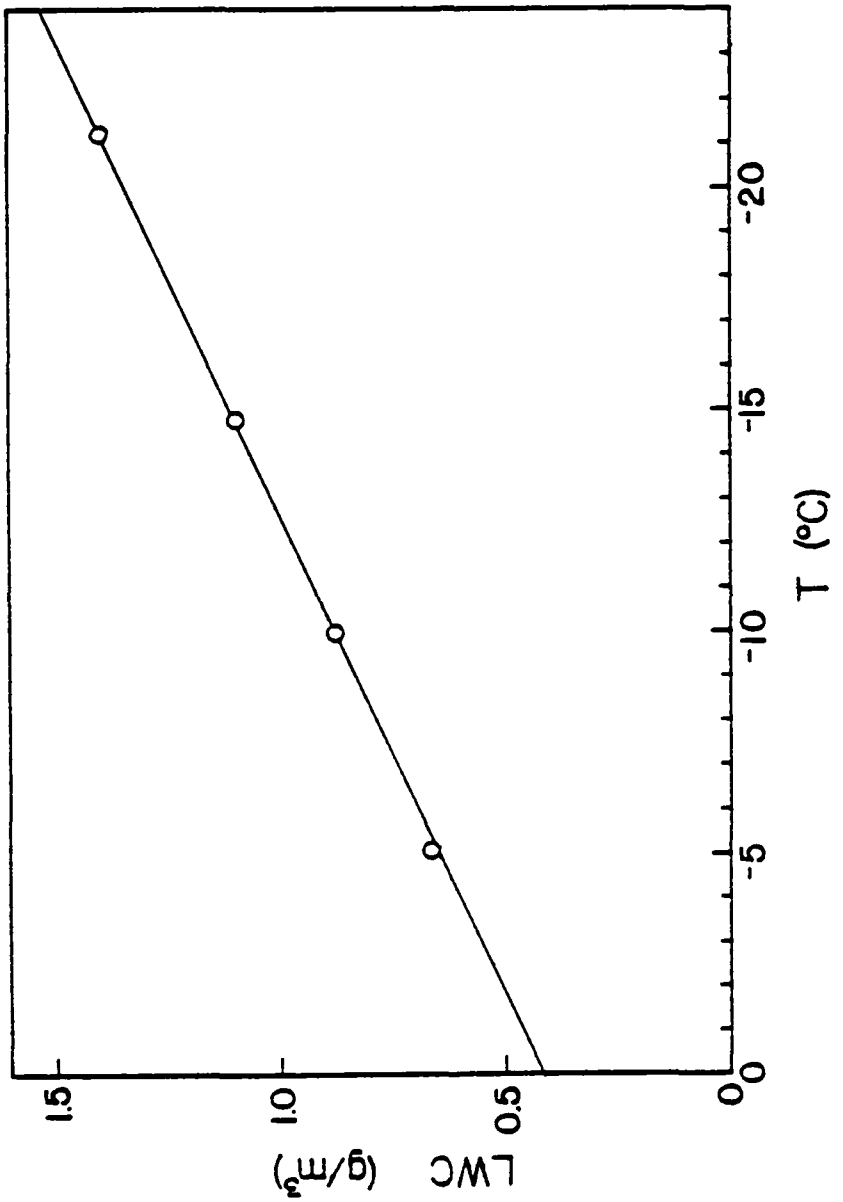

Figure 23. Liquid water content LWC plotted as a function of cold room temperature T.

of these measurements. Since all variables in the steam generator are held constant throughout the study, the graph accurately indicates the liquid water content of the supercooled fog used in this study as a function of cold room temperature. The liquid water content increases linearly with decreasing temperatures.

Tunnel Operation

Preparation

The first step in preparing the supercooled cloud tunnel for ice crystal growth measurements is to attain the desired temperature in the environmental cold room. Normally the desired temperature is set on the cold room temperature controls the evening before the day the experiments are to be conducted. This assures that all parts of the tunnel have cooled to the desired room temperature before the experiments start. This, in turn, assures that no transient convective currents are produced in the tunnel, which might occur, for example, if the chamber walls were significantly warmer than the air being pulled through the tunnel.

Appproximately 30 to 40 minutes before beginning an experiment, the vacuum cleaner, all of the tunnel lights, and all of the tunnel deicing heaters are turned on. This allows the cold room to adjust to the slight warming caused by these heat sources and allows it to stabilize at a new temperature level. At the same time, the steam generator heater is turned on to assure its water will heat up to 32.2°C before the experiment begins.

Ice Crystal Nucleation, Injection, Suspension, and Removal

After the temperature of the air passing through the tunnel has stabilized to a constant value, the compressed air to the steam generator is turned on at the pre-determined flow meter setting (3,825 cc/min in all of the present experiments). As the steam from the generator begins to enter the fog chamber, the baster, used to transfer ice crystals into the tunnel, is coated with ice by breathing into it. Also at this time, the microscope cover glass used to collect the crystals at the end of the experiment is coated with either motor oil or 3-in-1 household oil, depending upon the temperature. The cover glass is then placed in the crystal sampling device in the pre-collection orientation as described earlier. The depression in a microscope slide is filled with silicone oil at this time also.

As the supercooled fog begins to pass through the working/observation section, the ice crystals have to be nucleated in the ice crystal generation chamber. A supercooled fog is formed in the generation chamber by breathing into it. After approximately 30 seconds, a plastic bubble is popped inside the generation chamber, resulting in copius amounts of ice crystals. The baster (volume of 75 cc) is used to transfer some of the ice crystals from the generation chamber. These ice crystals are then injected into the working/observation section of the tunnel through a hole near the bottom of the front wall. At this instant, the timer is started and the foot operated recorder event marker switch is depressed for a second.

The ice crystals are allowed to rise to the holding position (14 cm square position) in the working/observation section. (This is

at the eye level when the observer is in the operating position). The suction valve is then used to adjust the flow speed in order to keep the crystals at this position. After approximately 30 to 90 seconds, attention is focused on a single crystal located near the centerline position. The flow speed is continually adjusted to keep this crystal at the holding position. After approximately 3 minutes, only this crystal remains at the holding position. The flow speed must be continuously adjusted (increased) in order to keep the crystal at the holding position as it grows. As described earlier, the convergent design of the working/observation section results in an airflow pattern that keeps the crystal near the centerline position.

At the end of the desired growth period, the alarm on the timer sounds. The foot activated recorder event marker switch is again depressed. At the same time the crystal sampling device is inserted into the tunnel, to a position below the crystal, with the collection glass oriented parallel to the airflow. The flow speed is then slightly decreased to bring the crystal to a position immediately above the collection glass. The glass is then rotated to an orientation perpendicular to the airflow and the crystal falls softly onto it. The entire crystal sampling device is then removed and the steam injection into the tunnel stopped by turning off the compressed air supplied to the fog generator.

Crystal Preservation, Examination and Photography

The procedure used to preserve the ice crystal for study under the microscope is similar to that used by Fukuta et al. (1979). The cover glass, upon which the crystal is caught in removing it from the

working/observation section, is either coated with motor oil or 3-in-1 household oil. The motor oil is used at temperatures as cold as -10°C. At colder temperatures, the motor oil becomes too viscous and the less viscous 3-in-1 oil is used. After removal from the tunnel, the cover glass holding the crystal is removed from the sampling device and placed, oil coated side down, on a depression microscope slide filled with Dow Corning 550 silicone oil. Care must be taken when performing this procedure at temperatures warmer than -7°C. If either the microscope slide or cover glass is touched by the bare hand, the crystal is immediately melted by the body heat. The crystal remains at the interface of the two oil layers since it is denser than the oil on the cover slide and less dense than the silicone oil on the microscope slide.

The microscope slide and cover glass are then placed on the microscope stage. After the ice crystal is located, it is photographed. The cover glass is then moved horizontally with a probe to produce a shear at the interface of the two oils. This allows the crystal to be turned so that a photograph can be taken of the side view of the crystal. With the above combination of oils, all types of crystals except for long columns and large dendrites can be turned so that both the a- and c-axis can be viewed and photographed. Figure 24(a) and (b) show photographs of ice crystals taken with this treatment. Figure 24(a) shows a crystal viewed from the top. Note that from this orientation it is impossible to determine whether the crystal is a single plate or a double plate. However, Figure 24(b) shows the same crystal as viewed from the side. It is obvious from this angle of view that the crystal is indeed a double plate.

In order to determine accurately the mass of the crystal, it

Figure 24. Photographs of ice crystals and water droplets using the crystal preservation technique.

(a). Top view; Growth time = 5 min; Temperature = -11.3°C; 2a = 0.23 mm and 0.20 mm.

(b). Side view of crystal shown in (a); c = 0.04 mm.

(c). Growth time = 9 min; Temperature = -14.8°C; 2a = 1.6 mm.

(d). Water droplets resulting after crystal shown in (c) melted.

(e). Growth time = 9 min; Temperature = -7/2°C; 2a = 0.10 mm.

(f). One water droplet and two air bubbles resulting after crystal shown in (e) melted.

AD-A107 263 AIR FORCE INST OF TECH WRIGHT-PATTERSON AFB OH F/G 8/12
DETERMINATION OF ICE CRYSTAL GROWTH PARAMETERS IN A SUPERCOOLED--ETC(U)
JUN 81 M W KOWA
UNCLASSIFIED AFIT-CI-81-36T NL

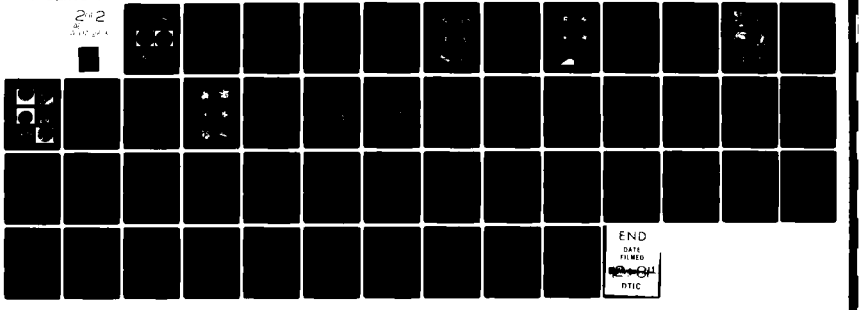

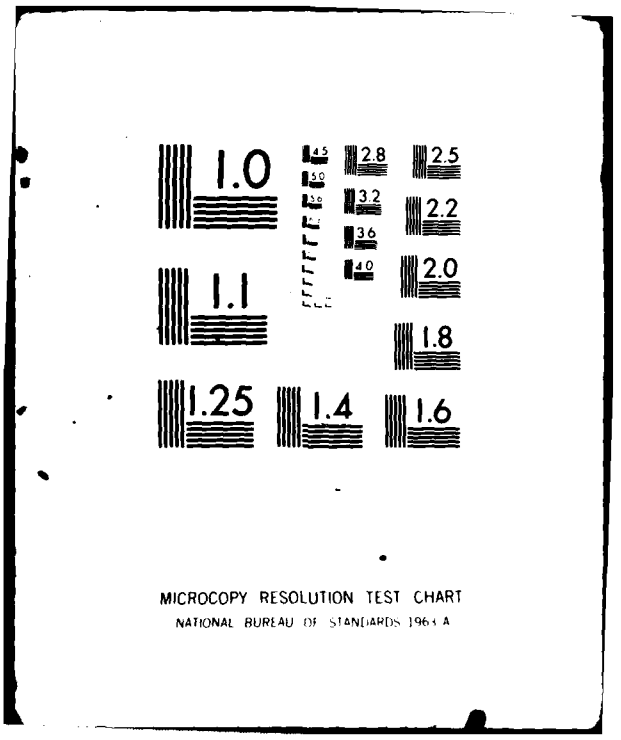
1.0
1.1
1.25
1.4
1.6
1.8
2.0
2.2
2.5
2.8
3.2
3.6
4.0
4.5
5.0
5.6
6.3
7.1
MICROCOPY RESOLUTION TEST CHART
NATIONAL BUREAU OF STANDARDS 1963 A

(a)

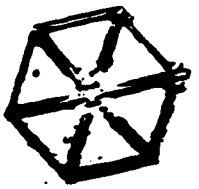

(b)

(c)

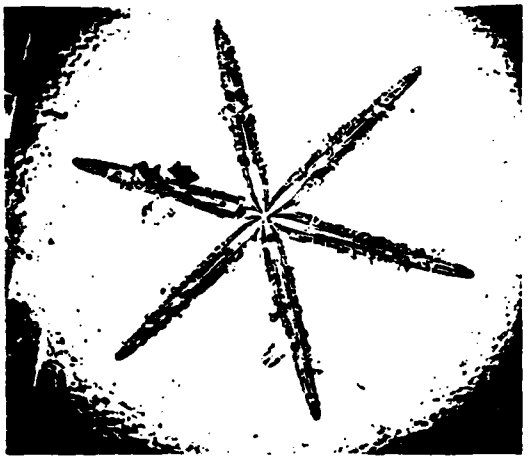

(d)

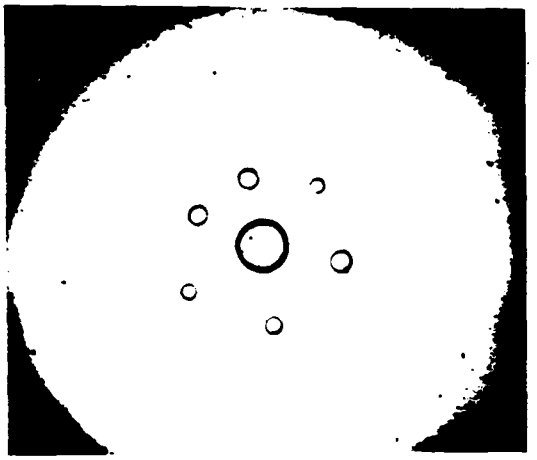

(e)

(f)

must be melted. This is accomplished by blowing a puff of hot air across the cover glass. A special tool is used for this (Figure 22(b)). A 10 cc syringe is attached to the handle of a soldering iron. Small copper tubing is wrapped around the heating element of the soldering iron and is attached to the syringe by rubber tubing. As air is forced from the syringe through the copper tubing, it is heated adequately to to melt the ice crystal. The resulting water droplet remains at the interface of the two coils and also retains its spherical shape, a necessity in order to measure the true diameter. A photograph is then taken of the water droplet. Figure 24(c) shows a stellar crystal. Figure 24(d) shows the same crystal after it has been melted. One large water droplet resulted from the central part of the crystal. Six smaller droplets resulted from the branches. All seven droplets must be measured to accurately determine the crystal mass. Figure 24(e) shows a column. Figure 24(f) shows the same crystal after melting. One large droplet resulted. Also present are two air bubbles. The presence of the two air bubbles is a unique feature of the melted column crystal. Care must be taken not to consider these air bubbles when determining the crystal mass. All the photographs taken of the crystals and water droplets are black and white.

Post Experimental Procedures

At the end of each experiment, the honeycomb is removed from the supercooled cloud tunnel to see if any frost build-up has begun. If so, it is replaced by a frost free honeycomb. Also, the baster and rubber hoses used to transfer the crystals from the generation chamber to the tunnel are flushed with dry air. This assures that no ice

crystals that may have stuck to the baster or tubing walls remain. The tunnel is then ready for the next experiment.

Growth Periods and Temperatures

Ice crystals were suspended for periods of 4, 5, 6, 7, 8, 9, and 10 minutes. Suspending crystals steadily for periods of less than 3.5 minutes was very difficult because at that point the crystals had not yet reached a fall velocity high enough to adequately develop the "velocity trap" in the working/observation section. The capability exists with this tunnel to freely suspend a crystal for indefinite periods of time. However, due to time constraints for this study, 10 minutes was chosen as the maximum growth period.

The warmest temperature at which crystals were grown was -3°C, while the coldest temperature routinely attainable in the environmental cold room was -25°C. Growth experiments were conducted at approximately 2°C intervals within this temperature range.

We found that for this study the best measurement routine was to first obtain the desired temperature in the environmental cold room. At that temperature, growth experiments were conducted for the seven different periods of time. The cold room temperature was then changed to another desired temperature and the routine repeated.

Chapter 5

RESULTS AND DISCUSSION

Ice Crystal Habit

From the large number of ice crystals grown and collected, the variation of ice crystal habit with temperature was analyzed. At temperatures warmer than -4.5°C both double and single plates were observed.

In the temperature range from approximately -4.5 to -7.0°C, columns were detected. Six column crystals grown in this temperature zone are shown in Figure 25. A feature unique to these column crystals is the presence of at least two air pockets in the tips of each column. These air pockets can be observed in Figure 25(a), (c), (d), (e), and (f) as cone-shaped cavities at each end. In Figure 25(b) the air pockets have a spherical shape. When the column crystals are melted, the two air pockets remain, being attached to the formed drop ((Figure 24(f)). This was observed in every column grown.

At temperatures near -9°C isometric crystals (2a- and c-axis equal) were observed. Six of the crystals grown hear this temperature are shown in Figure 26. For growth periods of four and five minutes the crystal surfaces were relatively smooth (Figure 26(e) and (f)). However, crystals suspended for more than five minutes began to grow small hexagonal appendages on the basal face at the crystal's corners. The appendages become more pronounced for longer growth periods up to ten

Figure 25. Photographs of column crystals. All photographs are the same scale.

(a). Growth time = 9 min; Temperature = -7.2°C; 2a = 0.10 mm; c = 0.21 mm.

(b). Growth time = 8 min; Temperature = -6.7°C; 2a = 0.07 mm; c = 0.30 mm.

(c). Growth time = 6 min; Temperature = -6.9°C; 2a = 0.05 mm; c = 0.20 mm.

(d). Growth time = 8 min; Temperature = -6.9°C; 2a = 0.07 mm; c = 0.28 mm.

(e). Growth time = 10 min; Temperature = -5.6°C; 2a = 0.08 mm; c = 0.48 mm.

(f). Growth time = 9 min; Temperature = -5.4°C; 2a = 0.07 mm; c = 0.55 mm.

(a)

(b)

(c)

(d)

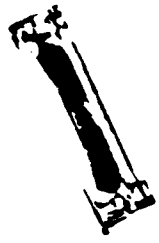

(e)

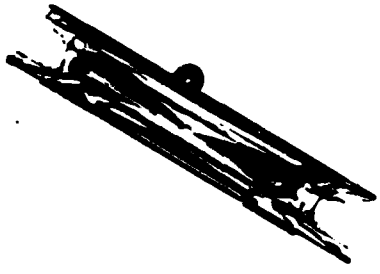

(f)

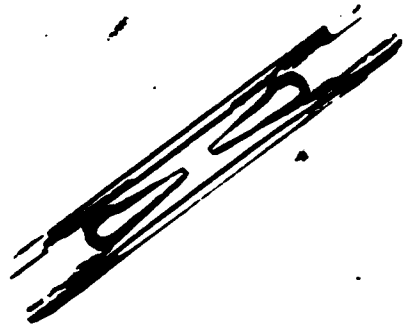

Figure 26. Photographs of isometric crystals. All photographs are the same scale.

(a). Top view. Growth time = 10 min; Temperature = -9.5°C; 2a = 0.17 mm.

(b). Side view of same crystal as shown in (a). c = 0.14 mm.

(c). Top view. Growth time = 8 min; Temperature = -9.1°C; 2a = 0.15 mm.

(d). Side view of same crystal as shown in (c). c = 0.15 mm.

(e). Top view. Growth time = 4 min; Temperature = -8.9°C; 2a = 0.09 mm.

(f). Side view of same crystal as shown in (e). c = 0.07 mm.

(a)

(b)

(c)

(d)

(e)

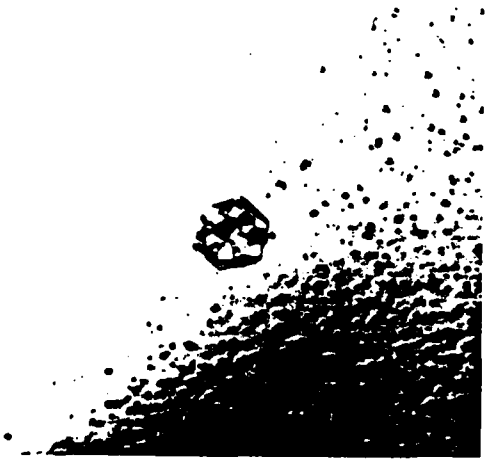

(f)

minutes (Figure 26, (a), (b), (c), and (d)).

Double plates were observed between -10.0 and -12.5°C. Examples of these double plates are shown in Figures 27 and 24, (a) and (b). Double plates suspended for short periods (three and four minutes) had the 2a-axis dimensions of each plate nearly equal. However, as the double plates were suspended for longer periods (up to ten minutes), the 2a-axis of one plate became larger than that of the other. The double plates with the top plate deformed into a shape like a bowl as shown in Figure 27, (c) and (d) were observed only after growth periods of eight minutes or more. These facts seem to indicate that initially edge growth dominates to develop the double plates of equal size. However, after approximately four minutes, one plate begins to grow faster than or at the expense of the other. This is likely due to the orientation of the crystal during its free-fall as well as the resultant aerodynamic flow of supercooled fog around the crystal. This aerodynamic flow apparently provides a more favorable condition of growth for the lower plate. Accordingly, the vapor field near the top plate becomes unfavorable for diffusional growth and leads to the growth of commonly observed single plate later.

The majority of crystals grown in the temperature zone between -13.0 and -16.0°C were dendrites. Six of these crystals are shown in Figures 28 and 24(c). In the warmer regions of this zone, the dendrites had long, thin branches as in Figures 28, (a), (c), and (f), and 24(c). In the colder regions of the zone, the dendrites had shorter, thicker branches as in Figure 28(b) and (d), until near -16°C where they became nearly platelike as in Figure 28, (e). In this temperature range, dendrites were always observed after three minutes of growth, the shortest

Figure 27. Photographs of dougle-plate crystals. All photographs are the same scale.

(a). Growth time = 8 min; Temperature = -11.8°C; 2a = 0.47 mm and 0.33 mm.

(b). Side view of same crystal as shown in (a). c = 0.04 mm.

(c). Growth time = 9 min; Temperature = -11.6°C; 2a = 0.55 mm and 0.27 mm.

(d). Growth time = 10 min; Temperature = -12.1°C; 2a = 0.66 mm and 0.34 mm.

(e). Growth time = 6 min; Temperature = -11.9°C; 2a = 0.33 mm and 0.27 mm.

(f). Side view of same crystal as shown in (e). c = 0.04 mm.

(a)

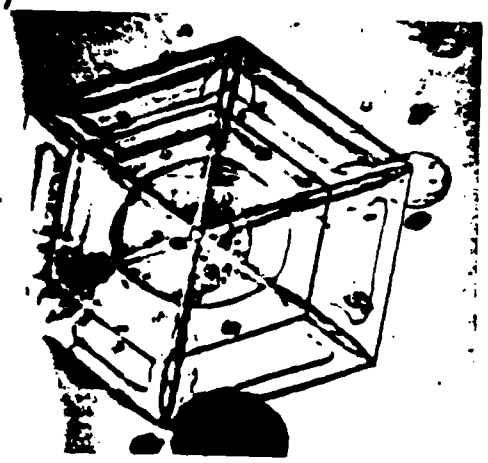

(b)

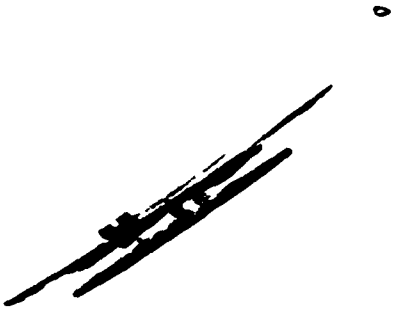

(c)

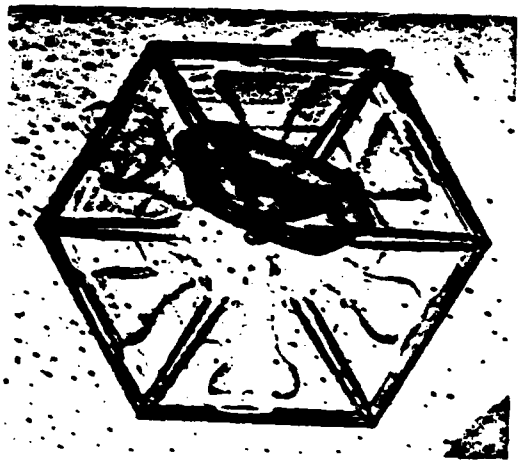

(d)

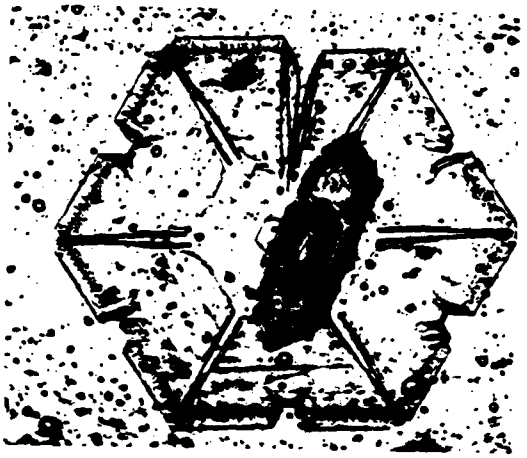

(e)

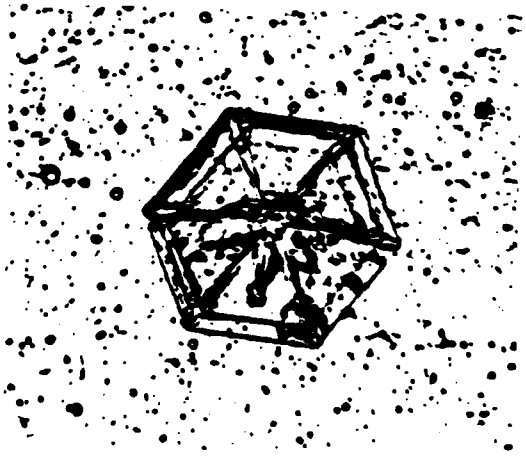

(f)

Figure 28. Photographs of dendritic crystals. (a), (c), and (f) are the same scale while (b), (d), and (e) are the same but larger scale.

(a). Growth time = 9 min; Temperature = -13.2°C; 2a = 1.17 mm.

(b). Growth time = 6 min; Temperature = -15.3°C; 2a = 0.68 mm.

(c). Growth time = 7 min; Temperature = -14.8°C; 2a = 1.12 mm.

(d). Growth time = 6 min; Temperature = -15.9°C; 2a = 0.57 mm.

(e). Growth time = 6 min; Temperature = -15.8°C; 2a = 0.49 mm.

(f). Growth time = 9 min; Temperature = -14.2°C; 2a = 1.65 mm.

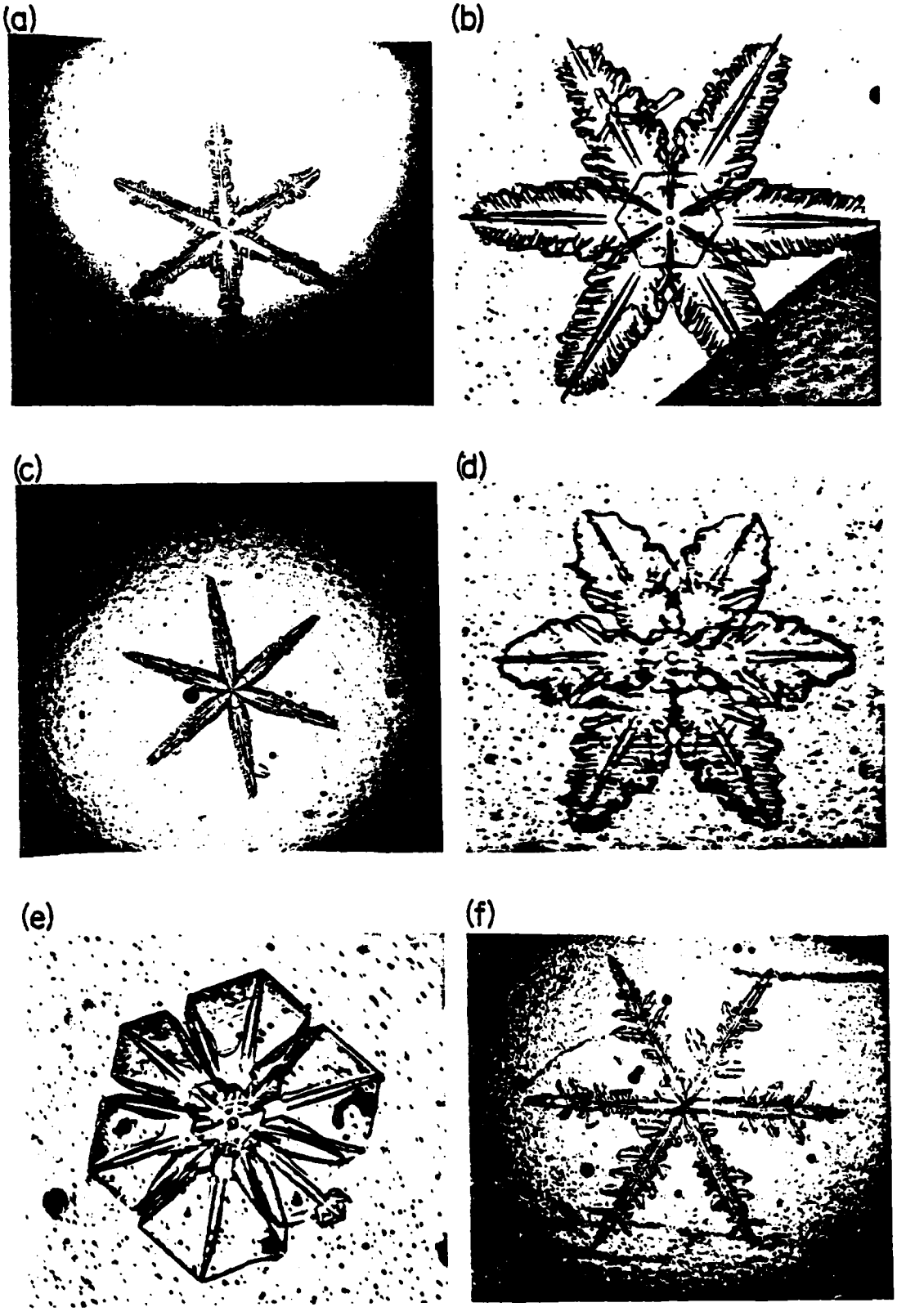
(a)
(b)
(c)
(d)
(e)
(f)

growth period in the present study. This indicates that initiation of dendritic growth takes place within the initial three minutes.

In the temperature range between -16.0 and -18°C, vaned crystals were common. An example of this type of crystal is shown in Figure 29(e) and (f). Figure 29(e) is a top view of the crystal. Figure 29(f) is a side view which plainly shows the two small vanes protruding from the basal face. A crystal may have one small vane to several large ones.

At temperatures between -18.0 and -23.0°C, complex crystals were observed. Examples of these are shown in Figure 29, (a), (b), (c), and (d). A significant feature noticeable in these crystals is the presence, in the center of the crystal, of an isometric crystal. After four minutes of growth, the isometric crystal begins to develop dendritic branches from its corners as shown in Figure 29(c). As the crystal grows for longer periods of time, the branches become more complex and better developed. This is shown in Figure 29(d) after six minutes of growth. Figure 29(a) shows that, by nine minutes of growth, the branches have become so well developed and complex that the isometric crystal nucleus is no longer easily identified. Close examination of these branches revealed that they are made up of many thick hexagonal plates, randomly attached to one another. It was noted earlier in Figure 23 that in our experiments the liquid water content increased with decreasing temperatures. It is probably that these complex crystals result, at least partly, because of these higher values of liquid water content at that temperature zone. Their growth seems to be attributable to the combined process of vapor diffusion and riming growth. Some supercooled water droplets collide with the crystal and stick.

Figure 29. Photographs of complex crystals. All photographs are the same scale.

(a). Growth time = 9 min; Temperature = -22.9°C; Sphere of best fit = 0.35 mm.

(b). Growth time = 8 min; Temperature = -18.6°C; Sphere of best fit = 0.37 mm.

(c). Growth time = 4 min; Temperature = -21.7°C; Sphere of best fit = 0.16 mm.

(d). Growth time = 6 min; Temperature = -21.4°C; Sphere of best fit = 0.26 mm.

(e). Growth time = 9 min; Temperature = -16.8°C; 2a = 0.37 mm.

(f). Side view of same crystal as in (e).

(a)

(b)

(c)

(d)

(e)

(f)

Next, each captured and frozen droplet begins to grow by vapor diffusion into a thick hexagonal plate. This growth process may well be a transition stage of growth between vapor diffusion and riming.

Crystal Dimensions

Figure 30 is a graph of the crystal 2a-axis, the longest dimension on the basal plane, plotted with respect to temperature, for growth periods of four, six, eight, and ten minutes. A 2a-axis minimum is found near -7°C, associated with the columnar forms of crystals in this temperature zone. With decreasing temperature, the 2a-axis increases to a maximum near -15°C where the dendritic crystals were detected. With further lowering in temperature from this point, the 2a-axis decreases to a secondary minimum between -18.0 and -21.0°C.

The relationship between the crystal c-axis and temperature, for growth periods of four, six, eight, and ten minutes, is shown in Figure 31. As would be expected, this graph is a near inverse of the 2a-axis vs. temperature relationship shown in Figure 30. A c-axis vs. temperature relationship shown in Fig. 30. A c-axis maximum is found in the column temperature zone near -5°C, a minimum in the dendrite temperature zone near -15.0°C, and a secondary maximum near -19°C.

Figure 32 shows the relationship between the logarithm of the 2a/c ratio and the temperature. Negative values indicate the temperature zone where column crystals were observed and positive values correspond to those for plates. The temperatures at which transitions from plates to columns and columns to plates occur are easily identified by the points where the logarithm becomes zero. Clearly evident is the temperature zone between -8.0 and -9.5°C where the isometric crystals

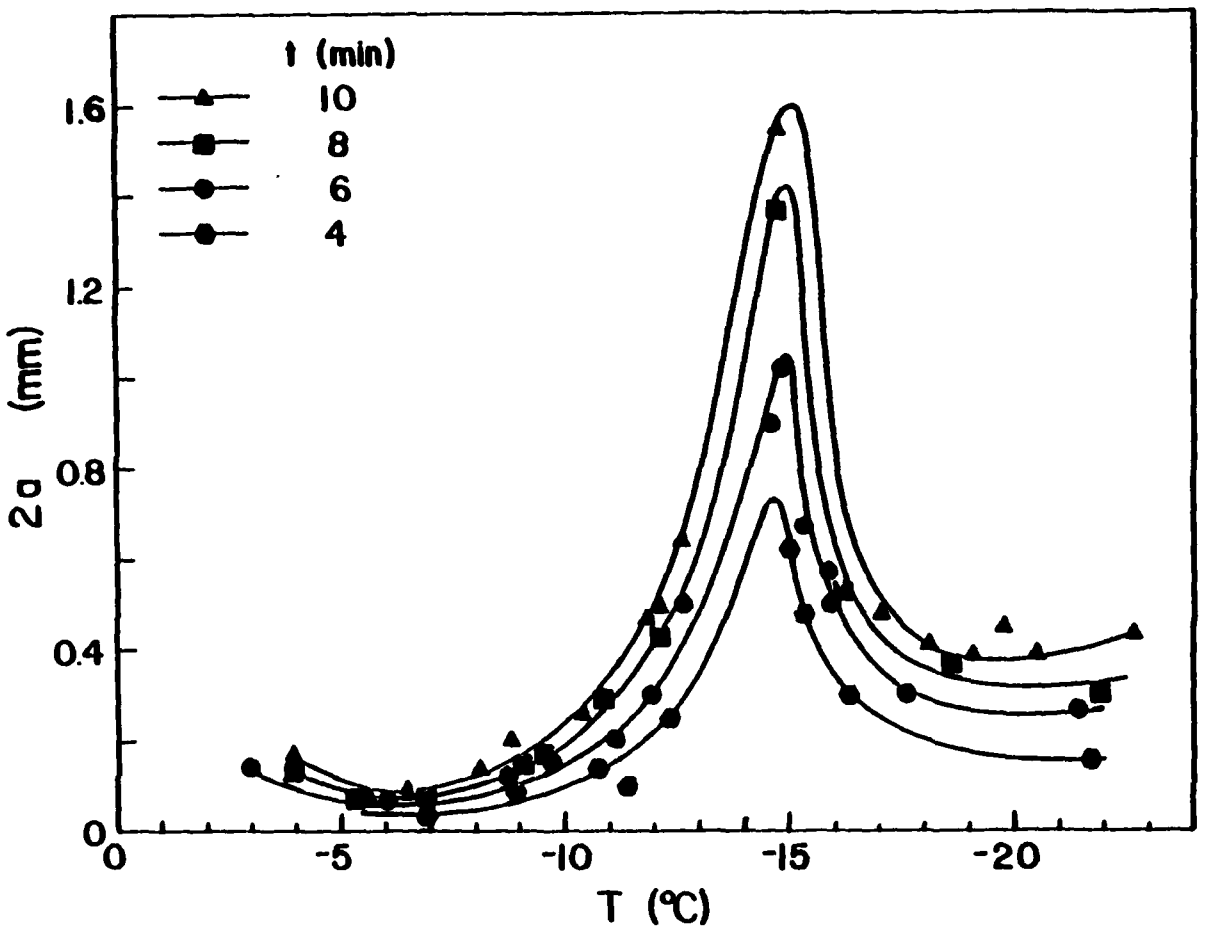

Figure 30. The ice crystal 2a-axial dimensions plotted as a function of temperature T at different growth time t.

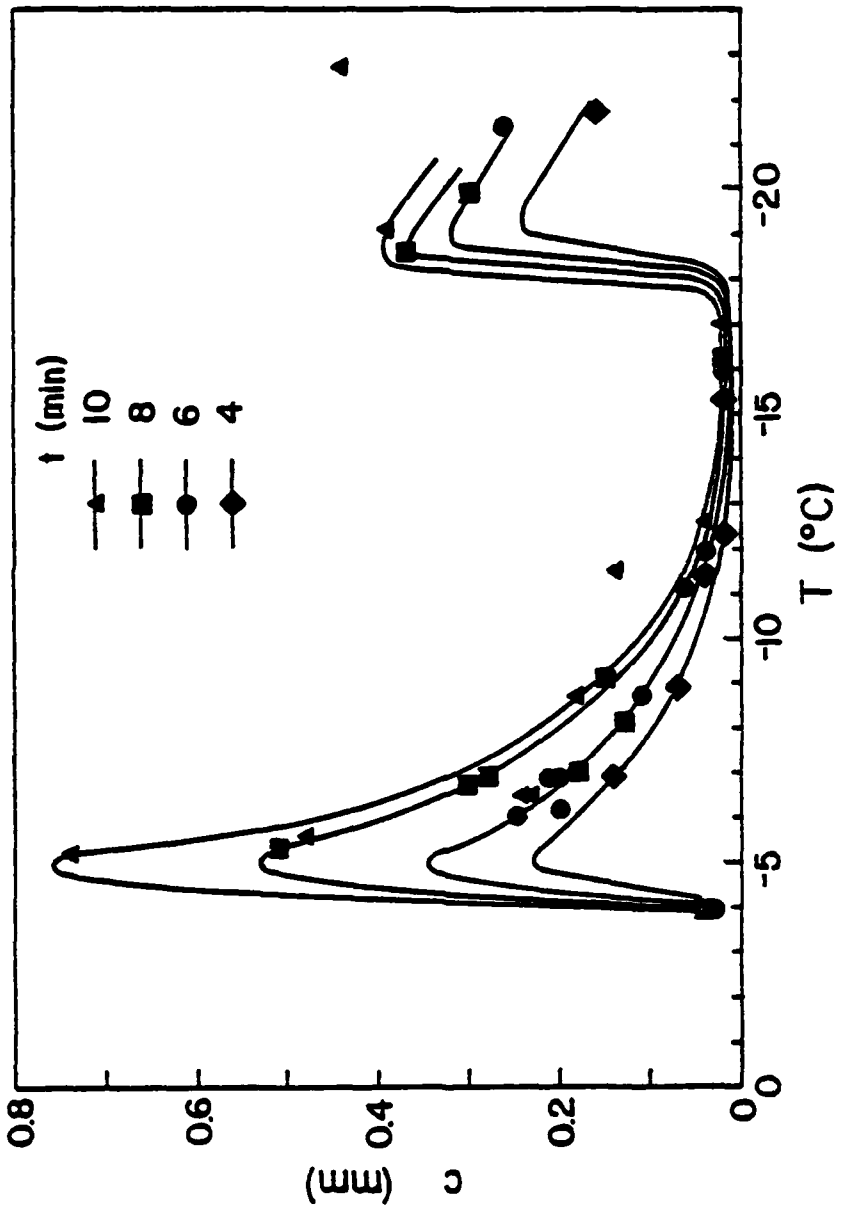

Figure 31. The ice crystal c-axial dimensions plotted as a function of temperature T at different growth times t.

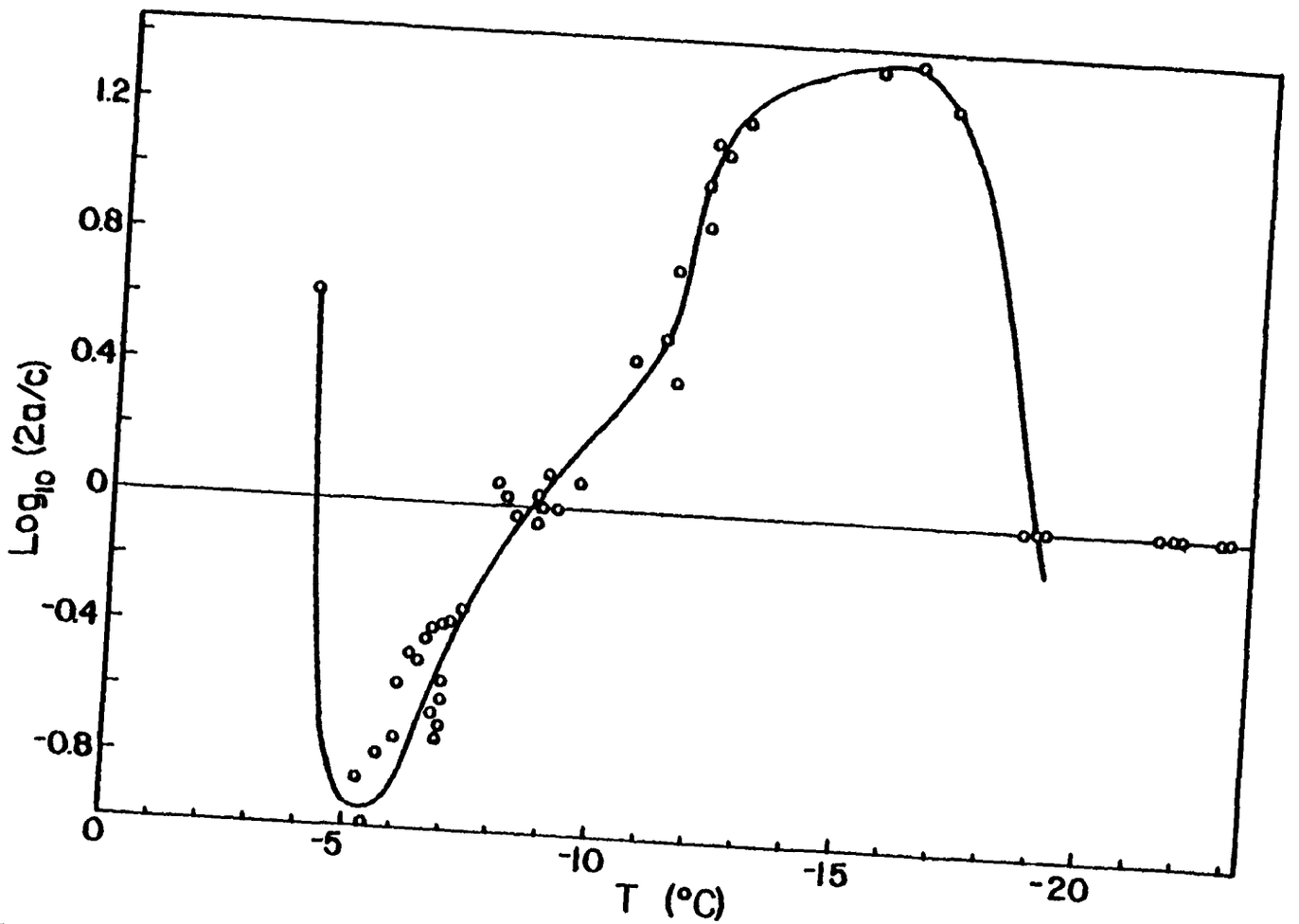

Figure 32. The ice crystal $\log_{10}(2a/c)$ value plotted as a function of temperature T for all growth periods from 4 to 10 minutes.

discussed earlier were observed. The largest negative values are found between -5.0 and -6.0°C, the temperatures where the longest, thinnest columns were observed. The largest positive values are found between -13.0 and -16.5°C, the temperatures where the largest dendrites were observed. The logarithm values of zero at temperatures below -18.5°C are due to the complex crystals observed and not for solid isometric crystals. Due to their complex structure, a determination of the exact 2a- and c-axis dimensions was impossible. Therefore, the diameter of the sphere just large enough to envelope the crystal was measured and plotted in the graph.

Figure 33 shows the variation of the crystal c-axis value with respect to growth time for three temperature zones. The c-axis values increased linearly with respect to time most rapidly in the temperature zone between -6.7 and -7.2°C where columns were observed and most slowly at temperatures between -11.8 to -12.3°C where double plates were found.

The same relationship is shown in Figure 34 for the crystal 2a-axis. In the temperature zones of -15.8 to -16.5°C, -11.8 to -12.3°C, 10.9 to -11.6°C, -8.3 to -9.1°C, and -6.7 to -7.2°C the 2a-axis values increased linearly with time. In the temperature zone of -14.6 to -15.3°C, the 2a-axis value grew at the increasing rate with increased growth periods. The 2a-axis value increased the fastest in the zone between -13.6 and -15.3°C where the largest dendrites were observed. The 2a-axis increased at the slowest rate in the temperature zone of -6.7 to -7.2°C where columns were found.

Growth Rate

Figure 35 illustrates the relationship between ice crystal mass

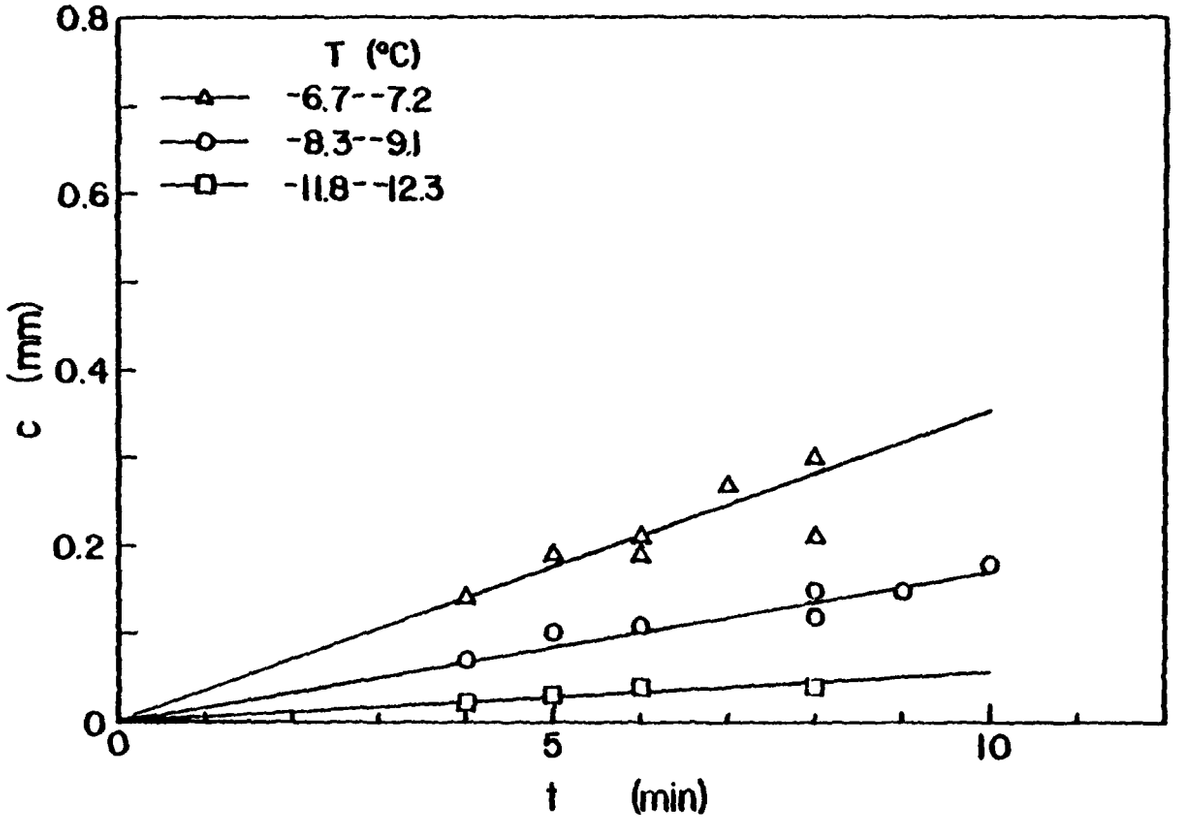

Figure 33. The ice crystal c-axial dimensions plotted as a function of growth time t at different temperatures T.

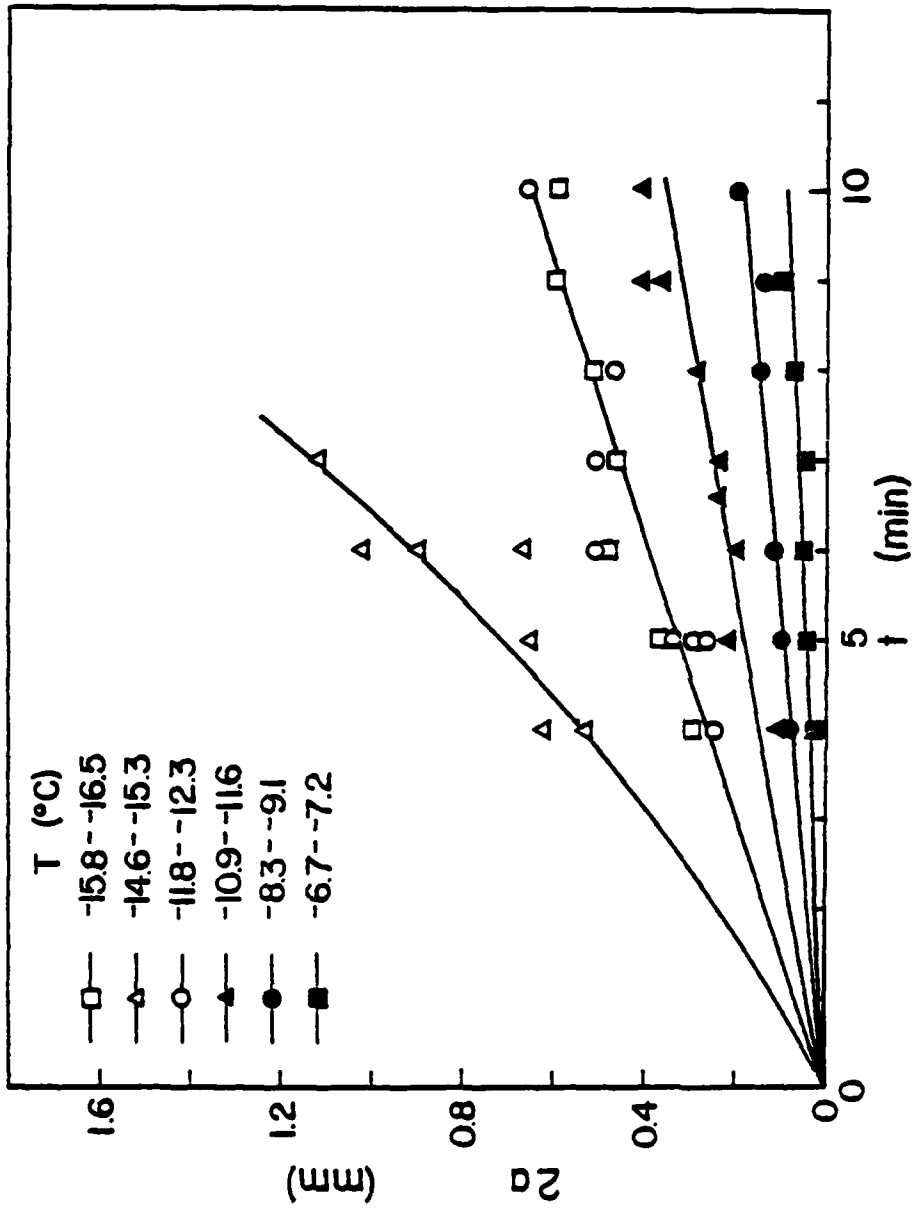

Figure 34. The ice crystal 2a-axial dimensions plotted as a function of growth time t at different temperatures T.

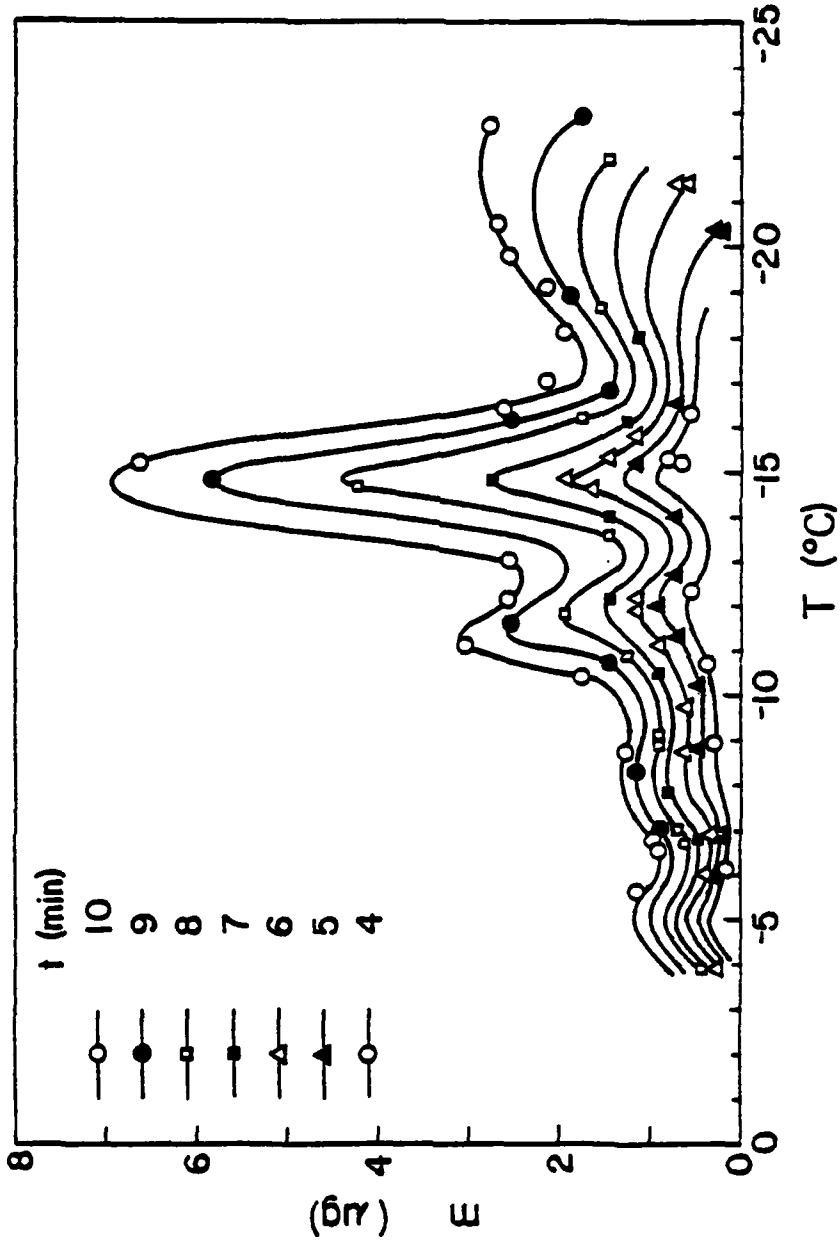

Figure 35. Ice crystal mass m plotted as a function of temperature T for different growth periods t.

and temperature for growth periods from four to ten minutes at one minute intervals. The most obvious feature of the figure is the strong peak near -15°C, associated with dendritic crystals. This peak agrees well with the results of Ryan et al. (1976) and Fukuta et al. (1979), who collected data for growth periods of up to 150 seconds. A secondary peak is located in the zone from -11.0 to -12.0°C, associated with the double plates observed at these temperatures. This secondary peak is well pronounced at the longer growth periods and less pronounced at the shorter growth periods. This may explain why this peak was not evident in earlier works where crystals were suspended for only a short period of time. Two small peaks occur near -5.0 and -8.0°C. The peak at -8.0°C corresponds well with the data reported by Ryan et al. (1976) and Fukuta et al. (1979). A peak is also located at temperatures below -18.5°C where the complex crystals were observed. This peak may be caused by the higher liquid water content values observed at these colder temperatures. Mass minima are found near -6.5°C, -9.0 to -10.0°C, -12.5 to -13.5°C, and -17.0°C. The location of all the maxima and minima in Figure 35 agrees quite well with those in data observed by Michaeli and Gallily (1976), who suspended crystals for 60 and 100 seconds. Only the relative magnitudes of the peaks and valleys with respect to each other differ.

Figures 36 and 37 show the relationship between crystal mass and growth time at different temperatures above -11.6°C and below -11.8°C respectively. At all temperatures the crystals grow at an increasing rate with time. After the initial three minutes, crystals at temperatures from -14.6 to -15.3°C, the dendritic zone, grow at the fastest rate. Crystals at -6.7 to -7.2°C, the column zone, grow at the slowest

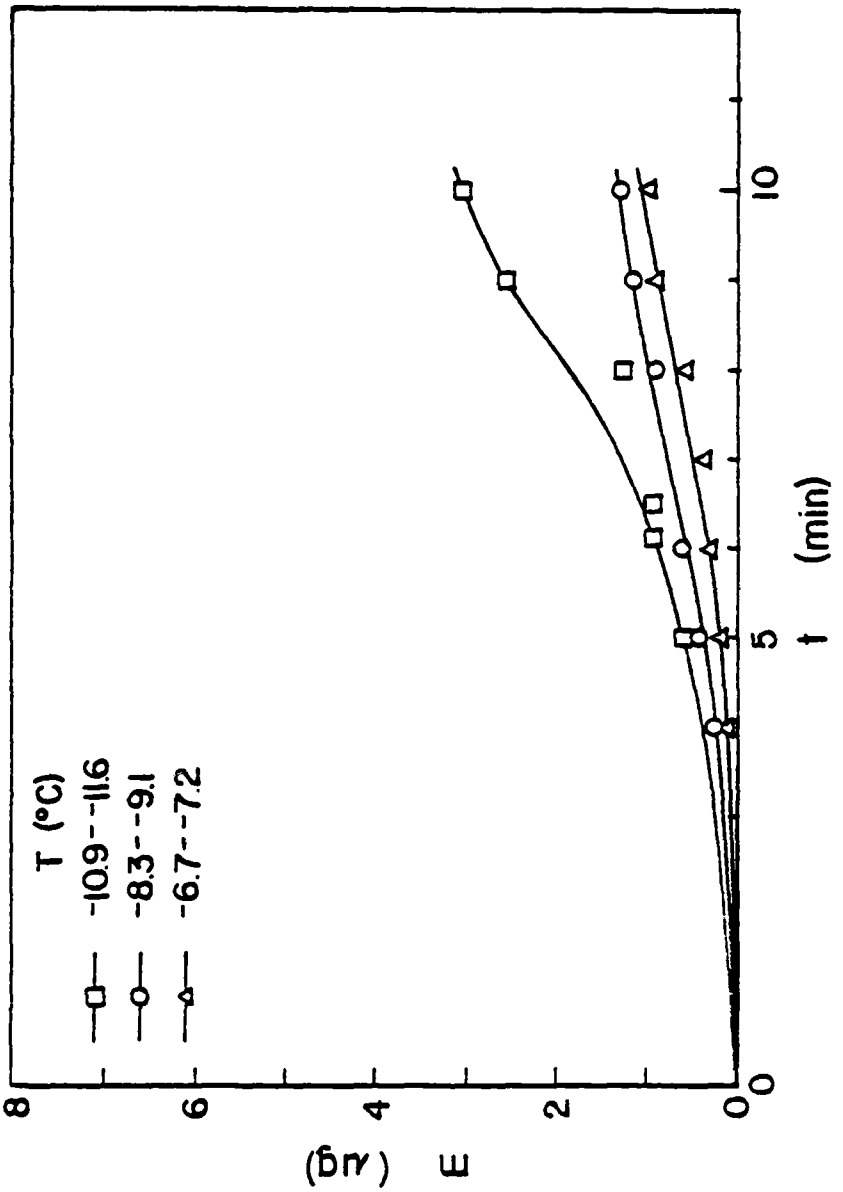

Figure 36. Ice crystal mass m plotted as a function of growth time t at different temperatures T above -11.6°C.

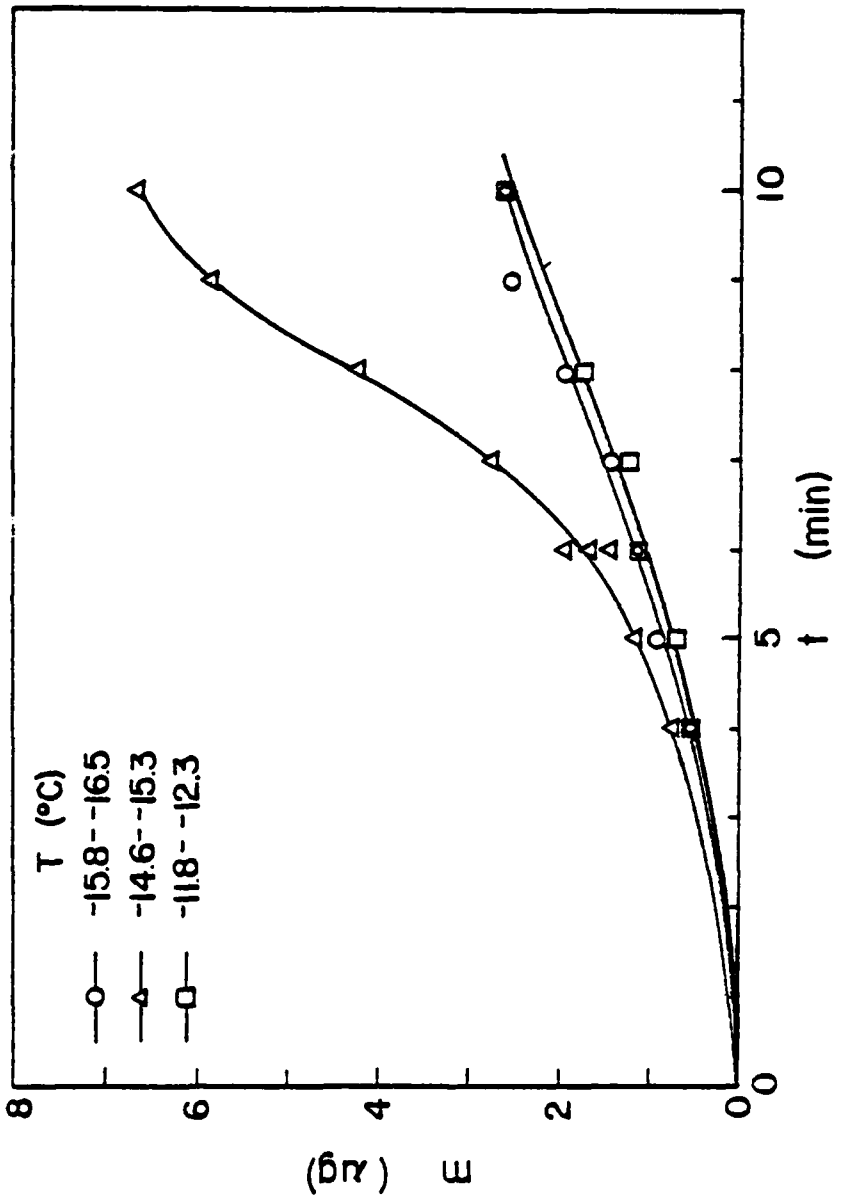

Figure 37. Ice crystal mass m plotted as a function of growth time t at different temperatures below -11.8°C.

rate.

It has been shown that, for simple Maxwellian growth of a near spherical ice crystal at constant supersaturation, temperature, and pressure (vapor diffusion growth), the mass of the crystal is proportional to $t^{1.5}$, where t is the growth time (Fukuta, 1969 and 1978). To examine this relationship, the log-log plotting of our data was made (Figure 38). The graph shows that the growth rate of crystals at -8.3 to -9.1°C and -10.9 to 11.6°C is proportional to this Maxwellian rate. Crystal growth rate at -11.8 to -12.3°C and -15.8 to -16.5°C increases only slightly faster than the Maxwellian rate, however, ice crystal growth rate increase a -6.7 to -7.2°C and -14.6 to -15.3°C is considerably faster than the Maxwellian rate. This indicates that the crystals that are nearly spherical, like the isometric and double plate crystals, grow at a rate proportional to the Maxwellian rate in the periods of this measurement. Also, it suggests that the effect of ventilation remains constant for those crystals under the period of observation in the present experiment. The crystals that varied the most from the Maxwellian growth ratio, the large dendrites and columns, are the least spherical. They also are the type of crystal that are affected the most by ventilation as they fall. This demonstrates the importance of the interaction between the ventilation and the shape, in addition to the deposition and thermal accommodation coefficient effect, when numerically describing ice crystal growth (Non-Maxwellian growth).

Apparent Density

By dividing the measured mass of an ice crystal by its volume, the apparent density of the crystal was estimated. The crystal volume

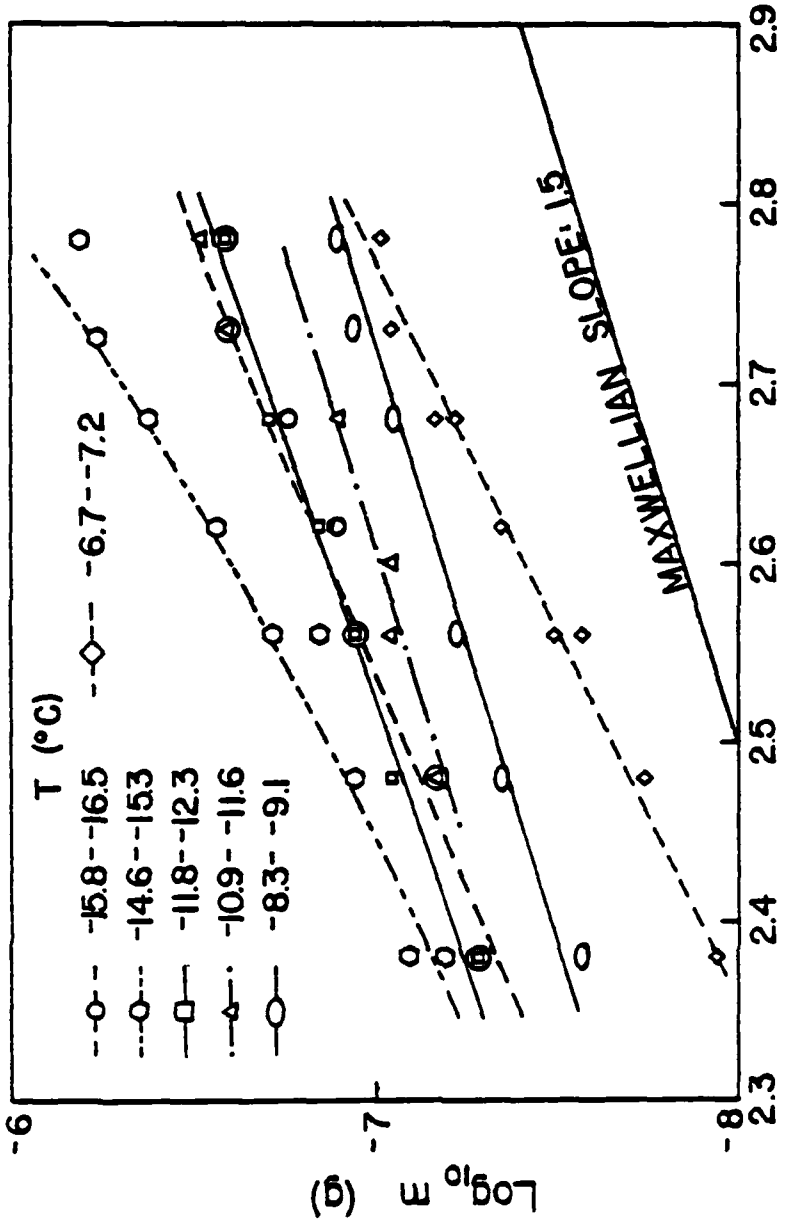

Figure 38. The logarithm of ice crystal mass m plotted as a function of the logarithm of growth time t at different temperatures T.

was estimated by determining the volume of a hexagonal plate or column which just envelopes the outer edges of the actual crystal. Due to their special structure, vaned and complex crystals were not considered. In addition, due to the difficulty in measuring the c-axis of dendritic crystals, they were assumed to have a c-axis of 0.02 mm (the value measured in the three cases where a dendrite was viewed from the side). Figure 39 shows the average apparent density of crystals grown for five, six, and seven minutes plotted as a function of temperature. A marked maximum is located near -9.0°C, the zone where isometric crystals were observed. A pronounced minimum is located near -14.0 to -15.0°C, the temperature zone where dendritic crystals were observed. A secondary minimum is located near -14.0 to -15.0°C, the temperature zone where a crystal mass minimum was observed, while the apparent density minima are located at temperatures where crystal mass maxima were detected. This data agrees very well with that of Fukuta (1969) for his crystals grown for 40-50 seconds. It agrees reasonably well with the data of Fukuta et al. (1979) for their crystals grown for up to 80 seconds, except that their data had the maxima and minima displaced 1°C colder than ours.

Fall Velocity

From the large number of ice crystal fall velocity measurements taken, the effects of both temperature and growth time on the fall velocity were studied. Figure 40 shows the crystal fall velocity plotted as a function of the temperature for growth periods of three to ten minutes. The most obvious feature of this graph is the pronounced fall velocity peak at -9°C, the zone where isometric crystals were observed.

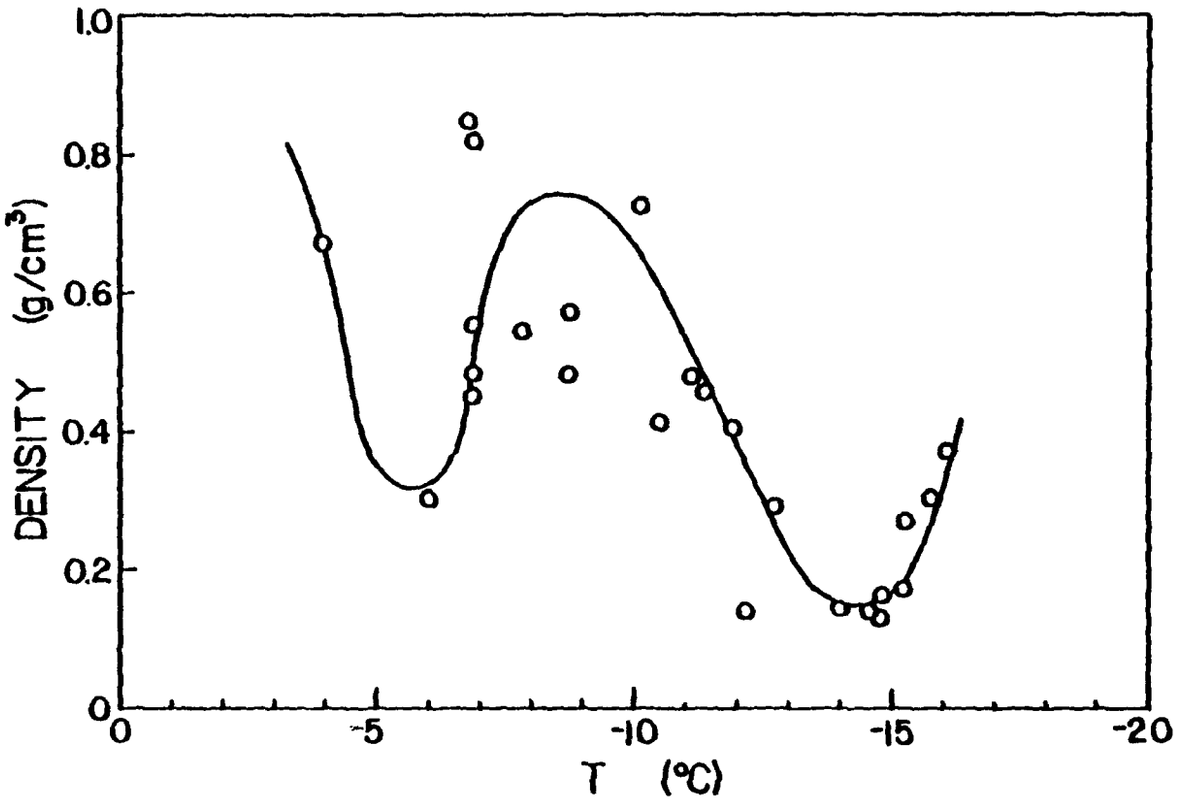

Figure 39. Ice crystal apparent density plotted as a function of temperature T. Plotted points represent the average values for growth periods of 5, 6, and 7 minutes.

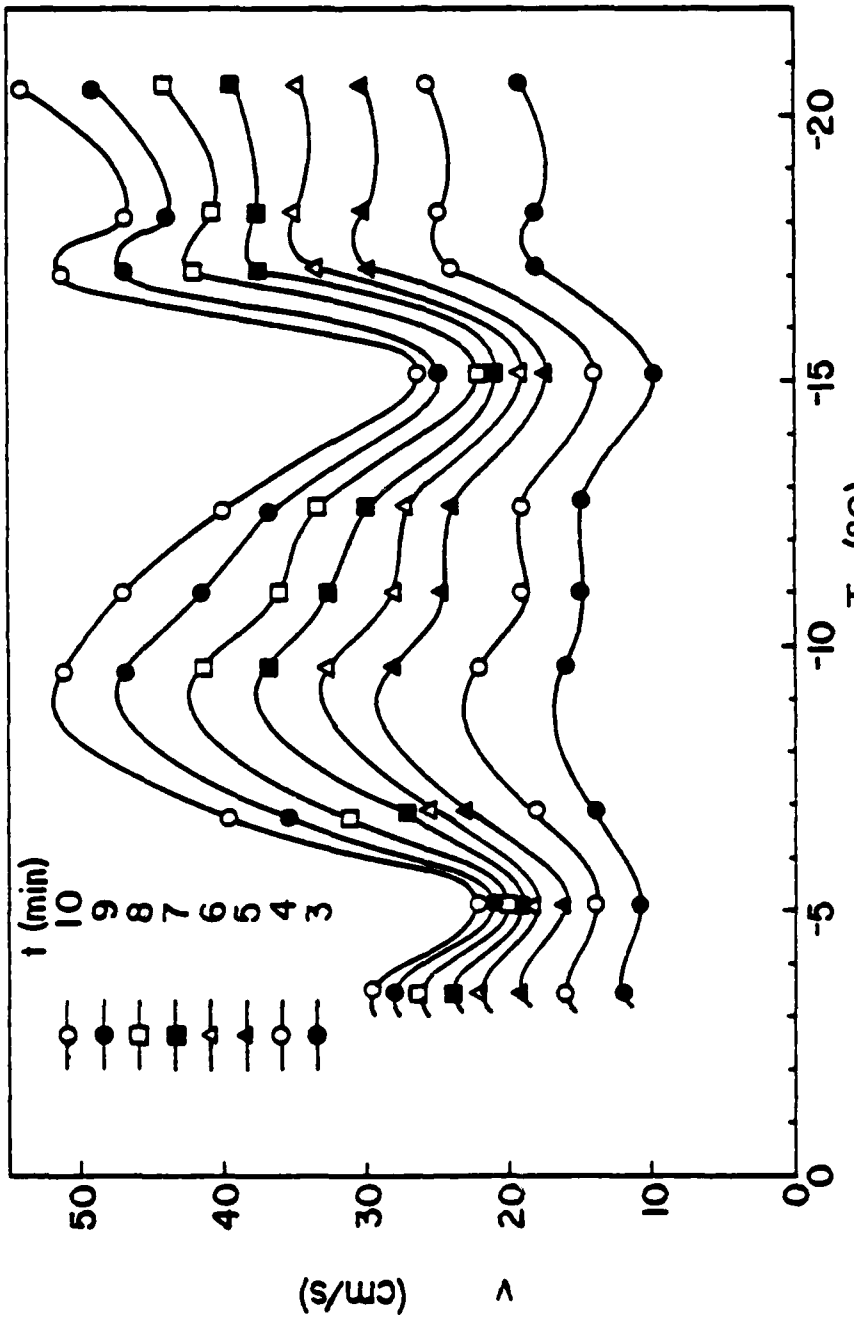

Figure 40. Ice crystal fall velocity v plotted as a function of temperature T for different growth periods t.

A second peak is observed at -17.0°C, the zone of vaned crystals, while a third peak located near -21°C, is associated with the complex crystals. It should be noted that the velocity peak at -9.0°C is nearly equal in magnitude to the peaks at -17.0 and -21°C, even though the ice crystals grew at -9°C under conditions with less liquid water content (Figure 23). If the liquid water content was kept at a constant value for all measurements, the peak at -9.0°C would be the fall velocity peak of highest magnitude. Fall velocity minima are located at -15.0°C, the zone of dendritic crystals, and -5.0°C, the zone of column crystals.

As was noted by Fukuta et al. (1979), the crystal fall velocity maxima were not associated with crystal mass peaks as might be expected. Instead, they were observed at the same temperatures as the mass minima. However, in comparing Figure 40 with Figure 39, it is apparent that the fall velocity peak at -9.0°C is found at the temperature where an apparent density peak exists. This demonstrates the relationship among the ice crystal spatial form, the mass growth rate and the fall velocity. Large columns and dendrites experience extensive aerodynamic resistance because of their spatial form and, therefore, have a slow fall velocity. Isometric crystals experience a minimum of aerodynamic resistance because of their near spherical form and have a fast fall velocity.

Figure 41 gives the ice crystal fall velocity plotted as a function of growth time for different temperatures warmer than -11.0°C. Figure 42 shows the same relationship for various temperatures colder than -12.6°C. Easily recognizable is the slow-down effect of the fall velocity development for the columns (-5.2°C) and dendrites (-15.2°C). In both cases, especially after five minutes of growth, the crystal shape begins to significantly affect the crystal fall velocity.

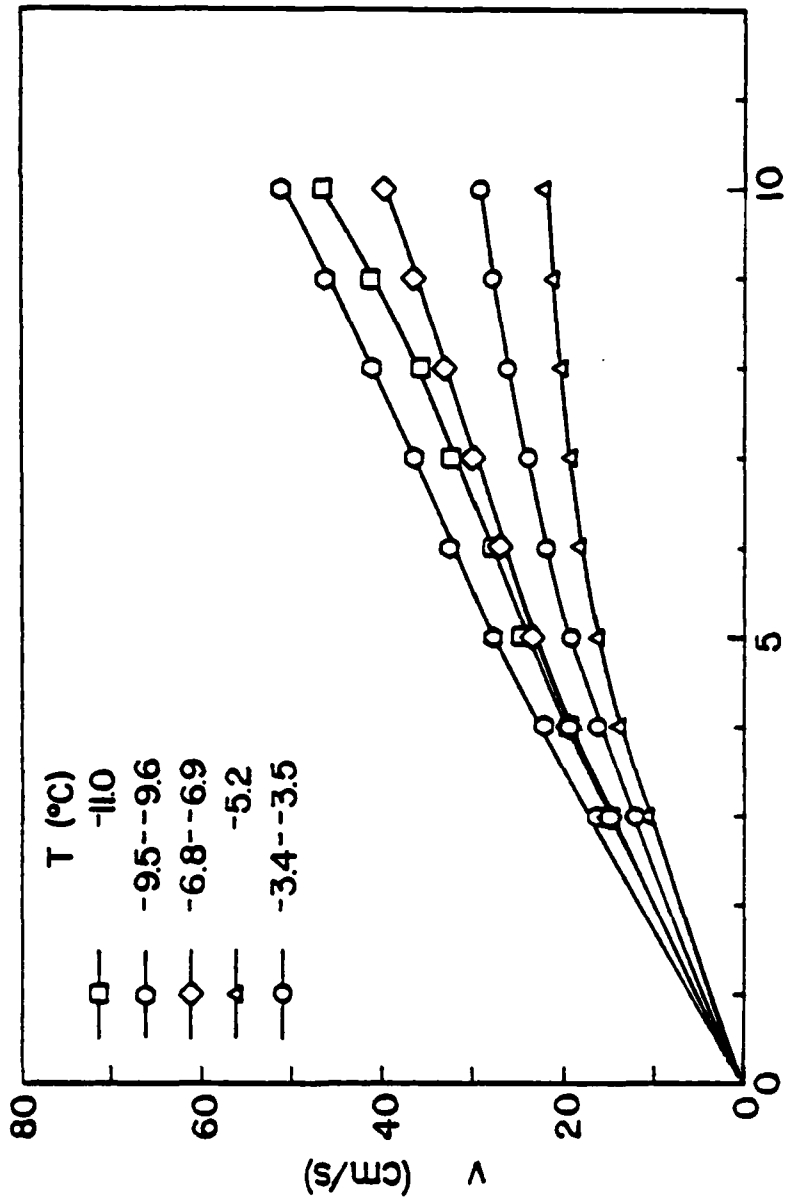

Figure 41. Ice crystal fall velocity v plotted as a function of growth time t for different temperatures warmer than -11.0°C.

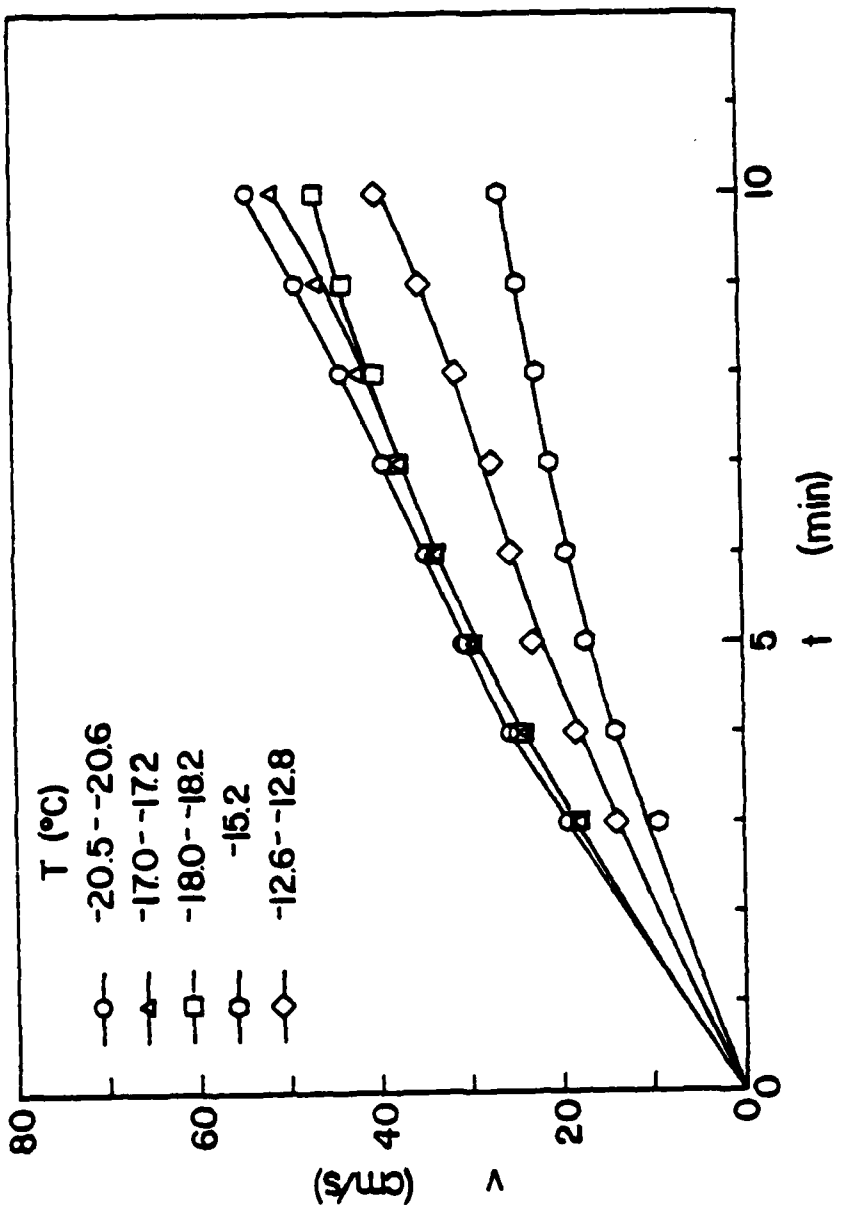

Figure 42. Ice crystal fall velocity v plotted as a function of growth time t for different temperatures colder than -12.6°C.

Conversely, the near isometric crystals (-9.5 to -9.6°C) continue to accelerate at approximately a constant (linear) rate.

Fall Behavior

While the ice crystals were being freely suspended in the supercooled fog stream, their behavior was closely observed. The easiest crystals to suspend were dendrites and large single plates. These crystals were oriented in the tunnel with their basal surface perpendicular to the stream. At the same time, the crystals rotated about their vertical axis. As the fall velocity became larger, the speed of rotation increased. Due to their large basal surface and the resultant high aerodynamic resistance, these crystals were very stable in the vertical direction, responding immediately to the slightest changes in the flow speed. In addition, because of their symmetrical shape, their stability in the horizontal plane was also very good and the crystal remained at the tunnel centerline.

Double plates were only slightly more difficult to suspend than the dendrites and large single plates. Their orientation and rotation characteristics were the same as the dendrites and large single plates. However, due to their smaller basal surface, they did not respond quite as fast to changes in flow speed. Their horizontal stability was about the same.

Columns were also reasonably easy to suspend. These crystals, however, were oriented with their prism surface perpendicular to the airstream. In this orientation, they rotated horizontally about an axis perpendicular to the prism plane. The faster the flow speed, the faster was the speed of rotation. Their stability in the vertical

direction was slightly less than that for the double plates. The horizontal stability was nearly the same.

Isometric crystals were more difficult to suspend. Due to their small aerodynamic resistance, they reacted much more slowly to flow speed changes than the previously discussed crystals. However, since they were nearly symmetrical, they did remain in the zone near the tunnel centerline. Approximately half of the isometric crystals were oriented with the basal surface perpendicular to the airflow while the other half had their prism surface perpendicular to the flow. It was not possible to determine if their crystals rotated while suspended.

The vaned crystals were the most difficult to suspend in the supercooled fog. During approximately the first five to six minutes of growth, the vaned crystals behaved as regular dendrites or plates. However, after this period of growth, they became very unstable in the horizontal direction. At this point, the crystals became nearly impossible to hold at the tunnel centerline. As they randomly moved to various positions in the horizontal plane, it became very difficult to keep the crystal suspended at the 14 cm square position of the working/observation section of the tunnel. This instability is likely caused by the presence of the vanes protruding from the crystal basal surface. After five to six minutes, the vanes have grown to a size where they significantly disrupt the aerodynamic characteristics of the crystal.

Chapter 6

CONCLUSIONS

In the process of developing a new supercooled cloud tunnel capable of freely suspending an ice crystal for extended periods of time, a number of new developments were made. By using this new supercooled cloud tunnel, many ice crystal growth measurements were conducted for periods well beyond the periods previously possible in the laboratory. The main contributions are listed below.

Apparatus Development

Using the principle of simultaneously measuring ice crystal mass, fall velocity, apparent density, and shape and size, first attempted by Fukuta (1969), and extending the capability of the supercooled cloud tunnel used by Fukuta et al. (1979), a new supercooled cloud tunnel was designed, built and tested successfully for suspending crystals for much longer periods of time than previously possible. The main features of the newly developed supercooled cloud tunnel are as follows:

1. A fog chamber with four vertical sections is used to make the supercooled fog homogeneous with respect to temperature and droplet concentration and number.
2. A honeycomb section is applied to develop the laminar supercooled fog flow necessary to freely suspend ice crystals.

The honeycomb is designed to be removable in order to keep it from icing.

3. A new design of working/observation section, converging from bottom to top, is developed to obtain maximum stability in both the horizontal and vertical direction. With this design, it is possible now to freely suspend an ice crystal in the supercooled fog airstream for indefinite lengths of time.
4. The suction chamber, placed above the working/observation section, insures that the flow is drawn evenly across the entire cross-section of the working/observation section.
5. The moisture for the supercooled fog is stably supplied by a specially designed steam generator. The amount of supercooled fog produced is determined and held constant by regulating the volume of compressed air flowing into the generator.
6. The flow speed of the supercooled fog through the working/observation section is controlled by a specially designed valve, which, at the same time, maintains the total flow and fog characteristics through the tunnel constant.
7. The flow-speed through the tunnel is measured by a pitot arrangement attached to an electronic manometer. The manometer output is displayed on a flatbed recorder to allow for real-time monitoring and later analysis.
8. Temperature is continuously measured by a thermocouple whose output is also displayed on the flatbed recorder.
9. A method is used to collect and preserve the ice crystals

for observation and photographing, both from the top and side. After melting, the resulting water droplets remain in their spherical shape, allowing accurate mass determination.

Main Findings

Using the new supercooled cloud tunnel, ice crystals were suspended for three, four, five, six, seven, eight, nine, and ten minutes at various temperatures between -3.0 and -22.0°C. The main findings are listed below:

1. Ice crystal habit: >4.5°C, single and double plates; -4.5 to -7.0°C, columns; -9.0°C, isometric; -10.0 to -12.5°C, double plates; -13.0 to -16.0°C, dendrites; -16.0 to -18.0°C, vaned; -18.0 to -23.0°C, complex.
2. Mass: A pronounced mass maximum was observed at -15.0°C. Secondary maxima were observed near -5.0, -8.0, -11.5, and -21.0°C. Minima were found near -6.0, -9.0, and -17.0°C. Ice crystals in the temperature zones from -8.3 to -9.1°C and from -10.9 to -16.6°C grew proportional to the simple Maxwellian rate. At other temperatures, growth rates were faster than the simple Maxwellian rate. Crystals grew the fastest at temperatures from -6.7 to -7.2°C and from -14.6 to -15.3°C.
3. Crystal apparent density was calculated. A maximum was observed near -8.5°C while minima were noted near -5.5 and -14.5°C.

4. From crystal fall velocity measurements, the most pronounced feature observed was a maximum at -9.0°C, associated with the isometric crystals. Minima were observed near -5.0°C, associated with large columns, and -15.0°C, associated with dendrites. Secondary maxima were noted at -17.0 and -20.5°C.
5. At temperatures between -18.0 and -23.0°C and liquid water contents between 1.25 and 1.50 g/m^3, complex crystals were observed. These crystals seem to have developed from a process that combined riming and vapor diffusion growths. They consisted of isometric crystals at the center with complex branches, made up of several randomly connected thick hexagonal plates extending radially outward in all directions.

Possible Future Applications

Since the new supercooled cloud tunnel provides the capability to freely suspend an ice crystal for indefinite periods of time and also can accurately control the liquid water content, many possible future applications are foreseen. A few of these applications are listed below:

1. Using the same experimental procedures that were used in this study, ice crystals should be grown for even longer periods of time.
2. By holding the temperature at which a crystal is grown constant and changing the liquid water content of the supercooled fog, the growth of a crystal in different types of

clouds may be simulated.

3. Due to the capability of holding an ice crystal freely suspended within 1-2 cm^2 of the same location, the possibility exists of taking time-lapse movie pictures of the crystal to more accurately observe and record its fall behavior.
4. By increasing the period of crystal suspension and carefully changing the liquid water content, an accurate determination of the riming threshold for different types of crystals may be possible.

APPENDIX

EXPRESSION FOR FLOW SPEED CALIBRATION

From the sketch of the working/observation section shown in Figure A1, it can be seen that

$$\frac{b - a}{y - a} = \frac{c}{x} . \tag{A1}$$

Rearranging and solving equation (A1) for y yields

$$y = a + \frac{b-a}{c} x . \tag{A2}$$

From the continuity of flow, the product of the cross-sectional area at any point in the working/observation section and the flow velocity, v, at the same point is constant; i.e.,

$$y^2 v = C . \tag{A3}$$

Substituting equation (A2) into equation (A3) and solving for v results in

$$v = \left[\frac{c}{ac + (b-a)x} \right]^2 C . \tag{A4}$$

Since

$$v = \frac{dx}{dt} , \tag{A5}$$

equation (A4) becomes

$$\left[\frac{ac + (b-a)x}{c} \right]^2 \frac{1}{C} dx = dt . \tag{A6}$$

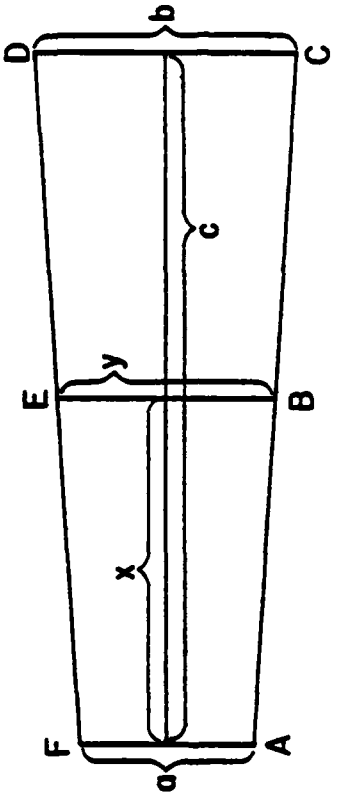

Figure A1. Dimensions of working/observation section of the wind tunnel.

Integration of equation (A6) over the limits of distance from 0 to c and time for 0 to t_b yields

$$C = \frac{c}{3t_b} (b^2 + ab + a^2) . \qquad (A7)$$

Substitution of equation (A7) into equation (A4) gives

$$v = \frac{c^3}{3t_b} \frac{(a^2 + ab + b^2)}{(ac + (b-a)x)^2} . \qquad (A8)$$

In equation (A8), the values for a, b, and c are dimensions of the working/observation section. t_b is the time required for a parcel of air to travel from the AF plane in the section to the CD plane. This time is measured during the smoke tests. The value for x is the distance measured from the AF plane to the position where the velocity determination is desired. For all of our experiments, the velocity calibration was made for the 14 cm square position in the working/observation section, since this was the position where the crystals were suspended. Therefore, the values for equation (A8) are as follows:

x = 38.2 cm

a = 9.6 cm

b = 18.0 cm

c = 72.8 cm

REFERENCES

Anderson, J. D., 1978: Introduction to Flight. McGraw-Hill, Inc., 432 pp.

Auer, A. H., and D. L. Veal, 1970: The dimensions of ice crystals in natural clouds. J. Atmos. Sci., 27, 919-926.

aufm Kampe, H. J., H. K. Weickmann, and J. J. Kelly, 1951: The influence of temperature on the shape of ice crystals growing at water saturation. J. Meteor., 8, 168-174.

_____, 1969: A determination of the terminal velocity and drag of small water drops by means of a wind tunnel. J. Atmos. Sci., 26, 1066-1072.

Beard, K. V., and H. R. Pruppacher, 1971: A wind tunnel investigation of collection kernels for small water drops in air. Quart. J. Roy. Meteor. Soc., 97, 242-248.

Bigg, E. K., 1953: The supercooling of water. Proc. Phys. Soc., 66, 688, 157-162.

Fukuta, N., 1968: Some remarks on ice nucleation by metaldehyde. Proc. Intl. Conf. on Cloud Phys., Toronto, 26 - 30 Aug. 1968, 194-198.

_____, 1969: Experimental studies on the growth of small ice crystals. J. Atmos. Sci., 26, 522-531.

_____, 1973: Thermodynamics of cloud glaciation. J. Atmos. Sci., 30, 1645-1649.

_____, 1978: Ice crystal growth kinetics and accommodation coefficients. Cloud Physics and Atmospheric Electricity Conference, Seattle, Washington, 31 July - 4 August, 1978.

Fukuta, N., L. R. Neubauer, and D. D. Erickson, 1979: Laboratory studies of organic ice nuclei smoke under simulated seeding conditions: ice crystal growth. Final report to NSF under Grant No. ENV 77-15346, January 1979.

Hallett, J., 1965: Field and laboratory observations of ice crystal growth from the vapor. J. Atmos. Sci., 22, 64-69.

Hallett, J., and B.J. Mason, 1958. The influence of temperature and supersaturation on the habit of ice crystals grown from the vapor.

Proc. Roy. Soc. London, A247, 440-453.

Hoffer, T. E., and S. C. Mallen, 1968: A vertical wind tunnel for small droplet studies. J. Appl. Meteor., 7, 290-292.

_____, 1970: Evaporation of contaminated and pure water droplets in a wind tunnel. J. Atmos. Sci., 27, 914-918.

Iribarne, J. V., and M. Klemes, 1970: Electrification associated with breakup of drops at terminal velocity in air. J. Atmos. Sci., 27, 927-936.

Jayaweera, K. O. L. T., and R. E. Cottis, 1969: Fall velocities of plate-like and columnar ice crystals. Quart. J. Roy. Meteor. Soc., 95, 703-709.

Jayaweera, K. O. L. F. and B. J. Mason, 1966: The falling motion of loaded cylinders and discs simulating snow crystals. Quart. J. Roy. Meteor. Soc., 92, 151-156.

Kinzer, G. D., and W. E. Cobb, 1956: Laboratory measurements of the growth and collection efficiency of rain drops. J. Meteor., 13, 295-301.

_____, 1958: Laboratory measurements and analysis of the growth and collection efficiency of cloud drops. J. Meteor., 15, 138-148.

Kinzer, G.D., and R. Gunn, 1951: The evaporation temperature and thermal relaxation time of freely falling water drops. J. Meteor., 8, 71-83.

Kobayashi, T., 1961: The growth of snow crystals at low supersaturations. Phil. Mag., 6, 1363-1370.

Lamb, D., and P. V. Hobbs, 1971: Growth rates and habits of ice crystals grown from the vapor phase. J. Atmos. Sci., 28, 1506-1509.

Macklin, W. C., 1961: Accretion in mixed clouds. Quart. J. Roy. Meteor. Soc., 87, 413-415.

Magono, C., and S. Tazawa, 1966: Design of snow crystal sondes. J. Atmos. Sci., 23, 618-625.

Mason, B. J., 1953: The growth of ice crystals in a supercooled water cloud. Quart. J. Roy. Meteor. Soc., 79, 104-111.

_____, 1971: The Physics of Clouds, Oxford University Press, 671 pp.

Michaeli, G., and I. Gallily, 1976: Growth rates of freely falling ice crystals. Nature, 259, 110.

Nakaya, N., 1954: Snow Crystals: Natural and Artificial. Harvard

University Press, 510 pp.

Ono, A., 1969: The shape and riming properties of ice crystals in natural clouds. J. Atmos. Sci., 26, 138-147.

_____, 1970: Growth mode of ice crystals in natural clouds. J. Atmos. Sci., 27, 649-658.

Pankhurst, R. C., and D. W. Holder, 1952: Wind-Tunnel Technique. Sir Isaac Pittman and Sons, LTD (London), 702 pp.

Petter, R. L., and H. R. Pruppacher, 1973: A wind tunnel investigation of freezing of small water drops falling at terminal velocity in air. Quart. J. Roy. Meteor. Soc., 99, 540-550.

Pflaum, J. C., J. J. Martin, and H. R. Pruppacher, 1978: A wind tunnel investigation of the hydrodynamic behavior of growing, freely falling graupel. Quart. J. Roy. Meteor. Soc., 104, 179-187.

Pflaum, J. C., and H. R. Pruppacher, 1979: A wind tunnel investigation of the growth of graupel initiated from frozen drops. J. Atmos. Sci., 36, 680-689.

Pope, A., and J. J. Harper, 1966: Low-Speed Wind Tunnel Testing. John Wiley and Sons, Inc., 457 pp.

Pruppacher, H. R., and K. V. Beard, 1970: A wind tunnel investigation of the internal circulation and shape of water drops falling at terminal velocity in air. Quart. J. Roy. Meteor. Soc., 96, 247-256.

Pruppacher, H. R., and J. D. Klett, 1978: Microphysics of Clouds and Precipitation. D. Reidel Publishing Co., Boston, 714 pp.

Pruppacher, H.R., and M. Neiburger, 1968: The UCLA cloud tunnel. Proc. Intl. Conf. Cloud Physics, Toronto, 389-392.

Rogers, R. R., 1979: A Short Course in Cloud Physics. 2nd edition. Pergamon Press, 235 pp.

Ryan, B. F., E. R. Wishart, and E. W. Holroyd III, 1974: The densities and growth rates of ice crystals between -5°C and -9°C. J. Atmos. Sci., 31 2136-2141.

Ryan, B. F., E. R. Wishart, and D. E. Shaw, 1976: The growth rates and densities of ice crystals between -3°C and -21°C. J. Atmos. Sci., 33, 842-850.

Schaefer, V. J., 1941: Method of making replicas of snowflakes, ice crystals and other shortlived substances. Museum News, 19, 11-14.

_____, 1946: The production of ice crystals in a cloud of supercooled water droplets. Science, 104, 457-459.

_____, 1949: A method of making snowflake replicas. Science, 93, 239-240.

_____, 1962: The vapor method of making replicas of liquid and solid aerosols. J. Appl. Meteor., 1, 413-418.

Smith-Johannsen, R. I., 1965: Resin vapour replication technique for snow crystal and biological specimens. Nature, 205, 1204-1205.

Telford, J. W., N. S. Thorndike, and E. G. Bowen, 1955: The coalescence between small water drops. Quart. J. Roy. Meteor. Soc., 81, 241-250.

VITA

Name	Mike Wayne Kowa
Birthplace	Olney, Illinois
Birthdate	19 January, 1952
High School	Northern High School Durham, North Carolina
Universities	North Carolina State University Raleigh, North Carolina 1970-1974
	University of Utah Salt Lake City, Utah 1979-1981
Degrees	Bachelor of Science, Mathematics, 1974 North Carolina State University
	Bachelor of Science, Meteorology, 1974 North Carolina State University
Professional and Honorary Organizations	American Meteorological Society Chi Epsilon Pi Phi Kappa Phi
Professional Position	Weather Officer United States Air Force

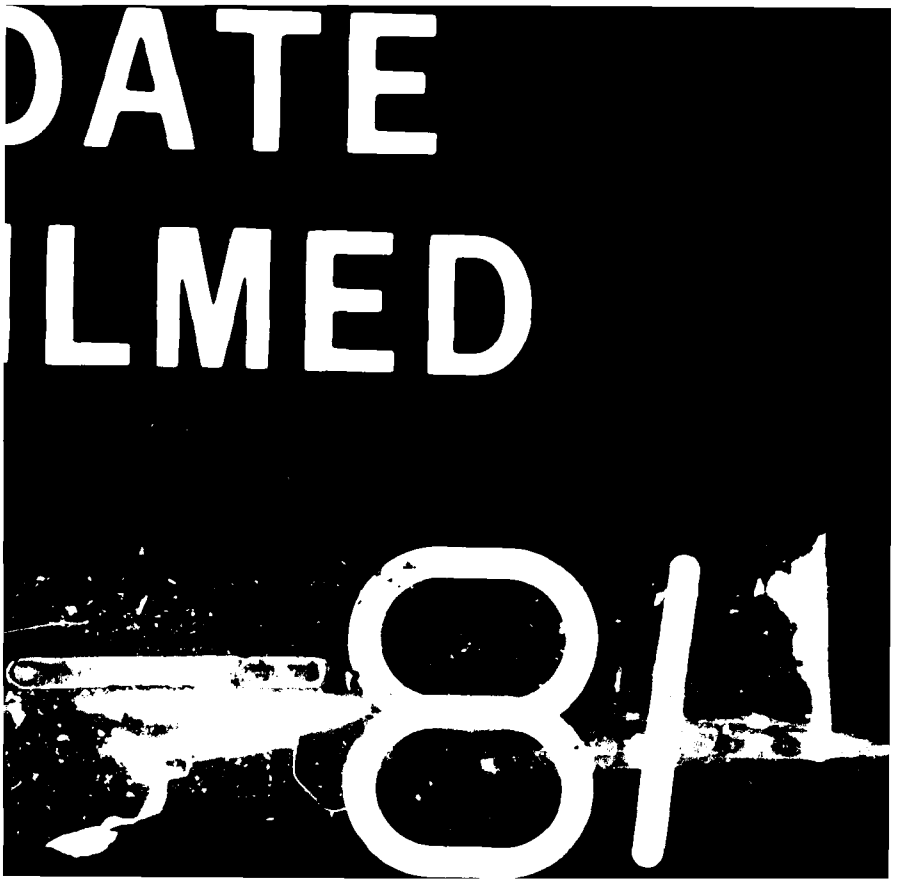
DATE
LMED
81